A STUDY ON THE BEARING CAPACITY OF SHALLOW FOUNDATIONS ON GEOSYNTHETIC REINFORCED SAND

C. Sanjei

158012A

Degree of Master of Science

Department of Civil Engineering

University of Moratuwa

Moratuwa

Sri Lanka

January, 2017

A STUDY ON THE BEARING CAPACITY OF SHALLOW FOUNDATIONS ON GEOSYNTHETIC REINFORCED SAND

Chitravel Sanjei

158012A

The research thesis was submitted in partial fulfillment of the requirements for the Degree of Master of Science

Supervised by Dr. L.I.N. De Silva

Department of Civil Engineering

University of Moratuwa

Moratuwa

Sri Lanka

January, 2017

DECLARATION

I declare that this is my own work and this thesis does not incorporate without acknowledgement any material previously submitted for a Degree or Diploma in any other University or institute of higher learning and to the best of my knowledge and belief it does not contain any material previously published or written by another person except where the acknowledgement is made in the text.

Also, I hereby grant to University of Moratuwa the non-exclusive right to reproduce and distribute my thesis, in whole or in part in print electronic or other medium. I retain the right to use this content in whole or part in future works (such as articles or books)

…… Date: January 7, 2017

C.Sanjei

The above candidate has carried out research for the Master thesis under my supervision.

…… Date: January 7, 2017

Dr. L.I.N. De Silva

ABSTRACT

A study on the bearing capacity of shallow foundations on geosynthetic reinforced sand

This thesis demonstrate a research study aimed at investigating the significance of bearing capacity improvement of shallow foundation supported on geocell, geogrid and combination of geocell and geogrid reinforced sand. To implement the objective, laboratory model test, numerical study using PLAXIS 3D and theoretical study were performed to investigate the behavior of reinforced soil foundation. Honeycomb shape HDPE geocell and biaxial geogrid were used in laboratory model test.

For geocell, initially single layer geocell was experimented with different cover thickness (geocell placing depth). From the results, suitable cover thickness was found at [depth (U)/width (B)] ratio between 0 and 0.5 for a square pad footing. Numerical modeling of the geocell has been an immense challenge due to their curved shape. The equivalent composite approach (ECA) is widely used to model the geocells. However, the composite method has a number of limitations, including the disregard of the effect of shape. The shape has a major influence in stress distribution. Hence a realistic model approach is essential to simulate the same experimental condition in numerical analysis. In this study, a 3D Auto Cad model was imported to PLAXIS 3D and modeled using geogrid structural element. Then the model was validated using experimental results where the results satisfied each other. According to the numerical analysis, optimum cover thickness for sand was found as 0.1B (width of footing). The static load test showed that with the provision of HDPE geocells, bearing capacity of soil can be improved by a factor up to 2.5 times of unreinforced soil. Further numerical investigations were carried out using double layer geocell for prototype footing to compare the bearing capacity improvement with single layer geocell. The results clearly depict that bearing capacity is improved by a factor of 2.75 and 3.5 times of unreinforced soil when using single layer and double layer geocell respectively. When doubly reinforced geocell was used, footing size is reduced by 40% and cost is reduced by 65%. It is apparent that using double reinforced geocell will lead to cost effective foundation designs. These ultimate bearing capacity results were validated by theoretical approaches. A good matching was found between experimental, numerical and theoretical approach.

For geogrid, laboratory model test and numerical modelling were performed to find the correlation between number of geogrid and bearing capacity, using optimum cover thickness and spacing. The experimental results show that both surface heaving and settlement are reduced with number of geogrid mattress. Moreover it was also observed that bearing capacity of reinforced soil increases with increasing number of reinforcement layers (at same vertical spacing). However, the significance of an additional reinforcement layer decreases with the increase in number of layers, and bearing capacity is improved by a factor of 2.86 times of unreinforced soil when four layer geogrid was used. Further validations were performed using (FHWA/LA.08/424) technical report.

Finally, a combination of geocell and geogrid was used as reinforcement. Two different cases were investigated, namely ‘geocell+geogrid’ combination and ‘geogrid+geocell’ combination. Optimum bearing capacity was obtained when geogrid was placed at the base and on the top of geocell in which bearing capacity is improved by a factor of 4.3 and 3.8, times of

unreinforced soil respectively. It shows that a layer of planar geogrid placed at the base of the geocell mattress improves the bearing capacity significantly compared with provision of geogrid above the geocell layer.

Based on the overall study, key recommendations are made, which can be made for the improvements of reinforced soil foundation design. The results stated in this study will be useful in construction of building and pavements on the weak soils to significantly improve the bearing capacity of shallow foundation.

Key words: Bearing capacity, shallow foundation, geosynthetic, honeycomb shape geocell, PLAXIS 3D, feasibility study

DEDICATION

To my ever-loving teachers

ACKNOWLEDGEMENT

First of all, I would like to express my sincere thanks and appreciation to my advisor, Dr. L.I.N. De Silva, senior lecturer at the Department of Civil Engineering of University of Moratuwa, for his patient guidance all through my master study. Without his advice, support, and encouragement, this thesis would not have been accomplished. It has been a great honor for me to have him as my advisor. His help and support are really appreciated. And I would like to thank to Dr. N.H. Priyankara and Dr. U. P. Nawagamuwa for serving on my progress review committee. I am truly grateful for their time and valuable comments.

I would like to extend my gratitude to Head of the Department, Prof. J.M.S.J. Bandara and former head Prof. S.M.A Nanayakkara, Department of Civil Engineering, University of Moratuwa in providing this opportunity. A special gesture of appreciation is also conveyed to department research coordinator, Prof. A.A.D.A.J. Perera, for giving his full support in research and evaluation.

The assistance received from Mr. K.R. Pitipanaarachchi, technical officer, Mr. D.G.S. Vithanage, technical officer and Mr. Ajith, lab assistant, of the Soil Mechanics Laboratory of the University of Moratuwa, during the laboratory-testing programme is acknowledged. Many thanks are extended to University of Moratuwa for the services provided during the research and to the Senate research council of University of Moratuwa (SRC/Capital/14/07), Sri Lanka for funding this research.

TABLE OF CONTENTS

LIST OF FIGUERS

LIST OF TABLES

LIST OF ABBREVIATIONS

Abbreviations	Description	Unit
ϕ	Friction angle	[^{o}]
c	cohesion	[kN/m^2]
δ	Interface friction angle	[^{o}]
k	Coefficient of permeability	[m/day]
γ	Dry unit weight	[kN/m^3]
BCR	Bearing capacity ratio	-
M	Secant modulus of the geocell material	[kN/m]
K_e	Young's modulus parameter of the unreinforced sand	-
n	Modulus exponent of the unreinforced soil	-
K_r	Young's modulus parameter of the geocell-reinforced sand	-
P_a	Atmospheric pressure	[kPa]
D_{10}	Effective particle size	[mm]
D_{50}	Mean particle size	[mm]
C_u	Coefficient of uniformity	-
C_c	Coefficient of curvature	-
G_s	Specific gravity	-
RD	Relative density	[%]
t	Thickness	[mm]
E	Young modulus	[MPa]
k	Interface shear modulus	[MPa/m]
T	Tensile strength	[kN]
J	Tensile modulus	[kN/m]
U	Cover thickness	[mm]
X	Spacing	[mm]
Bx	Width	[mm]
k_o	coefficient of active earth pressure	-
p	surcharge load	[kN/m]

c	cohesion of soil	[kN/m^2]
N_c	bearing capacity factor	-
S_c	loading shape factor related to cohesion	-
N_q	bearing capacity factor	-
S_q	loading shape factor related to surcharge load	-
B	loading width	[m]
N_γ	bearing capacity factor	-
S_γ	loading shape factor related to the soil unit weight	-
h/d	geocell aspect ratio	-
e	stress redistribution parameter	-
d	Geocell pocket size	[mm]
h	Geocell height	[mm]
D_f	embedment depth	[m]
E_s	Elastic modulus of sand	[kN/m^2]
$I_{\varepsilon p}$	strain influence factor	-

1 INTRODUCTION

1.1 Research background

Foundation design is the most significant part in the design of structures. Shallow foundation which represents the simplest form of load transfer from a structure to the ground beneath, is a widely used foundation type in construction of structures. The design of foundation is directly governed by soil type and ground condition. Statistics say that **80%** of soil existing soil in the world is average or weak based on their bearing capacity (Chesworth, 2007). According BS 8004, bearing capacity of soft clay, loose sand, firm clays, loose gravel and medium dense soil are less than 75kPa, less than 100kPa, 75-100kPa, 200kPa and 100-300kPa respectively.

Shallow foundations are constructed on top of the existing weak soil beds, resulting in low bearing capacity and excessive settlement problems. Structural damage, reduction in durability and deterioration are the expected causes. In conventional treatment, the increasing of the dimension of the footing is a common method used to improve the performance level. However, geosynthetic is an alternative and economical solution to improve the performance by reinforcing the soil. Inclusion of reinforcement generally increases the ultimate bearing capacity of soil and reduces the footing settlement. Geotextile, geogrid and geocell are the main reinforcing agents of geosynthetics.

Among geosynthetics, geogrid and geocell are mostly used to strengthen the weak soil. They provide faster, feasible and environmental friendly solutions.

(a) Geotextile **(b) Geogrid** **(c) Geocell**

Figure 1.1 Different types of geosynthetics

Geogrid is a planar reinforcement which could be used in the shallow depth soil improvement. It is designed as a 2D array of apertures between longitudinal and transverse elements. This geogrid increases the interaction between soil and geogrid. Geogrid reinforced soil foundation performs better than geotextile. Geogrids are made of polypropylene, polyester and polyethylene. Geogrid was developed in 1950 by Nelton.Ltd in the United Kingdom. Uniaxial, biaxial and triaxial geogrids are the three types of geogrids. Uniaxial geogrids are formed by the stretching of ribs in the longitudinal direction. So, in this case, the material possesses high tensile strength in the longitudinal direction than on the transverse direction. Uniaxial geogrid could be used as reinforcement in retaining walls, bridge abutments, slope sand slip repairs. Biaxial geogrids were manufactured by stretching the punched sheet of polypropylene in two orthogonal directions. This process resulted in a product with high tensile strength and modulus in two perpendicular directions. The resulting grid apertures were either square or rectangular. Biaxial geogrid could be used as reinforcement in

retaining walls, segmental block walls, foundations, paved and unpaved roads .Now, geogrids with triangular apertures have been developed for construction purpose. The triaxial geogrid is based on one of the most efficient, stable structural forms-the triangle. Where biaxial geogrids have inbuilt strength in two directions, with the triaxial it is multi-directional, providing greater stability and increasing bearing capacity. Triaxial could be used as reinforcement in highways, airport and heavy duty pavements and foundations.

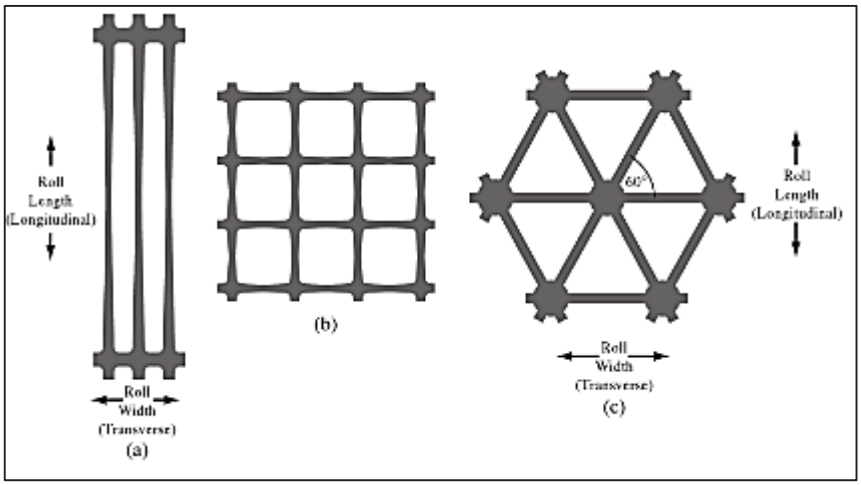

Figure 1.2 Geogrid (a) uniaxial; (b) biaxial; (c) with triangular apertures (Das, 2015)

Geocell is a three dimensional polymeric honeycomb like cellular material which could provide better lateral confinement to infill soils. Geocell was developed and introduced by US Army corps of Engineer in 1970, and it was used in military fields to improve the cohesionless soil. Nowadays geocell is made from High Density Poly Ethylene. Reinforced geocell soil has significantly high stiffness. With reinforcement improvement of stability and capacity and reduction of settlements and lateral deformation can be observed. These could be particularly, honeycomb three-dimensional cell structures which can provide containment of compacted fill soils. With their increased applications, research on their effect on soil stability is also needed. These geocells could be used in various types of geo-civil engineering projects like footing foundation and embankment foundation construction, slope erosion control and earth retaining wall construction.

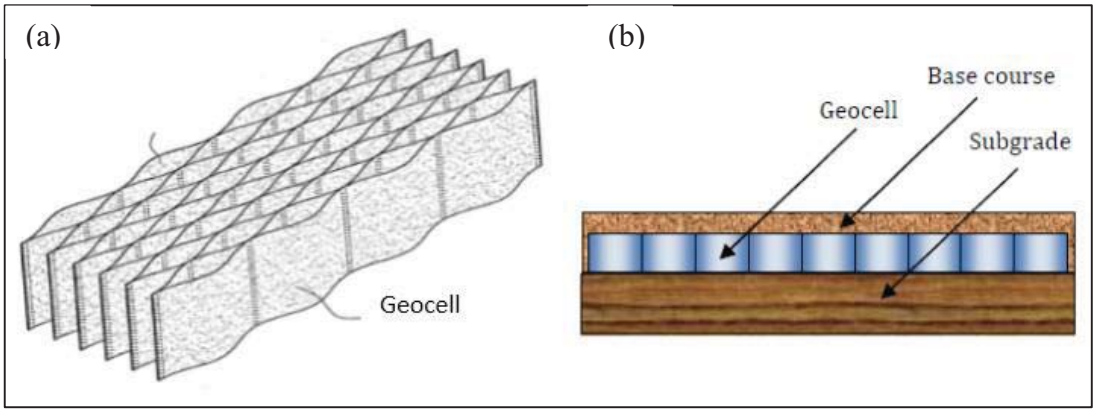

Figure 1.3 Geocell (a) honey comb shape geocell; (b) application of geocell in pavement (Yang, 2010)

1.2 Research Problem

Despite the successful application of geogrid and geocell in civil engineering projects, the bearing capacity improvement of shallow foundation on geogrid and geocell reinforcements have not been well understood, especially for static load applications. In the past, most of the research studies on the load-supporting geosynthetic reinforcement focused on planar geosynthetic products such as geogrid and geotextile. Only a limited number of studies aimed to develop the design methods for the geocell reinforcement and combination of geogrid and geocell.

Particularly, geocells with honeycomb three-dimensional cell structures can provide containment of compacted fill soils. With their increased applications, research on their effect on soil stability is also needed. Several experimental investigations can be found aimed at analyzing the bearing capacity of shallow foundations on geocell reinforced found adopting several methods. However most of these studies were conducted by employing field observations alone without much connection with numerical modeling. In designing complex structures as that involved in geocells, the numerical modeling would be helpful in better understanding of the behaviour. In addition, It is not always possible to depend on field studies for design calculations which are often time consuming and costly. Yet, only a few numerical analyses have focused to determine the bearing capacity of geocell-reinforced soil.

In numerical analysis, generally, equivalent composite approach (ECA) is used by most of researchers to model geocell in 2D and 3D modelling packages (Latha, 2000; Rajagopal et al., 2001; Latha and Rajagopal, 2007; Latha et al., 2008). ECA is a relatively simple and time saving method. However it has considerable limitations. For instance, ECA does not consider the shape and size of the geocell, but consider the material properties. Particularly the shape of the geocell has strong influence in the stress distribution patterns. Most geocells such as the ones that consist of honeycomb structure cannot be modeled as square boxes because of their curvature. When they are modeled as a square a box, which is rather easier, the stresses are likely to accumulate on the corner edges of the square box. However, in reality the honeycomb structures distribute the stresses uniformly along the periphery of the geocells, and it is a special positive attribute of most of the commercial geocells available nowadays. Such misrepresentations in erroneous models for honeycomb structures easily lead to inaccurate results.

Geogrid is a well-researched geosynthetic type but there is not clear explanation about how number of geogrid influence in the bearing capacity. Yet, some numerical analyses which are not familiar to geotechnical engineering have been carried out to determine the bearing capacity of geocell-reinforced soil. Most of the design are based on numerical and experimental studies even though there are some simplified calculation methods. So it is important to validate those theoretical approach and explain to civil industry which will lead to feasible design. Geogrid and geocell combination might produce high bearing capacity than themselves alone. Therefore, these combination should be analysed well using experimental and numerical methods.

Taking these factors in to account broadly, the need to investigate those gapes in geocell and geogrid was identified. Further it is apparent that in order to facilitate the

development of design methods for geocell and geosynthetic reinforcement for supporting the shallow foundation, the behavior of geosynthetic-reinforced soil under static loading conditions must be studied.

1.3 Objectives

The main objective of this study is to investigate the effect of geosynthetic type, spacing and cover thickness/placing depth on the bearing capacity of shallow foundation using experimental and numerical studies. In this research, Numerical analysis was used as major investigation tool to analyse bearing capacity improvement of shallow foundation. Furthermore geocell will be modelled as actual honey comb shape and the results will be validated using experimental results.

The findings of study will help to propose a set of guidelines on the selection of geosynthetic type spacing and cover thickness on the bearing capacity of shallow foundation. In addition, sustainable contribution of geocell and cost effective construction method were also studied with limited scope and factors.

1.4 Limitations

In order to make sure that enough focus on the topic can be reached, the following limitations were taken into account:

- In this study, timber footing model was considered instead of concrete footing.(timber thickness was selected based on flexure strength)
- Only three-dimensional models were taken into account because the behaviour of soil is typical a three-dimensional phenomenon, especially related to laterally loaded footings.
- In model test, actual size of geocell and geogrid were used as it satisfied the expected requirements.
- In laboratory model test, water level was not considered due to limited facilities to control the water level.
- In numerical approach, uniform settlements could be expected as long as the foundation material properties are homogeneous and rate of application of footing pressure is constant. However in experiments this is not the case as in reality it is nearly impossible to ensure such homogeneous soil properties.
- The bearing capacity of footing was determined by calculation methods described in BS 8004 which had not been calibrated to environmental condition.
- In this thesis, dynamic loads were not taken into account.

1.5 Research approach

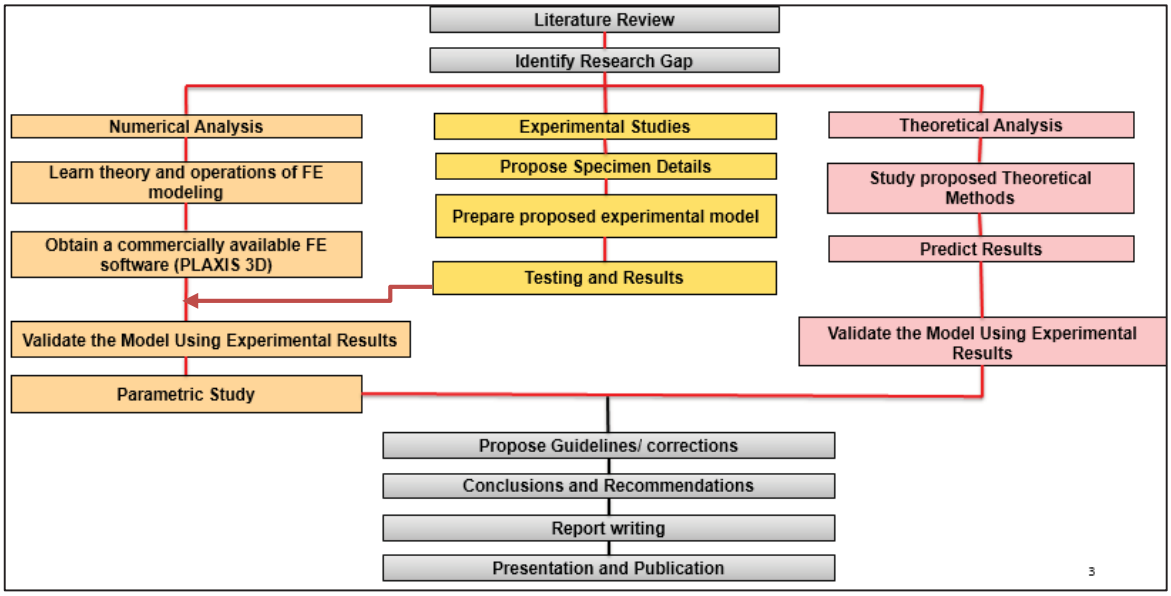

In this study, experimental, numerical and theoretical approach were used to investigate the bearing capacity of shallow foundation on the geosynthetic reinforced soil.

Initially **experimental studies** were done using geocell, geogrid and combination of both geocell and geogrid cases.

Geocell: initially single layer geocells were examined with different cover thickness (geocell placing depth). According to the experiment, optimum cover thickness for sand was estimated. Further investigations were made using double layer geocell for suitable spacing. An optimum spacing to achieve maximum bearing capacity with optimum cover thickness was estimated.

Geogrid: Laboratory model tests were performed to find the correlation between number of geogrid and bearing capacity, using optimum cover thickness and spacing. Number of geogrid range was 0 to 4.

Geogrid+geocell: Finally combination of geocell and geogrid was used as reinforcement. Two different cases were investigated, namely 'geocell+geogrid' combination and 'geogrid+geocell' combination.

Then **numerical models** were developed for geocell, geogrid and combination of both respectively using PLAXIS 3D. The same dimensions of test bed in the experiments were considered to model in the PLAXIS 3D.

Geocell: Geocell was modelled as actual honeycomb shape 3D cells with the help of AUTO CAD 3D. This model considers the curvature to increase the accuracy of the results. Then it was imported to PLAXIS 3D as solid structure and was modeled as a geogrid. Analysis was carried out by changing the prescribed vertical settlement.

Geogrid: Geogrid was modelled using direct option available in PLAXIS 3D and geogrid properties, which were given in specifications.

Geogrid+geocell: Combination of geocell and geogrid was modelled using both the described models of geocell and geogrid.

Theoretical approach was used to validate the final results of each case. Neto‘s (2013) proposed calculation and Koerner’s (1994) method were used for validation of bearing capacity of Geocell reinforced soil. Bearing capacity improvement of Geocell and Geogrid reinforced soil were validated using (FHWA/LA.08/424) (Chen, 2007; Radhey Sharma et al., 2008) technical report.

At last, a set of guidelines were proposed on the selection of geosynthetic type, spacing, and depth on the bearing capacity of shallow foundations. They are considered as useful in construction of building and pavements on the weak soils to significantly improve the bearing capacity of shallow foundation.

1.6 Dissertation Outline

The dissertation is comprised of seven chapters.

Chapter 1 explains research background and research problem.

Chapter 2 presents an extensive literature review of experimental and numerical studies of reinforced soil foundations. Focus is given to experimental and numerical studies of geocell and finite element study of geogrid and results reported by other researchers in this field.

Chapter 3 presents the experimental studies and results of reinforced soil foundation (geocell, geogrid and combination of geocell and geogrid).

Chapter 4 provides verification of the research methods by comparing the results obtained through the numerical analysis with the small-scale results.

Chapter 5 provides the further verification of analytical methods by comparing the results obtained through the numerical analysis and experimental studies.

Chapter 6 discusses the cost feasibility of geocell reinforced shallow foundation.

Chapter 7 summarizes the key findings and concludes the study, along with some suggestions for future research.

2 LITERATURE REVIEW

2.1 Overview

The ground improvement technique using geosynthetic was introduced around late of 20th century which could be applied in pavement and foundation engineering**.** Geosynthetic reinforced soil is the cost effective and feasible solution to improve the bearing capacity of shallow foundation without replacing the natural soil and increasing the footing dimensions**.** The concept of reinforced soil as construction material is based on the existence of soil-reinforcement interaction due to tensile strength, frictional and the adhesion properties of the reinforcement and it was first introduced by a French Architect and an Engineer Henri Vidal in the 1960s (Vidal , 1978). Since then, this technique has been widely used in geotechnical engineering practice.

This chapter discusses the existing background of geogrid and geocell and the problems which are explored in this research. Further, geocell and geogrid are reviewed in detail by covering the experimental and numerical studies separately.

2.2 Geocell Reinforced Foundations

2.2.1 Introduction

United States Corps of Army Engineer Waterways Experiment Station conducted a chain of studies on effective soil reinforcement techniques in late 1970s (Webster and Watkins, 1977; Webster, 1979a; Webster, 1979b). Those developed techniques could help to construct the roads on weak soils in battles to move the heavy vehicles. Webster and Watkins (1977) performed detailed studies on unpaved roads. After this study, a cellular confinement system, named “grid cell”, was soon developed, which was made up of square shaped grids and filled with sand. To assist design and application, both laboratory model test (Rea and Mitchell, 1978) (Rea, and Mitchell, 1978) and full-scale road test (Webster, 1979a; Webster, 1979b) were performed investigating a variety of factors that may influence the behavior of grid cell reinforced sand. The factors evaluated in those studies included grid size, grid shape, grid material, thickness of the sand-grid layer, subgrade stiffness, type of sand, compaction, load type and etc. Those test data were later summarized and analyzed by Mitchell et al. (1979), who then proposed some useful analytical formulas to predict the capacity of the grid cell reinforced sand base course against different failure modes.

The grid cell used in Webster’s (1979b) test study was made of paper and aluminum. Both materials have some drawbacks since paper has a poor resistance to water and aluminum is relatively expensive. Webster (1979b) further suggested that plastic might be a good material worth investigation. In 1980s, polymeric cellular confinement product was developed, and the general term “geocell” was first used to refer to this kind of products. Meanwhile, the benefit of using geocell reinforcement was widely demonstrated and studied in the U.S. as well as in Europe and Asia. Today, geocell has been successfully used in various types of civil engineering projects as a quick and effective technique of soil reinforcement.

2.2.2 Experimental Studies on Geocell Reinforced Soil Foundation

The behavior of geocell-reinforced soil supporting static load has been studied mostly through laboratory model tests. The purposes of running these tests were to demonstrate the benefit of using geocell by comparing reinforced cases with the unreinforced cases and to investigate the effect of different parameters. Some of the previous experimental studies are discussed below.

Dash et al (2001) conducted a laboratory model test to explore the reinforcing efficiency of the geocell mattress within sand bed under strip footing. More than 60 laboratory model tests were performed by varying the pattern of geocell formation, aspect ratio, pocket size and cover thickness. Tensile stiffness of the geogrids were used to fabricate geocell mattress and the relative density of the sand. The model tests were conducted in a steel tank with inside dimensions of 1200mm (length) × 332mm (width) × 700m (height). A rigid steel plate with dimensions 330mm (length) x 100mm (width) x 25mm (thickness) was used for model footing. This study was carried out using dry sand of effective particle size (D_{10}) of 0.22 mm, a uniformity coefficient (C_u) of 2.318, and a coefficient of curvature (C_c) of 1.03. Geocells was formed using polymer biaxial geogrids and non-oriented polymers NP-1 and NP-2 grids.

His model test results showed that settlement–bearing pressure relationship was linear up to settlements equal to about 50% of the footing width. Geocell should be placed at the depth of 0.1B in order to obtain optimum bearing capacity. Significant improvement could be obtained using geocell mattress if width was equal to footing width. Geocell matters will improve the bearing capacity and reduce the surface heaving. The optimum bearing capacity ratio (BCR) which is defined as the ratio of the bearing capacity of the reinforced soil foundation to that of unreinforced soil foundation was 8 when optimum cover thickness was used. The optimum width of geocell layer was 4 time of footing width. The optimum aspect ratio of geocell was 1.67 (Dash et al 2001).

This study further concluded that performance improvement is significant up to a geocell height equal to 2 times the width of the footing. Beyond that height, the improvement is only marginal. Chevron pattern for the formation of geocells is more beneficial than the geocells in diamond pattern. Better improvement in the performance of footing can be obtained by filling the geocells with denser soils because of dilation induced load transfer from soil to geocell.

Tafreshi and Dawson (2009) conducted a series of different pilot scale tests to develop a better understanding of the geocell reinforcement concept. The tests were conducted in a 150 mm wide, 750 mm long, and 375 mm deep steel box. A steel rigid plate with dimensions of 148mm long, 75 mm wide, and 20 mm thick was used as model footing. The foundation soil consisted of sand (SP) having specific gravity 2.68. Optimum cover thickness (U-depth to first reinforcement layer /B-width of footing) ratio and effect of (H [depth of the soil]/B-[width of footing]) ratios for optimum (U/B) were investigated using model test.

The model test results showed that bearing capacity improvement was more significant when the cover thickness was selected as (U/B) =0.1. At the meantime, the optimum reinforcement width was 4.2B. The maximum bearing capacity improvements were greater than 200% at U/B=0.1.The maximum BCR of 1.36 was achieved at U/B = 0.175 in their study. With the use of geocell reinforcement, the settlement could be reduced up to 75%.This study concluded that a significant improvement in bearing capacity and shallow foundation settlement could be achieved using a lesser quantity of geocell compared to geogrid.

Latha and Somwanshi (2009) studied to compare the relative performance of different form of reinforcement like geocell, planar layer and randomly distributed mesh elements in improving the bearing capacity and settlements. Experimental model test and numerical analysis were used to investigate the objects of research. The model tests were conducted in a steel tank with inside dimensions of 900mm (length) × 900mm (width) × 600m (height). A rigid steel plate with dimensions 150mm x 150mm x 25mm was used for model footing. This study was carried out using dry sand (poorly graded sand) of effective particle size (D_{10}) of 0.27 mm, a uniformity coefficient (C_u) of 3.04, and a coefficient of curvature (C_c) of 1.13.

Their test results showed that the footing on geocell reinforced soil could carry a load that was five times larger than the unreinforced soil's bearing capacity. They mentioned three factors to govern the bearing capacity of geocell reinforced soil, namely, cellular structure mattress, geocell reinforcement system and shear and bending rigidity of geocell.

Sitharam et al (2005) explored the performance of circular footing on the geocell reinforced soft clay soil using experimental study of model footings. . The model tests were conducted in a steel tank with dimensions of 900mm (length) × 900mm (width) × 600m (height). A rigid circular steel plate with diameter 150mm and 30mm thickness was used as model footing. The foundation soil consisted of clay (CL) having 100% passing the 0.075 mm opening sieve with a specific gravity of 2.66, and liquid and plastic limits equal to 40 and 17, respectively. The maximum dry density of the soil was 1895 kg/m^3 with an optimum moisture content of 26.5% as determined by the Standard Proctor test. Geocells was formed using biaxial geogrids. Ultimate tensile strength, initial modulus and secant modulus of geogrid material are 20kN/m, 183kN/m and 160kN/m at 5% strain respectively.

The results showed that the geocell should be placed just below the footing to obtain maximum improvement in bearing capacity of footing. The optimum BCR was 4.8 when optimum cover thickness was used. The optimum width of geocell layer was 4.9 time of the diameter of footing. The optimum aspect ratio of geocell was 1.8. Further, they mentioned that a provision of additional geogrid layer at the base of geocell matters would improve the bearing capacity and reduce the surface heaving.

Hedge and Sitharam (2013) studied the behavior of the foundations on commercially available geocell using model plate test and numerical studies. The tests were conducted in a 900 mm wide, 900 mm long, and 600 mm deep steel box. A square steel rigid plate with dimensions of 150mm long and 20 mm thickness was used as

model footing. The foundation soil consisted of sand (SP) having specific gravity 2.64. In another set, the foundation soil consisted of silt clay with specific gravity 2.66, liquid limit 40% and plastic limit 19%. Geocells and geogrids were used in this studies. Material properties of geocell are polyethylene, cell seam strength 2150N, density 0.95g/cm3 and short term yield strength 21.5kN/m. The experimental set up was simulated using FLAC 2D computer package and soil and geocell was modelled using Mohr-Coulomb model.

The model test results showed that bearing capacity improvement was more significant in clay (BCR=3.8) over sand (BCR=2.4). Provision of basal geogrid increased the bearing capacity of clay (BCR=6.2) over sand (BCR=3.2). This additional geogrid will reduce the surface heaving and prevents the footing from rotation failure.

Numerical results were in good matching with the model test results. However, numerical model overestimated the pressure by 15-20% at higher displacements. They pointed out the few short comings in 1-g model tests. However, Butterfield (1999) suggested that carful considerations of scaling law could be extrapolated to full scale model.

Dash et al (2007) carried out a series of model tests to explore the behavior of geocell reinforced sand under strip loading. The model tests were conducted in a steel tank with inside dimensions of 1200mm (length) × 332mm (width) × 700m (height). A rigid steel plate with dimensions 330mm x 100mm x 25mm was used for model footing. This study was carried out using dry sand of effective particle size (D_{10}) of 0.22 mm, a uniformity coefficient (C_u) of 2.318, and a coefficient of curvature (C_c) of 1.03. Geocells was formed using polymer biaxial geogrids. Ultimate tensile strength and secant modulus of geogrid material are 20kN/m and 160kN/m at 5% strain respectively.

From test results, they mentioned that the strain of geocell wall was the largest at the center and much smaller in the extended portions outside the footing width. The patterns of strain variation in the geocell wall indicated that the geocell mattress behave as a subgrade supported composite beam under the footing loading and for larger depth of the mattress, the deep beam, the effect became predominant. The optimum width of geocell layer was 4.0 time of width of footing. The dispersion angle represented the quasirigid nature of geocell, which was governed by cover thickness, geocell height, width and pocket size.

Thallak (2007) carried out laboratory model tests to explore the behaviour of geocell-reinforced soft clay foundations under circular loading. The tests were conducted in a 900 mm long, 900 mm wide, and 600 mm deep box in which the base was cemented. A steel rigid circular plate with diameter of 150mm was used as model footing. The foundation soil consisted of clay (CL) having 100% passing the 0.075 mm opening sieve with a specific gravity of 2.66, and liquid and plastic limits equal to 40 and 17, respectively. The maximum dry density of the soil was 1895 kg/m^3 with an optimum moisture content of 26.5% as determined by the Standard Proctor test. Geocells was formed using polymer biaxial geogrids. Ultimate tensile strength and secant modulus

of geogrid material are 20kN/m and 160kN/m at 5% strain respectively. In this studies, series of tests carried out by varying cover thickness, width of geocell mattress, height of geocell and influenced by an additional base geogrid layer.

The model test results showed that bearing capacity improvement was more significant when geocell should be placed just below the footing (U/D) =0. At the meantime optimum reinforcement width was 4.9D. The maximum bearing capacity was 4.85 times of the unreinforced bearing capacity under the optimum cover thickness (U-depth to first reinforcement layer /D-diameter of footing) =0 and aspect ratio (h-height of geocell/d-pocket size of geocell) =2.4. With the use of geocell reinforcement, the settlement could be reduced up to 92%. That additional geogrid reduced the settlement and improved the bearing capacity of footing. That study concluded that a significant improvement in bearing capacity and shallow foundation settlement could be achieved using a lesser quantity of geocell compared to geogrid.

2.2.2.1 Summary of Literature Findings

Many researchers in the past have demonstrated the beneficial aspects of geocells with the help of experimental and field studies (Yang et al., 2010; Tafreshi and Dawson, 2010; Pokharel et al., 2010; Lambert et al., 2011; Thakur et al., 2012; Tafreshi and Dawson, 2012; Tafreshi et al., 2013; Sitharam and Hegde, 2013; Hegde and Sitharam, 2014).

The influence of the placing depth of geocell was studied by Dash et al., 2001; Moghaddas & Dawson, 2009; Tafreshi et al., 2013.Further, optimum width of geocell was proposed by Adams and Collin,1997; Dash et al., 2001; Sitharam and Sireesh ,2005; Thallak et al., 2007. Bearing capacity improvement factor was between 3 and 7.5, when optimum depth and with was used in experimental studies. Yang et al. (2010), Hegde and Sitharam (2014a) carried out the experimental studies using honeycomb shape geocells. Improvement of bearing capacity vary with different shape of geocell and with other geometries The critical findings above studies , along with several others can be summarized and compared as in Table 2.1. The findings from that study used for designing and constructing, foundation for liquid storage tanks founded on soft soils, low cost unpaved roads over soft soils, large stabilized areas for parking of vehicles, platforms for oil drilling etc.

Table 2.1 Experimental studies reviewed on geocell-reinforced soil supporting static load

Reference	Footing	Infill soil	Under laying soil	Geocell	Remarks
Mandal and Gupta ,1994	Strip footing 205mmX73mm	Soft marine clay	Soft marine clay	Bonded non-woven geotextile	• The geocell layer exhibited a beam action up to a settlement ratio of 5-10%. After a settlement ratio of 20%, the geocell layer exhibited a membrane action. • BC Improvement factor= 7.5 • Settlement Improvement factor=6
Adams and Collin ,1997	Square (30,46,61,91)mm	Poorly graded soil	Poorly graded soil	Polyethylene	• Optimum width of geocell layer=4B/4D • BCR=3.5
Dash et al., 2001	Circular 150mm	Poorly graded sand	Low plastic silty clay	Bounded geogrid-square	• Optimum width of geocell layer=4B/4D • U/B=0.1 for max BCR
Dash et al., 2004	Strip footing 330mmX100mm	Poorly graded sand	Poorly graded sand	Bounded geogrid-triangular	• Optimum width of geocell layer=4B/4D • U/B=0.1 for max BCR
Wesseloo, 2004	Instrumented compression tests	Savuka Mine's backfilling plant soil	Savuka Mine's backfilling plant soil	Hyson Cell geocells-HDPE	• Analytical calculation procedure for the stress-strain behaviour of the fill confined with a single geocell was developed
Sitharam and Sireesh ,2005	Circular 150mm	Poorly graded sand	Low plastic clay	Geogrid cell	• Optimum width of geocell layer=5D

					• Improvement factor= 5.5-9.5(ultimate) • U/B=0.05 for max BCR • Performance increased with aspect ratio
Thallak et al., 2007	Circular 150mm	Low plastic silty clay	Low plastic silty clay	Bounded geogrid-triangular	• BCR = 4.85 (b/D = 4.9, and h/D = 2.4) • Maximum reduction in footing settlement (PRS)= 92% • Further improvement in performance was obtained with provision of an additional layer of Geogrid at the base of the geocell mattress.
Latha and Somwanshi, 2009	Square 150mm	Poorly graded sand	Poorly graded sand	Geocell and planar geogrid	• Aspect ratio=0.1 • Improvement factor=2.2 • Optimum width of geocell layer=4B
Sanat et al., 2009	Circular 150mm	sand	sand	HDPE,NPA	• Circular shape geocell more effective(elliptical) • Improvement factor=1.5-2.5
Madhavi et al ., 2009	Square 150mm	sand	sand	Geogid, geonet	• Improvement factor=5
Moghaddas and Dawson, 2009	Strip footing	Poorly graded sand	Low plastic silty clay	Planar geotextile thermo welded	• U/B=0.1 for max BCR • BCR =1.6-2.2 • PRS=63% • BCR=1 when U/B=1

Pokharel et al., 2009	Circurlar 150mm	Poorly graded sand	Poorly graded sand	Bounded geogrid-triangular	• BC improvement factors = 1.75 • Deformation improvement factor = 1.5
Yang et al., 2010	Circular 150mm	Poorly graded sand-Kansas	Poorly graded sand-Kansas	Polymer cell	• Improvement factor= 1.5 • Maximum tensile strain=0.56%
Hedge and Sitharam., 2013	Square footing-150mm	-Poorly graded sand -Clay-CI	-Poorly graded sand -Clay-CI	Honeycomb 3D structure	• BC improvement factor ✓ Sand bed=2.4 ✓ Clay bed=3.8 • Provision of basal geogrid increased the BC
Biswas et al., 2013	Circular 150mm	Dry river sand	Clay with low plasticity (CL)	biaxial geogrid-cells	• Sand layer with geocell reinforcement, maximum bearing capacity improvement was obtained for - soft subgrade -11.57 - stiff subgrade-3 • Thickness of the cushion layer giving maximum performance improvement was about 1.67D
Tafreshi et al ., 2013	Circular 300mm	well graded sand	Poorly graded sand	polypropylene -honeycomb shape	• Optimum embedded depth was approximately 0.2 times the footing diameter. • Combination of geocell and rubber–soil mixture layers was more effective than use of only geocell layers

2.2.3 Finite Element Studies on Geocell Reinforced Soil Foundations

Reinforced soil consists of two constituents, namely, the soil and the reinforcement. Finite element modeling of reinforced soil foundation could be carried out in two different ways which were presented by researchers.

In first approach, reinforced soil was modelled as equivalent composite material (Latha, 2000). In this category of method, the reinforced soil was treated as a macroscopically homogeneous composite material, the properties of which depend on properties of the geocell. This method is named as equivalent composite approach (ECA). ECA is a relatively simple and time saving method. However it has considerable limitations. For instance, ECA does not consider the shape and size of the geocell, only the material properties.

Latha (2000) proposed an equivalent composite model for geocell encased sand based on triaxial tests on sand encased in single and multiple geocells made of different geosynthetics. These triaxial tests are described in detail by Rajagopal et al. (1999). Later Rajagopal et al. (2001), Latha and Rajagopal (2007) and Latha et al. (2008) validated this model using experimental results from model tests on geocell supported embankments and strip footings on geocell-reinforced sand beds. A brief description of the model is presented below.

The ECA could be used to investigate the geocell in 2D or 3D frame. Using this method, Geocell reinforcement with filled soil could be modeled as a composite soil layer with improved strength parameters. Bathurst and Karpurapu (Bathrust, R.J. and Karpurapu, R, 1993) have proposed the approximate solution, (2.1) for estimating apparent cohesion C_r without performing large-scale triaxial tests on the geocell-soil.

$$C_r = \frac{\Delta\sigma_3}{2}\tan\left(\frac{\pi}{4}+\frac{\varphi}{2}\right) \quad \text{---------- (2.1)}$$

In (2.1), φ is the friction angle of the in-fill soil. The increased confining pressure $\Delta\sigma_3$ due to the membrane effect of the geocell can be estimated using (2) derived by (Henkal,D.J and Gilbert,G.D, 1952). 'd' and 'ε_a' notate the equivalent diameter of geocell pocket and tensile stress-strain response.

$$\Delta\sigma_3 = \frac{2M}{d}\left(\frac{1-\sqrt{1-\varepsilon_a}}{1-\varepsilon_a}\right) \text{---------- (2.2)}$$

The increased stiffness of geocell-reinforced soil was studied by (Latha,G.M, 2000), who proposed an empirical equation to estimate the modulus number of the geocell-soil composite from the modulus value of soil.

$$K_r = K_e + 200M^{0.16} \quad \text{---------- (2.3)}$$

The equivalent initial tangent modulus (Ei) of the geocell layer is calculated using the equation suggested by Janbu (Janbu.N, 1963).

$$E_i = K_r P_a \left(\frac{\sigma_3}{P_a}\right)^n$$ ---------- (2.4)

where,

M - Secant modulus of the geocell material (kN/m)

K_e -Young's modulus parameter of the unreinforced sand (dimensionless)

K_r -Young's modulus parameter of the geocell-reinforced sand (dimensionless)

P_a - Atmospheric pressure (kPa)

n - Modulus exponent of the unreinforced soil

The second group models the reinforcement and soil as two separate components (Han et al., 2008; Yang, 2010; Hedge, 2014). The reinforcement is generally treated as a linear elastic material in these studies. The soil model used by different researchers includes Duncan-Chang model (Evan, 1994; Latha, 2009), Drucker-Prager model (Mhaiskar and Mandal, 1996) and Mohr-Coulomb model (Han et al, 2008).

Han et al (2008) modeled first three-dimensional numerical model by considering soil and geocell separately. Detailed laboratory model test was carried out for reinforced and unreinforced condition. Three-dimensional polymeric honeycomb geocells was used in this study. Numerical studies was carried out by FLAC3D, Mohr-Coulomb model and linearly elastic membrane model were used to model sand and geocell respectively. Geocell was modelled as square box instead of honeycomb shape due to difficulties in modelling the actual shape. It was found that benefit of geocell on the bearing capacity shown in the test cannot be simulated using this model because Mohr-Coulomb model ignored the stress-dependency of soil. In order to match the test result, modulus of the soil inside the geocell has to be increased about 1.9 times.

Latha and Somwanshi (2009) used finite element analysis to complement the findings of the laboratory study and to understand the effect of form of reinforcement further in the light of stress and strain distributions underneath the footing. Model tests on planar reinforced and geocell-reinforced square footings in the tank are simulated in. numerical models using FLAC3D .The geocell encased sand bed is modeled as an equivalent composite model with enhanced strength and stiffness properties. The elastic–perfectly plastic Mohr–Coulomb model, available in FLAC3D, was used for modeling the behavior of soil.

Yang (2010) performed numerical simulations on circular footings resting on sand. The model Duncan-Chang model was used to model the behavior of sand. Reinforcement was modeled as Elastic plate model. The geocell pockets were modeled in a diamond shape by taking a photo after expansion of geocell in experimental studies, which is more appropriate than a sine curve for a multi-cell situation.

For the particular case modeled in the parametric study, the bearing capacity of the road was greatly improved (by about 43%) with the inclusion of geocell. The stiffness of the soil was also increased, but the benefit started to exhibit after about 5mm displacement was developed on the top surface. This result is consistent with the static load test data obtained from the geocell-reinforced sand.

Hedge et al. (2014, 2015) performed finite element analyses (FEA) on Square footing using the commercial FLAC2D and FLAC3D program. The soil is simulated as an elastic-perfectly Mohr-Coulomb model. The geocell was modelled using the geogrid structural element. Linear elastic model was used to simulate the behaviour of the geocell. The interfaces between the geocell and the soil were linearly modelled with Mohr Coulomb yield criterion. Analyses were carried out under controlled velocity loading of 2.5 x E-5 m/step. Only quarter portion of the test bed was modelled using symmetry to reduce the computational effort. Once the given model was validated with a single cell, the model was extended to multiple cell geocells. The digitizing technique was used to obtain the actual curvature of the geocells. In addition to geocells, the combination of geocell and geogrid case and only geogrid case were also modelled. The numerical results were compared with the results of the experimental studies.

The model was validated with the experimental studies and found that the results are in good agreement with each other. The results suggested that the geocells distribute the load to a shallower depth as compared to the unreinforced bed and the geogrid reinforced beds. Instead, the load will be distributed in the lateral direction to the wider areas and hence by reducing the vertical stress on the subgrade. It was also found that geocell with textured surface yields better performance than the geocell with smooth surface. The provision of the additional geogrid below the geocell further improves the performance reinforced soil beds by virtue of the membrane mechanism.

Ghareh (2015) carried out the numerical modeling of the laboratory samples using ABAQUS 6.11. This software was used in this analysis because it has the capability of solving problems ranging from a simple linear analysis to the most complex non-linear modeling. Clay was modeled as the CAM CLAY model and Sand's behavior was simulated using the DRUCKER PRAGER model. Effects of changing the shape of the footing from circular to square was investigated using validated numerical model.

By comparing the effective factors on footing's loadbearing capacity such as the width (b) and height (h) of the geocell element, it can be seen that if geocell elements are used to reinforce the soil, the footing's load-bearing capacity increases approximately 165% compared to the non-reinforced sample while the footing's settlement percentage increases by only 15% approximately. The results showed that increasing the geocell width (b) results in an increase in the footing's load-bearing capacity. Also as the geocell height (h) increases, stability and therefore the bending and shear stress of the geocell element increases. This increases the footing's load-bearing capacity and decreases its settlement.

2.2.3.1 Summary of Literature Findings

These findings suggest that numerical modeling of the geocells are not so easy due to its complex 3D honeycomb structure. Generally, the equivalent composite approach is used to model the geocells (Bathrust and Knight, 1998; Latha and Somwanshi, 2009; Hegde and Sitharam, 2013). But this approach is very simple, it is unrealistic to model geocells as the soil layer.

Geocell reinforcement is 3-dimensional in nature and hence, 3-dimensional modelling approach should be preferred. Han et al. (2008) modelled single cell geocell using FLAC3D. Due to the difficulties in modelling the actual shape, the cell was modelled as the square box in their study. Similarly, Hegde and Sitharam (2014a) carried out the numerical simulation of the single cell geocell by adopting the circular shaped pocket geometry. Saride et al. (2009) modelled the multiple cell geocell in FLAC3D by assigning the square shape to the geometry of the cell pocket. However, Yang et al. (2010) modelled the actual shape of the single cell geocell in their study. Recently Hedge et al (2013, 2014, 2015) carried out more advanced analyse using FLAC3D. Ghareh (2015) and Biabani et al. (2016) also successfully modeled the geocell in ABAQUS. Those discussed numerical studies summarized in detailed in Table 2.2 .

Table 2.2 Numerical modeling studies reviewed on geocell reinforced soil supporting static load

Reference	Model	Program	Soil	Geocell Model	Remarks
Mhaiskar and Mandal ,1996	Square Footing	ANSYS-3D	Clay Sand	Composite material-Druker –Pragel Model	• Same result as experimental • BC Improvement Factor =5
Hen et al ,2008	Rectangular footing	FLAC3D	sand	• Mohr-Coulomb model • Linearly elastic membrane	• maximum displacement and the maximum tension within the geocell existed close to the bottom of the cell • Applied load increased by approximately 65%
Madhavi Latha et al, 2009	Strip footing	GEOFEM-2D	sand	Composite material-Hyperbolic model (Duncan & Chang)	• BCR difference due to apparent cohesion • BC Improvement Factor =2.5 • Full scale structure required for validation
Madhavi Latha and somwanshi ,2009	Square footing	FLAC3D	sand	Composite material Hyperbolic model (Duncan & Chang)	• Model was validated with experimental results • Improves the BC by transferring the footing load to deeper soil layers
Yang et al, 2010	Circular footing	FLAC3D	sand-Kansas	• Geocell- Mohr-Coulomb	By modelling geocell and the soil separately. Following features can be simulated.

				• Infill soil-(Duncan & Chang)	• The effect of geocell on the increase in the strength of the reinforced composite • The confining effect of geocell on the infill soils
Hegde and Sitharam ,2013	Square footing	FLAC2D	Poorly graded sand and clay	Composite-Mohr-Coulomb	• Overestimate the bearing pressure by 15-20% • Failure settlement was smaller than experimental failure settlement
Hegde and Sitharam, 2014	Square footing	FLAC2D, FLAC3D	Poorly graded sand	• Composite-Mohr-Coulomb • Honeycomb 3D structure	• Model was validated with experimental results • Textured geocell best • 3D more accuracy (2D)
Hegde and Sitharam, 2015	Square footing	FLAC3D	Sand, Silty clay	Honeycomb 3D structure-Cam-Clay model	• 50% reduction in stress • Additional geogrid under geocell for better BCR • Investigated factors affecting the performance
Soheil Ghareh, 2015	Circular footing	ABAQUS	coarse soil containing sand and gravel	Clay- Cam-Clay model Sand- Drucker Prager model	• the footing's load-bearing capacity increased approximately 165% • geocell element's height (h) increased the stability

2.3 Geogrid Reinforced Foundations

2.3.1 Introduction

The concept of reinforced soil as construction material is based on the existence of soil-reinforcement interaction due to tensile strength, frictional and the adhesion properties of the reinforcement and was first introduced by the French architect and engineer Henri Vidal in the 1960s (Vidal , 1978). Since then, this technique has been widely used in geotechnical engineering practice.

The reinforcing materials that have been developed over the years range from stiff to flexible geosynthetic materials and can be classified as either extensible or inextensible reinforcements (McGown et al., 1978). Recently, geosynthetics have been used extensively as reinforcements for improving the load-settlement characteristics of soft foundation soils. Their use has been proven to cost-effectively improve the bearing capacity and settlement performance of earth structure (Basudhar et al., 2007; Ghazavi and Lavasan, 2008). The most common types of geosynthetics include Geogrids, Geotextiles, Geomembranes, Geosynthetic Clay Liners, Geonets, and Geopipes (Koerner, 1997), whereby Geogrids are one of the most commonly used forms of reinforcement, which, as they offer superior interface shear resistance due to interlocking.

In the present study, geogrid reinforced foundations will be examined. Extant studies have shown that geogrid reinforced foundations can increase the ultimate bearing capacity and reduce the settlement of shallow footings, compared to the conventional methods, such as replacing strong soils or increasing footing dimensions

2.3.2 Experimental Studies on Geogrid Reinforced Soil Foundation

Bearing capacity of reinforced soils has been studied experimentally by many researches (e.g. Guido et al., 1986; Das et al., 1994; Adams and Collin, 1997; Dash et al., 2001; Latha and Somwanshi ,2009 ;Tafreshi and Dawson, 2010; Kolay et al. 2013;Abu-Farsakh et al., 2013). These studies demonstrated the overall effects of using geosynthetic material in increasing the bearing capacity of shallow foundations. The roles of different parameters such as reinforcement length, spacing between reinforcing layers, depth to the upper geosynthetic layer, number of layers, and types of geosynthetics that contribute to the bearing capacity were also investigated in these studies. Here some recent studies are discussed.

Latha and Somwanshi (2009) performed experimental studies on square footings resting on sand. Experimental model test and numerical analysis were used to investigate the objects of research. The model tests were conducted in a steel tank with inside dimensions of 900mm (length) × 900mm (width) × 600m (height). A rigid steel plate with dimensions 150mm x 150mm x 25mm was used for model footing. This study was carried out using dry sand of effective particle size (D_{10}) of 0.27 mm, a uniformity coefficient (C_u) of 3.04, and a coefficient of curvature (C_c) of 1.13. Biaxial geogrid (WG) was used in the studies.

The test results showed that the footing on geogrid reinforced soil could carry a load which was two times larger than the unreinforced soil's bearing capacity. Studies indicated that the bearing capacity improvement factor is significantly affected by the form of reinforcement.

Biswas et al. (2012) Present carried out experimental studies to develop an understanding of the performance of geogrid reinforced foundation systems having clay subgrades of different undrained shear strengths (C_U) of 7, 15, 30, and 60 kPa. Different series of physical model tests were conducted by varying different parameters such as the soil configuration with reinforcement systems. A typical geogrid-reinforced layered foundation system (1× 1×1 m) with a circular footing of diameter D was considered in this study. Two types of soils which were; top fill soil was sand and bottom native soil was clay were used. Planar geogrid reinforcement was placed at the sand-clay interface.

The results showed that the performances of foundation systems are largely dependent on the subgrade strength, thickness of the sand layer, and footing settlement level. Further, it was concluded that the improvement factor for bearing pressures in the layered foundation systems decreases with increase in subgrade strength. The experimental results showed that bearing pressures of layered foundation systems were increased for the geogrid reinforcement placed at the sand-clay interface. The benefits of the interface geogrid are attributed to the membrane resistance which enhanced with mobilized strain level through footing settlement. However, geogrid-induced improvements were reduced with increase in layer thickness of the unreinforced sand and stiffness of the underlying clay subgrades, due to insufficient strain mobilization for the membrane actions.

Kolay et al. (2013) investigated the bearing capacity of two layers of soil (i.e., a thin sand layer underlain by silty clay) and also of single-layer silty clay soil (for comparison purpose) with varying the number of biaxial geogrid at different layers and by keeping other properties constant.

A model footing, with the dimensions of length (L) equal to 284.48 mm, width (B) equal to 114.3 mm, and thickness (D) equal to 48.26 mm, was used in the experimental study. The footing dimensions were selected based on the model tank's dimension. The model footing was designed in such a way that its width is less than 6.5 times the depth of the model tank so that the effect of the load could not reach the bottom of tank. The bottom surface of the model footing was made rough by cementing a layer of sand with epoxy glue to increase the friction between the footing base and the top soil layer. Two types of soils were used to conduct the experimental study, that is, silty clay soil and sand. The silty clay soil and sand used are classified as CL and SP, respectively, based on the Unified Soil Classification System (USCS). Biaxial geogrid was used in the present experimental study. In study the silty clay soil was used at the bottom part of the model tank over laid by a small thickness of sand layer at the top.

A number of model tests were performed to evaluate the load-carrying capacity of a rectangular model footing. Load bearing capacity was increased by 7%, when top clay

layer was replaced by 76.2mm of sand. The bearing capacity for the two-layer soil increases with an average of 16.67% and 33.33% using one with the u/B equal to 0.667 and 0.33 respectively. Bearing capacity improvement increases with the number of geogrid.

Abu-Farsakh et.al (2013) conducted experimental studies to investigate the behavior of geosynthetic-reinforced sand foundations and to study the effect of different parameters on their improved performance. A series of laboratory model footing tests were conducted on geosynthetic reinforced sand foundation at the Geotechnical Engineering Research Laboratory (GERL) of the Louisiana Transportation Research Center (LTRC). The model tests were conducted in a 1.5m long, 0.91 m wide, and 0.91 m deep steel test box. The model footings used in the tests were 25.4 mm thick steel plates with dimensions of 152 mm × 152 mm (B×L) for square footings and 152 mm×254 mm (B×L) for rectangular footings, which were chosen, based on the dimension of box, to minimize the boundary effect. The testing procedure was performed according to the ASTM D 1196–93 (ASTM, 1993).

The model footing test results showed an optimum top layer spacing of 0.33B (B: footing width) for the embedded square model footing on geogrid reinforced sand and an influence depth of 1.25B for placing geosynthetic reinforcement regardless of the type of reinforcement and embedment depth. Further, immediate settlement was reduced by 20% at all footing pressure levels with two or more layers of geogrid. A ‘‘surcharge effect’’ was brought by the inclusion of geosynthetic reinforcement for surface footing condition. It was found that an effective geosynthetic reinforcement length is 6.0B.

2.3.2.1 Summary of Literature Findings

Recent research studies on geogrid reinforced soil only discussed here. Most of researchers carried out experimental studies to explain how to maximize the reinforcement benefits. Very detail laboratory model tests studies were conducted by Chen et al., 2007; Abu-Farsakh et al., 2013 to study the behavior of reinforced soil foundation. The Table 2.3 summaries the optimum top layer spacing (u), the optimum vertical spacing (h), the effective length of reinforcement (b) and the number of geogrids (N) which are reported by different researchers .

Table 2.3 Summary of optimum parameters for reinforced soil foundations

Reference	Footing	Soil type	Reinforced type	cover thickness –U	Spacing-X	Mattress width-b	Number of layers-N
Guido et al.,1985	Square	Sand	geotextile	0.5B	-	-	3
Ramaswamy and Purushothaman, 1992	Circular	Clayey soil	Geogrid	0.5B	-	-	-
Mandal and Sah, 1992	Square	Clayey soil	-	0.175B	-	-	-
Yetimoglu et al., 1994	Rectangular	Sand	Geogrid	0.25B-0.3B	0.2B-0.4B	4.5B	-
Das et al., 1996	Strip	Clayey soil	Geogrid	0.4B	-	-	-
Alawaji, 2000	Circular	sand	Geogrid	0.1D	-	4D	-
Maharaj ,2003	Strip	Clayey soil	Geogrid	0.125B	-	-	-
Patra et al., 2005	Strip	Sand	Geogrid	0.35B	0.25B	5B	-

Reference	Footing	Soil type	Reinforced type	cover thickness –U	Spacing-X	Mattress width-b	Number of layers-N
Basudhar et al., 2008	Strip	Sand	Geotextile	0.6B	-	-	-
Alamshahi & Hataf, 2009	Strip	Sand	Geogrid	0.75B	0.75B	-	-
Kolay et al., 2013	Rectangular	Sand	Geogrid	0.33B	0.33B	6.444B	4
Abu-Farsakha et al., 2013	Rectangular	Sand	Geogrid	0.33B	0.167B	6.0B	4

2.3.3 Finite Element Studies on Geogrid Reinforced Soil Foundations

Numerical analysis is an alternative way to study stresses and strains within a given soil-geosynthetic system. The finite element method has been proven to be effective in the analysis of reinforced foundations problems (Yetimoglu et al., 1994; Yogarajah and Yeo, 1994; EI Sawwaf, 2007; Zidan, 2012; Belal et al., 2015; Hussein and Meguid, 2016; Mosallanezhad et al., 2016). In these studies, modeling geogrid reinforcement was often simplified either using truss elements (in 2D analysis), a continuous sheet (in 3D analysis) or actual sheet 3D model. In addition, the interaction between the simplified 3D geogrid models and the surrounding soil was often captured using interface layers in which the contact properties were considered while the interlocking effect was represented in actual shape model (Hussein and Meguid, 2016; Mosallanezhad et al., 2016). It shows that soil-geogrid interlocking plays an important role in the load-carrying capacity of foundations.

El Sawwaf (2007) studied the relationships between the footing response and the variable parameters including replaced sand depth, relative density of sand, location of the footing relative to slope crest and geosynthetic configurations using PLAXIS 2-D. The non-linear behavior of sand was modeled using hardening soil model, which is an elastoplastic hyperbolic stress–strain model, formulated in the framework of friction hardening plasticity. The interaction between the geogrid and soil is modeled at both sides by means of interface elements, which allow for the specification of a reduced wall friction compared to the friction of the soil. Effect of number of geogrid layers, Effect of geogrid layer length Effect of depth to top layer, vertical spacing of the geogrid were studied and he concluded that for optimum response, the recommended depth of reinforcing geogrid and geogrid spacing are 0.6 and 0.5 of the footing width. The geogrid length should be greater than or equal to five times the footing width and the recommended number of geogrid layers is 3.

Ahmed et al. (2008) used finite element analysis to investigate the performance of embankment construction over weak subgrade soil. Two-dimensional plain strain condition was adopted and only half of the physical model is considered due to an axisymmetric at the center of the footing. The displacement is restricted to zero in x-direction along the centerline of the model due to symmetry and the right side of the model for subgrade layer only. All the dead load was defined and separate solved as a linear elastic model. They adopted modified cam-clay model for clay and non-linear elastic-plastic (i.e hyperbolic) model for sand. Linear elastic model was used to represent geosynthetics materials and slip surface model was used to model the interaction characteristics between soil and reinforcement.

They reported that geogrid performed much better than geotextile. The best performance was achieved when geosynthetic reinforcement were located nearest to the footing. The strain within geosynthetics became almost negligible after a distance equal six times of the footing width. Better stress distribution and deformation pattern within embankment were obtained when the geosynthetics were introduced.

Latha and Somwanshi (2009) performed numerical simulations on square footings resting on sand. The elastic-perfectly Mohr-Coulomb model was used to model the behavior of sand. Reinforcement was modeled. Effect of the type and tensile stiffness of geosynthetic material, the depth of reinforced zone, the spacing of reinforcement layers and the width of reinforcement were studied and they concluded that the layout and configuration of reinforcement play a vital role in bearing capacity improvement rather than the tensile strength of the geosynthetic material. They also reported that the effective depth of the zone of reinforcement below a square footing is twice the width of the footing. Within the effective reinforcement zone, the optimum spacing of reinforcing layers is about 0.4 times the width of the footing. Optimum width of reinforcement is about 4 times the width of the square footing.

Alamshahi and Hataf (2009) carried out finite element analyses to investigate strip footings on sand slopes reinforced with geogrid using PLAXIS 2D. The initial stress condition was implemented first by applying the gravity force due to soil weight in steps with the geogrid reinforcements in place. Six node triangle plane strain elements are selected for the soil and three node tensile elements are used for the footing and the geogrid. They used the non-linear Mohr–Coulomb criteria to model the sand for its simplicity, practical importance and the availability of the parameters needed. The interaction between the geogrid and soil was modeled at both sides by means of interface elements, which enabled for the specification of a decreased wall friction compared to the friction of the soil. Results showed that the load-settlement behavior and bearing capacity of the rigid footing can be considerably improved by the inclusion of a reinforcing layer. The depth to the top geogrid layer, number of geogrid layers, vertical spacing of the geogrid were all investigated and based on their particular case, the optimum embedment depth and vertical spacing of the reinforcement layer was about 0.75 times the width of the footing. The optimum number of reinforcements was 2.

Zidan (2012) investigated the aspect of enhancement of the bearing capacity and settlement reduction under a circular footing due to static and dynamic loading using PLAXIS 2-D V8.2. Static loading case only discussed here. The model geometry is simulated by means of an axisymmetric model in which the circular footing and load are positioned along the axis of symmetry. Both the soil and footing are modelled with 15-noded elements. The depth and width of model are taken 15d where d is the diameter of footing. A Hardening-soil model was used to simulate the non-linear behavior of sand. The interaction between the geogrid and soil was modeled at both sides by means of interface elements. The presence of interface element allows the relative movement takes place between reinforcement, footing and surrounding soil.

From finite element analysis of circular (diameter-D) footing on reinforced soil, it was concluded that optimum top layer spacing and spacing between geogrid layers, were found to be around 0.19D and 0.2D respectively in reinforced soil. Further, the influence of geogrid becomes practically negligible when the ratio of depth of first layer to the footing diameter is equal to 0.5 and no significant effect of spacing between

geogrid layers was observed when the ratio of depth of first layer to footing diameter greater than 0.3.

Belal et al. (2015) carried out the numerical simulations on square footing resting on geosynthetic reinforced sand. The main objective of this research study was to investigate the behavior of geogrid layers and different reinforcement parameters in improving the bearing of the system. Numerical studies were carried out on square footing rested on reinforced and unreinforced sand using ANSYS. Drucker-Prager's model was used to simulate the sand. The reinforcement was modeled using Linear Isotropic model as material model and Link8 as element type. It was noticed that there was a good agreement between numerical and experimental results. Optimum depth of geogrid layers, influence depth of reinforced zone, vertical spacing of the geogrid, geogrid width were all investigated which are 0.5B,2.0B,0.5B and 4.0B respectively .

Hussein and Meguid (2016) developed the numerical model for square footing on geogrid-reinforced sand-bed using the finite element software ABAQUS. The crushed stone backfill was modeled using elastoplastic Mohr-Coulomb failure criteria with non-associated flow rule and the soil domain was discretized using 8-node linear brick elements (C3D8). Geogrid was modeled as a constitutive model that is capable of simulating the nonlinear elastoplastic material with isotropic hardening. The load-settlement results obtained using the developed numerical model agreed reasonably well with the experiment data.

The proposed model was able to capture the 3D response of the soil-geogrid system with one or more geogrid layers installed under the footing. Increasing the number of geogrid layers resulted in an increase in the ultimate bearing capacity of the system. The geogrid deformations and tensile stresses decreased with the number of geogrid layers. Hence, the proposed FE approach has proven to be efficient in capturing the 3D responses of both unconfined and soil-confined geogrid and can be adopted by researchers for soil-geogrid interaction analysis.

2.3.3.1 Summary of Literature Findings

Several studies that employ finite and discrete element methods to analyze geogrid-reinforced structures have been reported in the literature (Yogarajah and Yeo, 1994; EI Sawwaf, 2007; Zidan, 2012; Belal et al., 2015; Hussein and Meguid, 2016; Mosallanezhad et al., 2016). Most of these studies focused on the overall response of the reinforced structure while adopting simplifying assumptions related to either the details of the geogrid geometry or the constitutive model of the geogrid material except few studies carried out. It is summarized in Table 2.4.

Table 2.4 Summary of Finite Element Material Models of Reinforced Soil Foundations

Author	**Footing type**	**Analysis type**	**Reinforcement model**	**Soil type**	**Soil model**	**Interaction Model/ Interface Element**
Yetimoglu et al. ,1994	Rectangular	Axi-symmetric	Linear elastic Shell element	Sand	Modified Duncan (1980)	Friction
Sugimoto, 2003	Strip	Plane-Strain	Nonlinear Truss Elements	Sand	Drucker- Prager	Line interface element
EI Sawwaf,2007	Strip	Plane-Strain	Beam element	Sand	friction hardening plasticity	Friction
Ahmed et al.,2008	Strip	Plane-Strain	Linear Elastic	Clay & Sand	Modified Cam and hyperbolic	Slip-surface model
Alamshahi and Hataf, 2009	Strip	Plane-Strain	Linear elastic Tensile element	Sand	non-linear Mohr Coulomb	Friction
Zidan , 2012	circular	Plane-Strain	Linear elastic Tensile element	Sand	Hardening-soil model	Friction
Belal et al.,2015	Rectangular	3D	Linear Isotropic model	Sand	Drucker- Prager	-
Hussein and Meguid ,2016	Rectangular	3D	nonlinear elastoplastic material	Sand	Mohr-Coulomb	Friction (master/slave surface)
Mosallanezhad et al ,2016	-	3D	a linear elastic plastic	Sand	elasto-plastic Mohr Coulomb model	Slip-surface model

3 EXPERIMENTAL STUDIES

3.1 Overview

The testing program designed in this study aimed at investigating the potential benefits of using the reinforced soil foundations to improve the bearing capacity and to reduce the settlement of shallow foundations on soils. For this purpose, geocell and geogrid were investigated in small scale laboratory test by changing the different parameters involved in the design. Another important purpose of running these tests is to validate and calibrate the numerical models created in this study. A poorly-graded dry sand was used as the infill material. HDPPE geocell and biaxial geogrid were tested.

3.2 Material used

3.2.1 Sand

A poorly graded dry sand with specific gravity of 2.64 was used in the study. Other properties of soil was effective particle size (D10) of 0.3 mm, coefficient of uniformity (C_u) of 3.02, coefficient of curvature (C_c) of 1.05, maximum void ratio (e_{max}) of 0.81, minimum void ratio (e_{min}) of 0.51, and angle of internal friction (φ) of 38°which was estimated using Direct shear test. The sand can be classified as poorly graded sand with symbol SP according USC System**.** Particle distribution curve of sand is represented in Figure 3.1. The geocell was made up of HDPE. The properties of the geocells appear in Table 3.1 .

Air-pluviation technique was used to prepare sand beds of 550mm thickness with relative density 70% which was estimated using void ratio relationship equation. The falling height-800mm was selected to prevent punching failure during the loading.

Table 3.1 Properties of sand used in experimental studies

Property	Symbol	Unit	Values
Effective particle size	D_{10}	mm	0.3
Mean particle size	D_{50}	mm	0.55
Coefficient of uniformity	C_u	-	3.02
Coefficient of curvature	C_c	-	1.05
Specific gravity	G_s	-	2.5
Friction angle	φ	o	38
Cohesion	C		0
Relative density	RD	%	73
Selected dry unit weight of sand	γ	kN/m^3	15.8

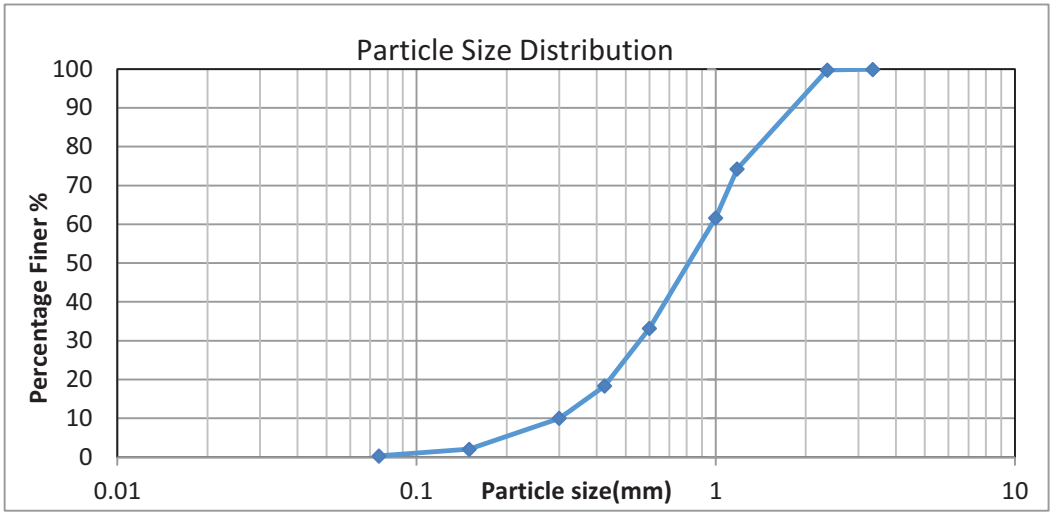

Figure 3.1 Particle size distribution of sand

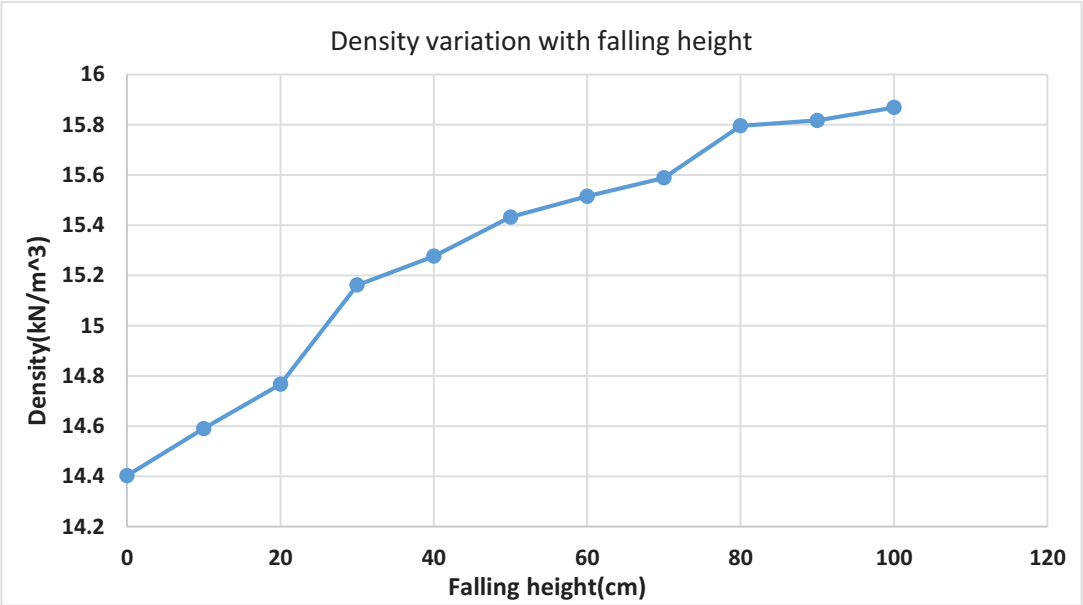

Figure 3.2 Density variation with falling height –Pluviation technique

3.2.1.1 Sequence of filling of geocell

Geocell should be filled using proper filling sequences. A filling sequence proposed by the John 1987 was adopted. In the sequences, first of all, sand was filled the half height of the two row of geocell. Second, sand was filled the first row to full length of the geocell. Thirdly, sand was filled the half height of the third row of geocell. And fourth, sand was filled the full height of second row of geocell. Finally, the same sequence of filling as given in the step 1 to 4 was repeated until the whole geocell row was filled. The cell pockets were filed up with the clear sand using pluviation technique to maintain uniform density. The filling sequence is give in the Figure 3.3.

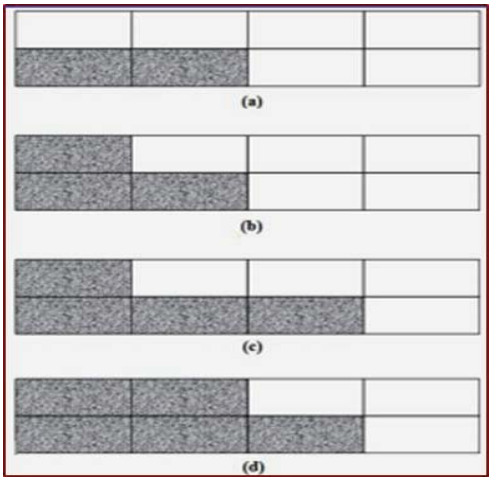

Figure 3.3 Sequence of filling of geocell (John, 1987)

3.2.1.2 Pluviation technique

In this study, density of sand should be maintained uniformly. There are several methods to fill the sand with uniform density. Here, air pluviation technique was used. Dry sand was allowed to fall through a funnel with the constant falling height. Initially, pluviation test was carried out using different height and density was estimated. Then falling height vs. density graph was plotted to select proper falling height.

Then suitable height was selected from graph and prepared dry sand was allowed to fall by keeping the constant height. (Kolbuszewski 1948)

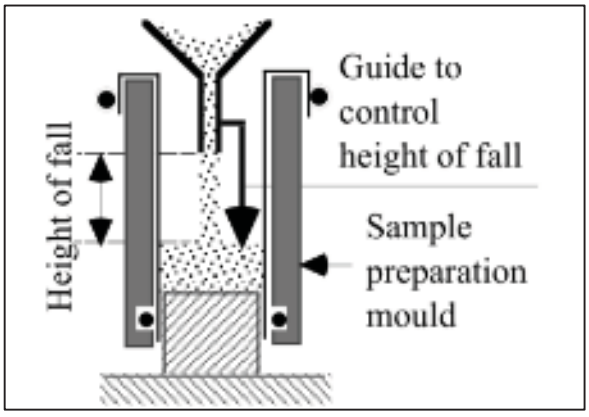

Figure 3.4 Air pluviation technique of sample preparation (Towhata, 2008)

3.2.2 Geocell

HDPE geocell which is made from strips of welded high density polyethylene was used in this research study. The properties of the geocell was referred from geocell specification manual of the product which is given in Table 3.2.

Table 3.2 Geocell Specification (from manual) used in experimental studies

Sheet Thickness ,mm	1.25	
Bonded Ranges,mm	530	
Cell depth,mm	100	
Properties	**Test Method**	**Value**
Material		HDPE
Standard Colour		Black
Surface		Textured
Sheet Thickness ,mm	ASTM D5199	1.25
Density,g/cm^3	ASTM D792	0.94
Carbon Black Content,%	ASTM D1603	2
Environmental Stress Crack Resistance,hrs	ASTM D1693	4000
Seam Peel strength	COE GL-86-19	1200

3.2.3 Geogrid

Geogrid is a planar reinforcement which could be used in shallow depth soil improvement. In this study, biaxial geogrid (tensar) was used. The physical and mechanical properties of geogrid are summarized in Table 3.3.

Table 3.3 Properties of geogrid used in experimental studies

Property	Symbol	Unit	Values
Thickness	t	mm	1.5
Young modulus	E	MPa	250
Interface shear modulus	k	MPa/m	2.36
Density	ρ	g/cm^3	1.05
Tensile strength	T	kN	12.2
Tensile modulus	J	kN/m	420

3.3 Test setup and procedure

The main purpose of experimental studies was to validate the numerical models and explore the research objectives. The experiments were conducted at the Department of Civil Engineering at the University of Moratuwa in Sri Lanka.

Figure 3.5 shows the model test setup used in the experimental studies. The model box was made of 5mm thick perspex panels and rigid steel and rigid composite base to avoid the deformation due to heavy loading. Steel angles were used to prevent buckling of surrounding perspex panels. Internal dimension of test tank were 1300 mm length, 1300 mm width, and 550mm height. The tank was connected to the steel stable frame that was attached to a fixed hand jack. A square timber plank of 200 mm width and 50mm thickness was selected as the footing of the model.

Model bed preparation was started using sand pluviation technique. Initially, sand was filled as layers which was approximately 50mm height. Then geosynthetic reinforcement was installed at proposed depths and was filled with sand using proper

sequences. Finally foundation plate was placed horizontally carefully. A proving ring with sufficient capacity was connected to timber column plank to measure the applied load. Dial gauge was fixed on the footing top surface to record the footing settlement with loading.

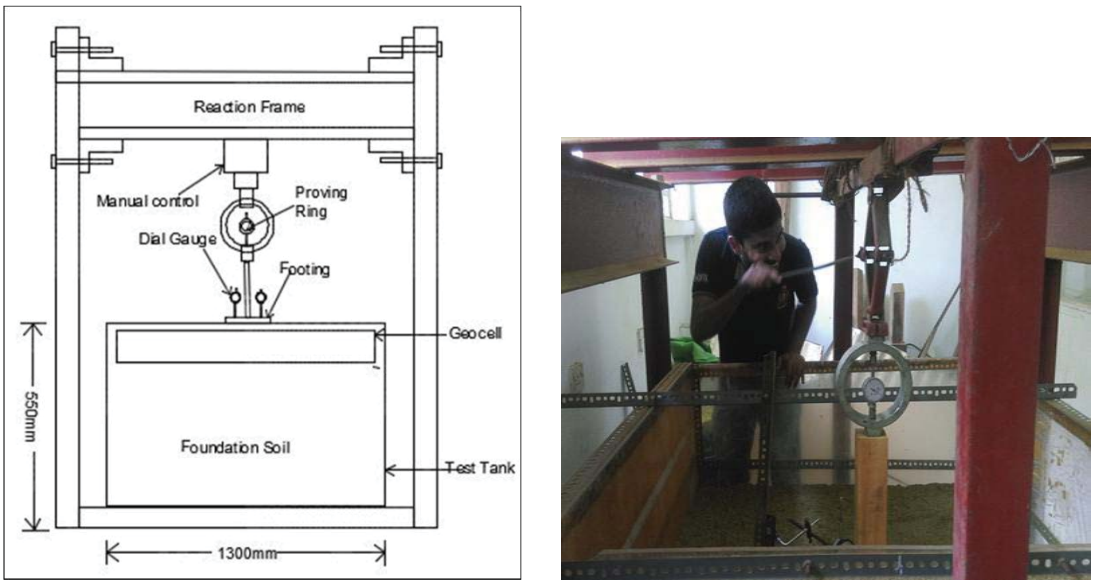

Figure 3.5 Model test setup

3.3.1 Testing program-Geocell

Geometry of the test configuration of geocell reinforcement is shown in Figure 3.6. Experimental studies were carried out by changing the placing depth of geocell (cover thickness), initially, experimental study was carried for unreinforced condition.

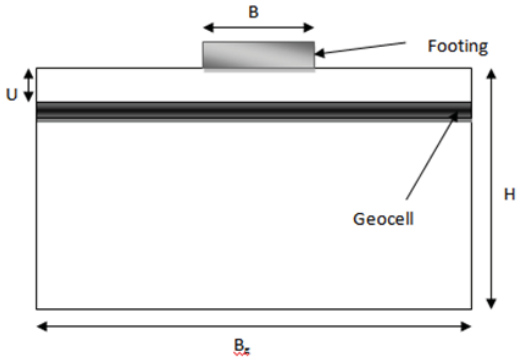

Figure 3.6 Geometry of the geocell reinforced foundation

Reinforcement of width 6B was placed at the depths of 0B, 0.25B, 0.5B and 1.0B (where B is the width of the footing). To maintain uniform density, pluviation technique was used to fill the geocell pockets with the reference of filling sequence method (Sladen and Handford., 1987). Then footing was placed on top surface of soil and the load was applied manually. The footing was placed on the center of the geocell pocket.

Table 3.4 Parameters used in geocell experimental studies

Test No	U(mm)	U/B	B_g/B	h/d
1	0	0	6	0.5
2	50	0.25	6	0.5
3	100	0.5	6	0.5
4	200	1.0	6	0.5

3.3.1.1 Test results and discussion

Structural performance due to provision of geocell could be estimated using non - dimensional improvements which are Bearing capacity ratio-BCR and percentage reduction-PRS in footing settlement. Here, BCR was used in calculations. It is defined as follows:

$$BCR = \frac{q_{rf}}{q_{urf}} \quad \text{..... (3.1)}$$

Where q_{rf} *and* q_{urf} are the bearing pressure of reinforced soil and unreinforced soil at a given settlement, respectively.

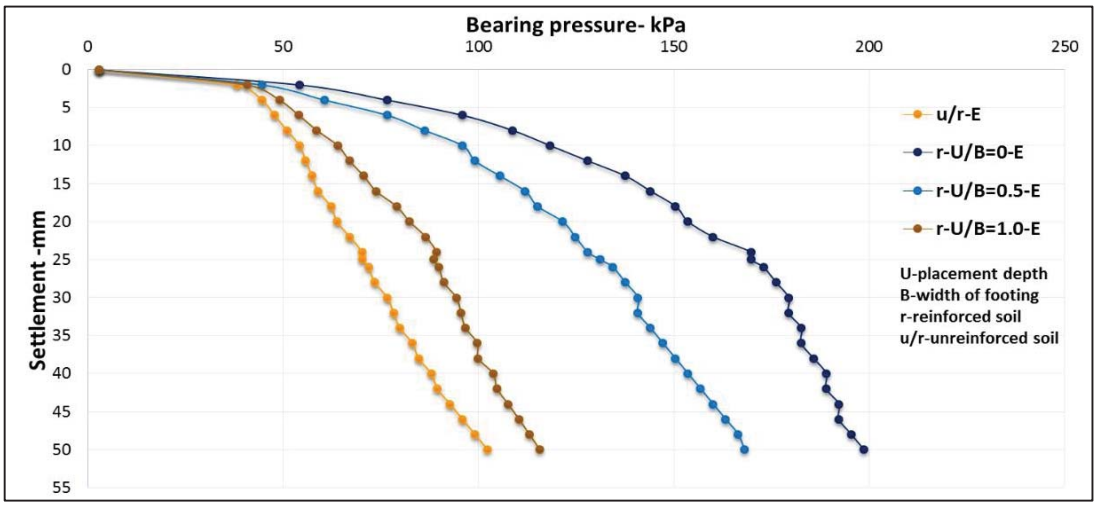

Figure 3.7 Bearing pressure – settlement behaviour of footing under various condition

Figure 3.7 shows the bearing pressure-settlement curves obtained from experimental studies for different reinforced conditions. Ultimate bearing capacity was estimated from experimental results. Ultimate bearing capacity of vertically loaded footing was consistently defined as the load corresponding to a vertical displacement equal to 10 % of the foundation width (s/B =0.1) (Amar et al., 1994). Hence ultimate bearing capacity is estimated for a settlement of 20mm. In unreinforced bed case, ultimate bearing capacity was observed in the range of 65kPa. Estimated bearing capacity using Terzaghi's methods is 70.2kPa. A Steep gradual increment curve was observed in the slope of the pressure-settlement. After 30mm settlement, punching was clearly observed. Bearing capacity of reinforced sand was estimated in different U/B ratio. The results clearly showed that geocell reinforcement increased the bearing capacity of the sand. Maximum bearing capacity was observed in the case of U/B ratio between 0 and 0.5. It was observed that the geocell is not effective after U/B>1. Further analysis

was carried using numerical analysis to estimate the cover thickness of geocell placement.

Modulus of subgrade reaction (Ks) will give the stiffness of the soil bed at lower settlements. It is defined as the pressure corresponding to the settlement- **s** in the load settlement behavior (Hegde and Sitharam, 2013). It is defined as follows(K_s in kNm^{-3})

$$K_s = \frac{q_s}{s \times 10^{-3}} \quad \text{..... (3.2)}$$

Table 3.5 Modulus of subgrade reaction (Ks) of geocell reinforced soil

Material	**Modulus of subgrade reaction (Ks in kNm^{-3})**			
	unreinforced	Geocell U/B=0	Geocell U/B=0.5	Geocell U/B=1.0
Sand(1.25mm)	37586	53633	44005	40257
Sand(25mm)	3170	6916	5248	3596

Table 3.5 shows the estimated modulus of subgrade reaction (Ks) for different cases in sand beds. It shows that improvement of Ks value is not significant in sand beds at initial settlement even with the addition of geocell reinforcement. Therefore, soil reinforcements show marginal improvement in stiffness of composite mass. However, bearing pressure was suddenly increased when the load was applied gradually on bed.

The test result also showed that the slopes of the pressure-settlement curves for reinforced and unreinforced cases were initially close to each other. The curves started to separate when the displacement reached 1mm. In another word, geocell reinforcement needs some displacement to take effect. The reason for this phenomenon may be the hoop stress from the geocell is proportional to the tensile stress of geocell. So, the geocell provides more and more confining stress to sand as the tensile stress (or strain) in the geocell increases.

3.3.2 Testing program-Geogrid

Cross sectional view of the test configuration of geogrid reinforcement is shown in Figure 3.8. Experimental studies were carried out by changing the number of geogrid layers. Initially experimental study was carried for unreinforced condition.

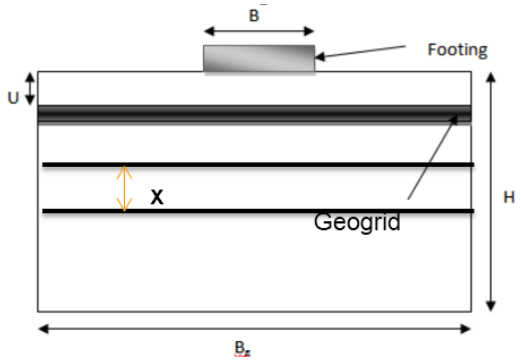

Figure 3.8 Geometry of the geogrid reinforced foundation

In model test, the optimum values of cover thickness (u), layer spacing of reinforcement(x) and width of reinforcement layer (B_x) were defined according to the

literature review. Experimental studies were conducted by changing number of geogrid layers. Number of geogrid (N) was changed from 0 to 4.The depth of the reinforcement (d) below the bottom of the foundation can be calculated by using the equation:

$$d = U + (N - 1) \times h$$

Where, U, N and h are cover thickness, number of geogrids and vertical spacing of geogrids respectively. By considering the previous findings, it was decided to use the following parameters shown in Table 3.6 in the present research studies. Table 3.7 shows the parameters used in the model test.

Table 3.6 Optimum parameters used in experimental studies

Parameters	Symbol	Optimum Value	Current Experimental value
Cover thickness	U	0.2B	0.2B
Spacing	X	0.2B	0.2B
Width	Bx	4.5B	6.5B

Table 3.7 Geometry parameters of model

Parameter	Symbol	Unit	Values
Footing width	B	mm	200
Cover thickness	U	mm	50
Spacing	x	mm	50
Depth	H	mm	550
Width	Bx	mm	1300

To maintain uniform density, pluviation technique was used to fill the tank. The footing was placed on top surface of soil and load was applied manually. The footing was placed on the center of the tank surface. The loading rate was kept constant in each model test .The load and settlement were measured using proving ring and dial gauge, respectively.

3.3.2.1 Test results and discussion

Structural performance due to provision of geogrid could be estimated using non - dimensional improvements which are bearing capacity ratio- BCR and percentage reduction-PRS in footing settlement. Here BCR was used in calculations and it is defined as follows:

$$\text{BCR} = \frac{q_{rf}}{q_{urf}} \quad \text{..... (3.3)}$$

Where, q_{rf} and q_{urf} are the bearing pressure of reinforced soil and unreinforced soil at a given settlement, respectively.

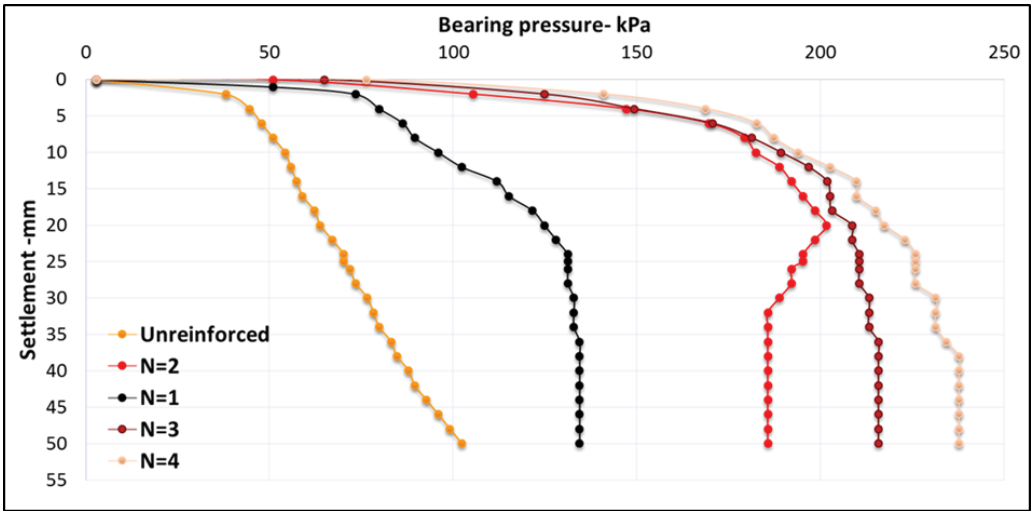

Figure 3.9 Variation of bearing pressure with different number of geogrid layers

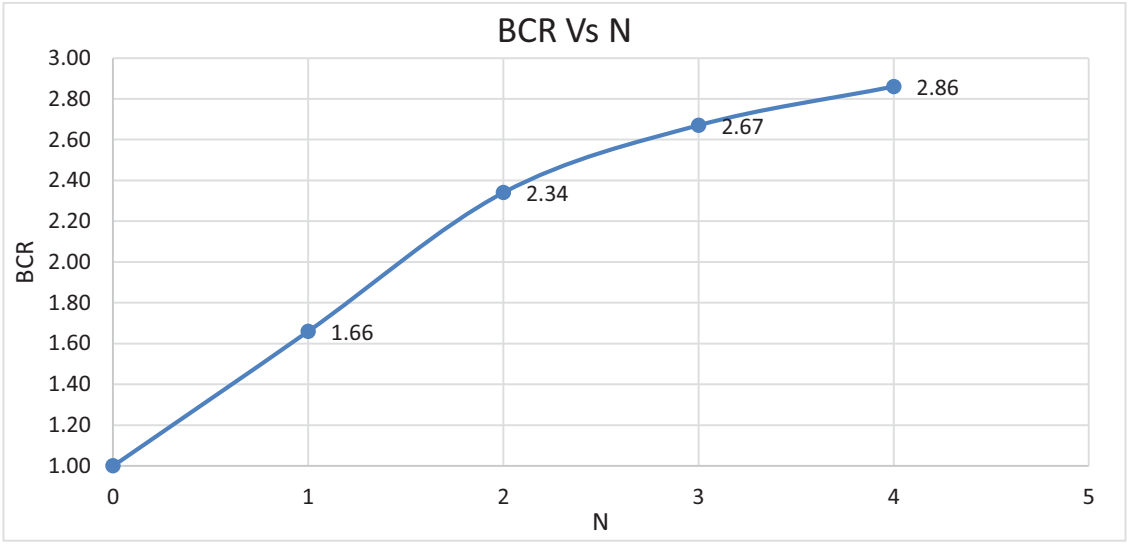

Figure 3.10 Variation of bearing capacity ratio with the number of geogrids (spacing 0.25B)

Figure 3.9 shows the bearing pressure-settlement curves obtained from experimental studies for different number of geogrid layers. Ultimate bearing capacity was estimated from experimental results. In unreinforced bed case, ultimate bearing capacity was observed in the range of 65kPa. A steep gradual increment curve was observed in the slope of the pressure-settlement. The results clearly showed that geogrid reinforcement increased the bearing capacity of the sand. Surface heaving and settlement were reduced with number of geogrid mattress. Maximum bearing capacity improvement was observed when four layer geogrid (N=4) used as reinforcement which was 2.86 times of unreinforced bearing capacity. It was observed that bearing capacity increment rate reduces after second layer. Further analysis was carried using numerical analysis to investigate further.

Table 3.8 Modulus of subgrade reaction (Ks) of geogrid reinforced soil

Material	Modulus of subgrade reaction (Ks in kNm^{-3})				
	unreinforced	N=1	N=2	N=3	N=4
Sand(1.25mm)	37586	45290	49120	63895	73990
Sand(25mm)	3170	5248	7422	8429	9039

Table 3.8 shows the estimated modulus of subgrade reaction (Ks) for different cases in sand beds. It shows that improvement of Ks value is not significant in sand beds at initial settlement even with the addition of geocell reinforcement. Therefore, soil reinforcements show marginal improvement in stiffness of composite mass. However, bearing pressure was suddenly increased when the load was applied gradually on bed.

3.3.3 Testing program-Geogrid –Geocell combinations

In some geotechnical problems, it is required to improve the bearing capacity very high. In those situations, double layer geocell or multiple layer geogrid could be used. But there may be some construction conflicts. Geocells are the speedy solution over geogrid in most of geotechnical problems. Here combination of geogrid and geocell was analysed using experimental studies. Two different cases were investigated, namely 'geocell+geogrid' combination and 'geogrid+geocell' combination which are shown in Figure 3.11.

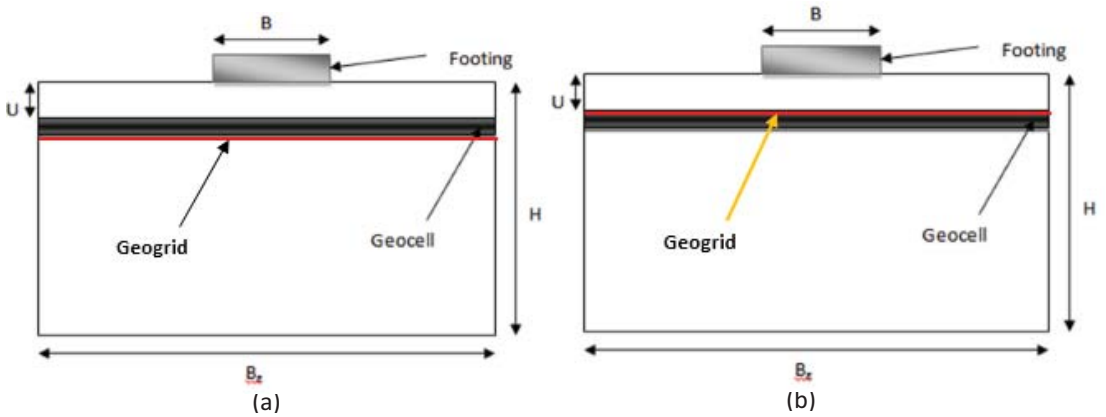

Figure 3.11 Geometry view of (a) Geocell– Geogrid layer reinforced soil (b) Geogrid –Geocell layer reinforced soil

The dimensions of model shallow foundations used in the numerical analysis are shown in Table 3.9 . The parameters of the sand is summarized in Table 3.1. Balau timber plank was used as rigid square footing with 50mm thickness and 200mm width. General properties of geocell are presented in Table 3.2. Table 3.3 show the properties of geogrid used in experimental study.

Table 3.9 Geometry parameter of model foundation

Parameter	Symbol	Unit	Values
Footing width	B	mm	200
Cover thickness (a)	U(a)	mm	20
Cover thickness (b)	U(b)	mm	20
Depth	H	mm	550
Width	Bx	mm	1300

3.3.3.1 Test results and discussion

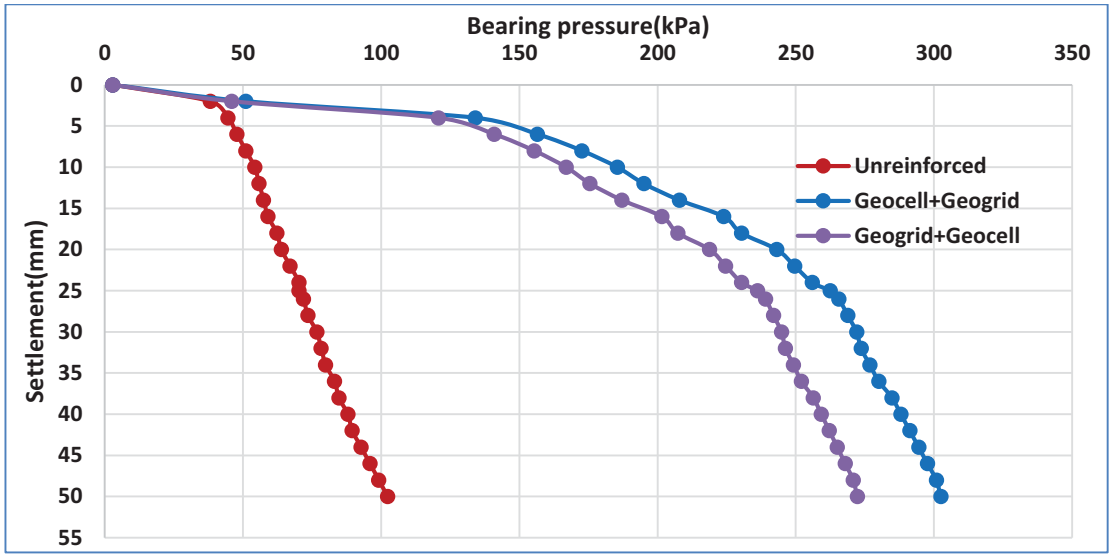

Figure 3.12 Bearing pressure – settlement behaviour of footing under various condition

Figure 3.12 shows the bearing pressure-settlement curves obtained from experimental studies for different reinforced conditions. Ultimate bearing capacity of 'geocell+geogrid' combination and 'geogrid+geocell' combination are 262kPa and 236kPa, respectively. It shows that a layer of planar geogrid placed at the base of the geocell improves the bearing capacity over a layer of planar geogrid placed at the top of the geocell. This section is discussed in numerical studies with detailed.

3.4 Summary

This chapter describes the static load test conducted in this study. The data obtained from these tests will be used to verify and calibrate the numerical models created in this study.

3.4.1 Geocell

Based on the results of the experimental analysis of geocell reinforced soil under footing, the following conclusions can be drawn:

- From the results, suitable cover thickness was found at [depth (U)/width (B)] ratio between 0 and 0.5 for a square pad footing. Further anlayse is carried out using numerical methods to estimate the exact cover thickness.
- The static load test showed that with the provision of HDPE geocells, bearing capacity of soil can be improved by a factor up to 2.5 times of unreinforced soil for optimum cover thickness
- Punching shear failure was observed after 30mm settlement.
- Estimated modulus of subgrade reaction (Ks) for different cases in sand beds showed that improvement of Ks value is not significant in sand beds even with the addition of geocell reinforcement. Therefore, soil reinforcements show marginal improvement in stiffness of composite mass. However, bearing pressure was suddenly increased, when the load was applied gradually on bed.
- Geocell reinforcement needs some displacement to take effect. The reason for this phenomenon may be the hoop stress from the geocell is proportional to the tensile stress of geocell. Therefore, the geocell provides more and more confining stress to sand as the tensile stress (or strain) in the geocell increases.

3.4.2 Geogrid

Based on the results of the experimental analysis of geogrid reinforced soil under footing, the following conclusions can be drawn:

- The inclusion of reinforcement resulted in increasing the ultimate bearing capacity of soils and reducing the footing settlement.
- Surface heaving and settlement are reduced with number of geogrid (N) mattress. However, improvement rate was reduced with N.
- The bearing capacity of reinforced soil increases with increasing number of reinforcement layers (at same vertical spacing). However, the significance of an additional reinforcement layer decreases with the increase in number of layers.
- Maximum bearing capacity improvement was observed when four layer of geogrids (N=4) was used as reinforcement which was 2.86 times of unreinforced bearing capacity.

3.4.3 Geocell-Geogrid combination

A layer of planar geogrid placed at the base of the geocell will improve the bearing capacity over a layer of planar geogrid placed at the top of the geocell.

4 NUMERICAL ANALYSIS

4.1 The Finite Element Approach

Performance of geosynthetic reinforced soil should be evaluated in the design stage of structures. It is not always possible to depend on field studies for design calculations, which are often time consuming and costly. Yet, only a few numerical analyses have been carried out to determine the bearing capacity of geocell/geogrid-reinforced soil. In designing complex structures as that involved in geocells, the numerical modeling would be helpful in better understanding of the behaviour.

It is important to create a model with a realistic geometric representation of the project when using the finite element model. A geometry model should append a representative division of the subsoil into distinct soil layers, structural objects, loading conditions, and construction stages. The model must be sufficiently large so that the boundaries do not influence the results of the studied problem.

In the study, PLAXIS was chosen for analysis. PLAXIS is based on finite element solution scheme to solve the initial and boundary value problems. In this numerical study, both PLAXS 2D and PLAXIS 3D were employed. Using PLAXIS 2D the equivalent composite approach (ECA) of geocell modelling was analyzed and justified for the results obtained. The actual 3D curved structure of the geocell was modeled using the PLAXIS 3D and Auto CAD 3D.It is discussed in following sections.

4.1.1 Description of PLAXIS

The PLAXIS program was originally developed in 1986, as a jointed project between Delft University of Technology and the Dutch Ministry of Public Works. The goal was to provide a practical means to use the finite element method in geotechnical engineering problems. In 1993, the PLAXIS Company was formed and it took over the activities from Delft University of Technology. Since then, many features were added to the software to extend its capability to cover most areas of geotechnical engineering (PLAXIS).

Usually, geotechnical problems could be approximated to either plane strain or axisymmetric conditions. But some remain very three dimensional which can’t be solved in 2D analysis. Full three dimensional numerical analysis should be carried out to solve these problems. In wither (*decay) plane strain or axisymmetric model, it is implied that displacements in one particular direction are zero, which is a simplification of real case. However, in actual geotechnical problems three dimensional components of displacement should be taken into account to get more accurate information. Especially when the domain is an irregular shape rather than a circle or square, the corner effect has significant influence in the behaviour of structures.

For PLAXIS 3D, the basic soil elements of the 3D finite element mesh are the 10-node tetrahedral elements (Figure 4.1). In addition to the soil elements, special types of elements are used to model structural behaviour. For beams, 3-node line elements are used, which are compatible with the 3-node edges of a soil element. In addition, 6-node plate and geo-grid elements are used to simulate the behaviour of plates and geo-grids respectively.

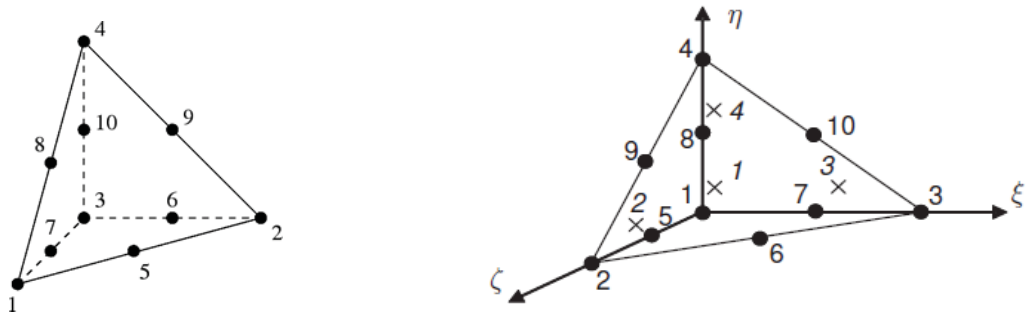

Figure 4.1 3D soil elements with 10-node tetrahedrons (source: PLAXIS 3D reference manual, 2015)

4.2 Foundation material properties

4.2.1 Sand

The constitutive models and parameters of the sand is summarized in Table 4.1

Table 4.1 *sand properties*

Parameters	**Name**	**Sand**	**Unit**
Material model	model	M-C model	-
Type of material behavior	type	drained	-
Soil unit weight	γ_{bulk}	15.8	kN/m^3
Permeability in horizontal direction	k_x	0.36	m/day
Permeability in vertical direction	k_y	0.36	m/day
Young's modulus	E_{ref}	12,500	kN/m^2
Poisson's ratio	v	0.25	-
Cohesion	C_{ref}	0.1	kN/m^2
Friction angle	φ	38	°
Dilatancy angle	ψ	8	°
Strength reduction factor	R_{inter}	1	-

4.2.2 Timber

Balau timber plank was used as rigid square footing with 50mm thickness and 200mm width. Constitutive model properties of timber is shown in Table 4.2.

Table 4.2 Timber properties

Parameters	Name	Sand	Unit
Material model	model	Plate	-
Type of material behavior	type	Isotropic	-
timber unit weight	γ_{bulk}	9	kN/m^3
Young's modulus	E_{ref}	9,000,000	kN/m^2
Poisson's ratio	v	0.1	-

4.3 Numerical analysis of Geocell

Numerical simulations of the geocells are not so easy due to its complex 3D honeycomb structure. Generally, the equivalent composite approach is used to model the geocells. But this approach is very simple, it is unrealistic to model geocells as the soil layer. Anyhow, it was validated using PLAXIS 2D in this research to check the accuracy of model.

Most of 3D numerical analyses were also carried out using this composite approach. But some researchers modelled as square boxes. Most geocells such as the ones that have honeycomb structure cannot be modeled as square boxes because of their curvature. When they are modeled as square a box, which is rather easier, the stresses are likely to accumulate on the corner edges of the square box. However, in reality the honeycomb structures distribute the stresses uniformly along the periphery of the geocells which is a special positive attribute of most of the commercial geocells available nowadays. Such misrepresentations in erroneous models for honeycomb structures easily lead to inaccurate results. Hence, modelling of actual honeycomb shape also carried out using PLAXIS 3D.

4.3.1 Numerical analysis - Equivalent Composite Approach-ECA

The ECA could be used to investigate the geocell in 2D frame. Using this method, Geocell reinforcement with filled soil could be modeled as a composite soil layer with improved strength parameters. Bathurst and Karpurapu (Bathrust, R.J. and Karpurapu, R, 1993) have proposed the approximate solution, (4.1) for estimating apparent cohesion C_r without performing large-scale triaxial tests on the geocell-soil.

$$C_r = \frac{\Delta\sigma_3}{2}\tan\left(\frac{\pi}{4}+\frac{\varphi}{2}\right) \quad \text{---------- (4.1)}$$

In (4.1), φ is the friction angle of the in-fill soil. The increased confining pressure $\Delta\sigma_3$

due to the membrane effect of the geocell can be estimated using (4.2) derived by (Henkal,D.J and Gilbert,G.D, 1952). 'd' and 'ε_a' notate the equivalent diameter of geocell pocket and tensile stress-strain response.

$$\Delta\sigma_3 = \frac{2M}{d}\left(\frac{1-\sqrt{1-\varepsilon_a}}{1-\varepsilon_a}\right) \text{---------- (4.2)}$$

The increased stiffness of geocell-reinforced soil was studied by (Latha,G.M, 2000), who proposed an empirical equation to estimate the modulus number of the geocell-soil composite from the modulus value of soil.

$$K_r = K_e + 200M^{0.16} \text{ ---------- (4.3)}$$

The equivalent initial tangent modulus (Ei) of the geocell layer is calculated using the equation suggested by Janbu (Janbu.N, 1963).

$$E_i = K_r P_a \left(\frac{\sigma_3}{P_a}\right)^n \text{---------- (4.4)}$$

Where,

M - Secant modulus of the geocell material (kN/m)

K_e -Young's modulus parameter of the unreinforced sand (dimensionless)

K_r -Young's modulus parameter of the geocell-reinforced sand (dimensionless)

P_a - Atmospheric pressure (kPa)

n - Modulus exponent of the unreinforced soil

ECA approach is a useful simplification that could be applicable to three-dimensional problem when using two-dimensional numerical software. The parameters used in modelling are shown below.

Table 4.3 properties of sand and geocells

Parameters	**Value**
Sand	
Young modulus(MPa)	12.5
Poisson's ratio	0.25
Geocells	
Young modulus (MPa)	225
Poisson's ratio	0.45
Interface friction angle(°)	38
Pocket diameter-mm	210

Table 4.4 shows the parameters which were calculated using ECA approach. These parameters were used in geocell composite design.

Table 4.4 equivalent composite properties of geocell layer

Parameters	Symbol	Value
Composite soil		
confining pressure -kPa	$\Delta\sigma_3$	30.3
Coefficient of passive earth pressure	K_p	4.4
Young's modulus parameter of the unreinforced sand	K_e	500
Young's modulus parameter of the reinforced sand	K_r	1040
Apparent cohesion (kPa)	C_r	31.8
Initial tangent modulus (MPa)	E_i	31.5
Friction angle(°)	φ	38

Figure 4.2 illustrates the 2D FEM model. It was noticed that there was a large bearing capacity variation between experimental results and FEM results. Bearing capacity was highly overestimated in FEM when using ECA approach. This is because the equivalent model cannot accurately simulate the interaction between the infill soil and the geocell. One problem with this method is that the axial strain of the geocell-reinforced soil at failure has to be first estimated in order to calculate apparent cohesion from the above discussed equations. Mitchell et al. (1979) pointed out that the confining stress in the cells beneath the loading area is much larger than that in the cells outside the loading area, which means the apparent cohesion and the modulus of the reinforced soil under the loading area should be larger than that outside the loading area. In reality, the strain value may vary from cell to cell, especially when the geocell reinforcement is supporting load in a limited area

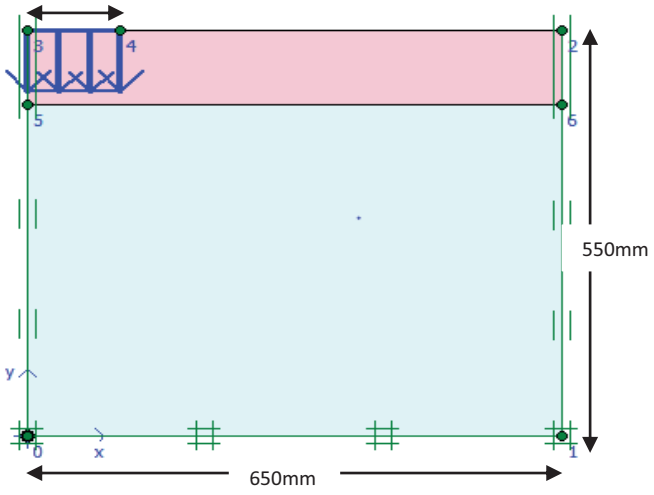

Figure 4.2 FEM model of equivalent composite approach-PLAXIS

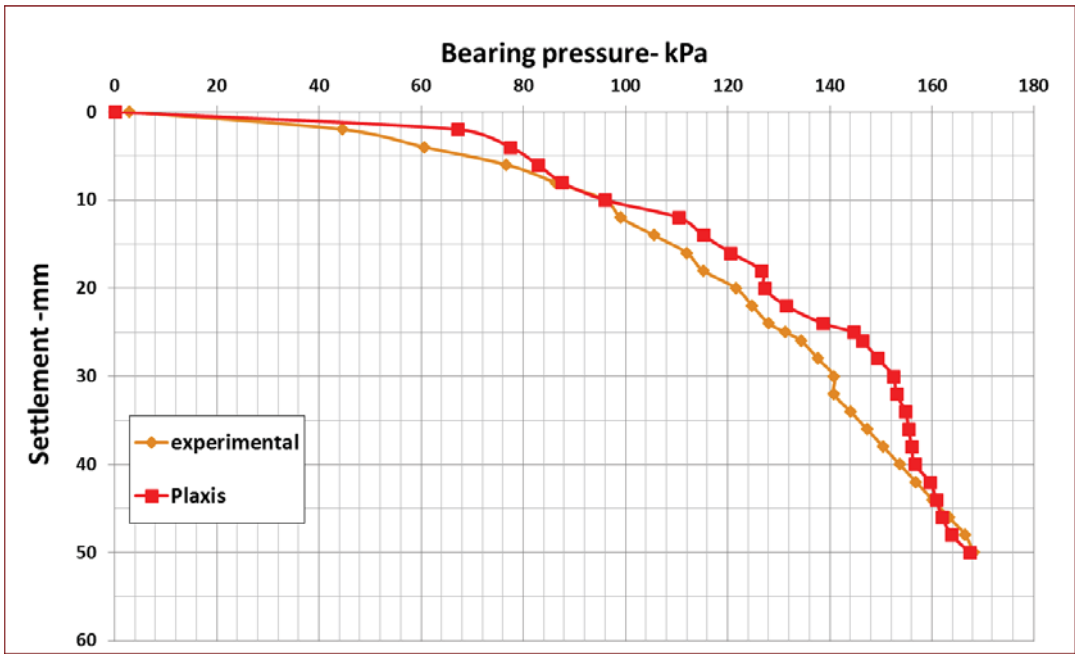

Figure 4.3 Settlement Vs Bearing pressure curve of ECA model

A good match was obtained between both results when elastic modulus of composite soil was reduced by 50%. Figure 4.3 shows the bearing pressure curve of updated elastic modulus. Hedge and Sitharam (Hegde and Sitharam, 2015a) (Hegde and Sitharam, 2015b) made similar observations, where they determined the elastic modulus of the geocell-soil composite layer from the slope of the experimental pressure-settlement behaviour in order to obtain a good match. However, there are some limitations in using this ECA approach. One is the overestimation of bearing capacity. Another one is that this method could not be applicable to combination of reinforcements. Further, this method is not a realistic modeling approach. Hence, 3D modelling is the most appropriate technique for these situations.

4.3.2 Numerical analysis-3D Modelling

PLAXIS3D was used for the 3D modelling of the shallow foundation model. PLAXIS 3D is a finite element program specially designed for solving the three dimensional geotechnical engineering problems. The dimension of test bed used in the experiments was used to model in the PLAXIS 3D.

One quarter of the test model was modeled using PLAXIS 3D to simplify the problem due to the symmetry of the problem. A steadily increasing static displacement was applied within the rectangular area of 0.2m×0.2m. Experimental observations were used to validate numerical simulation results. Here, geosynthetic reinforcement were used, which has a very small thickness compared with the model. Hence fine mesh was used in the model. Soil was modeled using Mohr-Coulomb model and Footing model as plate model. Material properties used in the model are given in Table 4.1 and Table 4.2. Generated 3D model and mesh are show in Figure 4.4 and Figure 4.6.

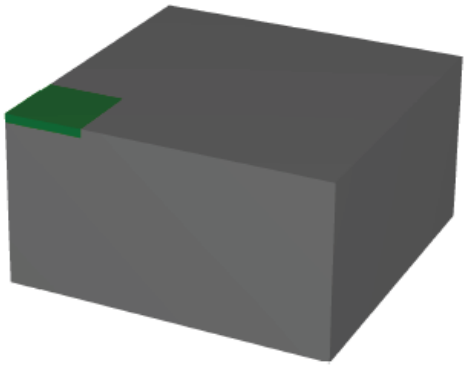

Figure 4.4 3D model of foundation foundation

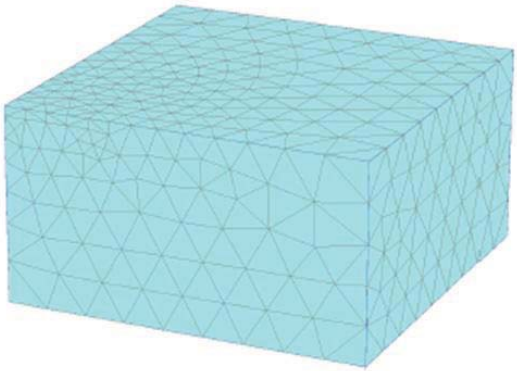

Figure 4.5 Generated 3D mesh of

4.3.2.1 3D Model of Honeycomb Geocell

Generally, equivalent composite approach (ECA) is used by most of researchers to model geocell in 2D and 3D modelling packages. ECA is a relatively simple and time saving method. However it has considerable limitations. For instance, ECA does not consider the shape and size of the geocell, but only the material properties. Particularly shape of the geocell has strong influence in the stress distribution patterns. Most geocells such as the ones that have honeycomb structure cannot be modeled as square boxes because of their curvature. When they are modeled as square box, which is rather easier, the stresses are likely to accumulate on the corner edges of the square box. However, in reality the honeycomb structures distribute the stresses uniformly along the periphery of the geocells, which is a special positive attribute of most of the commercial geocells available nowadays. Such misrepresentations in erroneous models for honeycomb structures easily lead to inaccurate results.

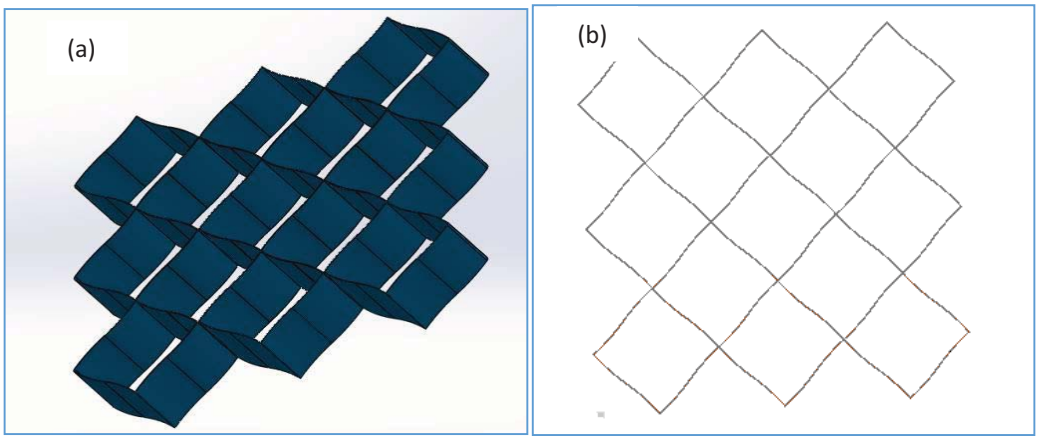

Figure 4.6 (a) Honey comb 3D model of geocells (b) geocell front elevation

Taking these factors in to account, broadly, this study aims to build an accurate enough numerical model for the bearing capacity of the honeycomb geocells reinforced soil; use the experimental results to validate the results from numerical analysis. The numerical model pays particular attention to correctly represent the geometrical structure of the geocells. It considers the curvature of the cells and hence, aims to increase the accuracy of the results.

Geocells are modeled as honeycomb structures. This model considers the curvature to increase the accuracy of the results. Geocells was modeled using Auto CAD-3D (

Figure 4.6). Then it was imported to PLAXIS 3D as a solid thin structure Later it was defined as geogrid type structures. The geogrid structural elements can resist the membrane stresses, but cannot resist the bending stresses. The rigid nature of the geocell joint was simulated by fixing the nodes representing the joints (Yang, 2010). A linear elastic model was used to simulate the behaviour of the geocell. The interfaces between the geocell and the soil were linearly modelled with Mohr Coulomb yield criterion. General properties of geocell and constitutive models are presented in Table 4.5, the geocell used in this study was a rough texture geocell.

Table 4.5 Geocell properties

Parameters	Name	Geocell	Unit
Material model	model	geogrid	-
Type of material behavior	type	Isotropic Elastic	-
Axial/Normal Stiffness	EA	800	kN/m

Figure 4.7 shows the very fine mesh of PLAXIS 3D models used in the analysis. Here, a very fine mesh was used because of the small thickness of geocell (1.25mm). These FE analysis require large computer memory and time. In these studies each analysis took 1-3 hours to mesh and analyze the results.

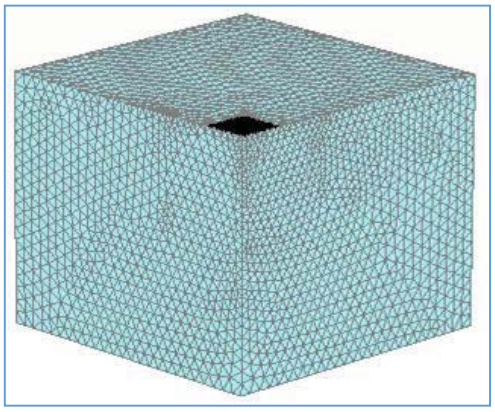

Figure 4.8 3D model of foundation

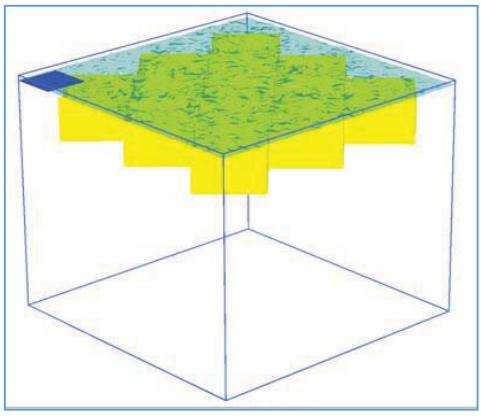

Figure 4.9 Placement of geocell

Then studies were carried out with different U/B (U-depth of geocell placement/B-width of footing) ratio with increasing vertical prescribed settlements. Figure 4.10 shows the actual PLAXIS 3D models used in the analysis. The numerical results were compared with experimental results and later it was validated using theoretical approach (Neto et al., 2013) (the equations derived from experimental and analytical knowledge) as well. Using the validated model, the distribution of stress and settlement under footing were obtained.

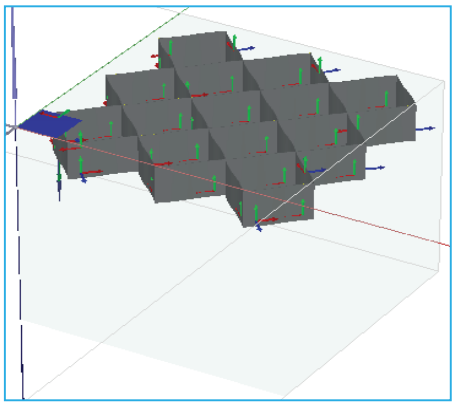

Figure 4.10 geocell with displacement vectors

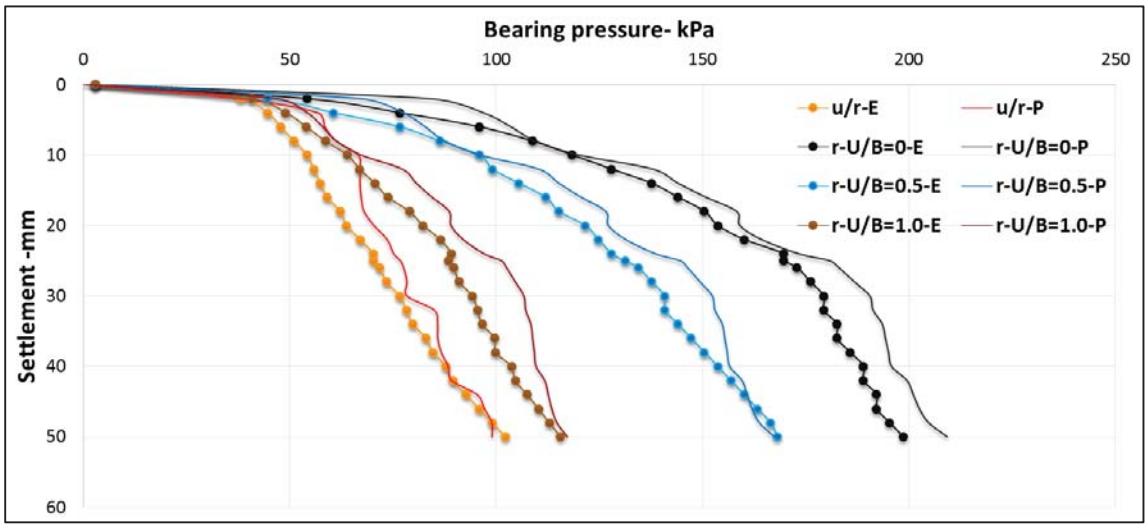

Figure 4.11 Bearing pressure – settlement behaviour of footing under various conditions

The bearing pressure-settlement curves obtained from numerical and experimental studies for different reinforced conditions presented in Figure 4.11. Ultimate bearing capacity was estimated from using numerical analysis and compared with experimental studies. In unreinforced bed case, ultimate bearing capacity was observed in the range of 70kPa. Variation between numerical and experimental result was less than 10kPa.This variation might occurred because of geocell properties which were directly used from manufacture's specifications. A steep gradual increment curve was observed in the slope of the pressure-settlement. After 30mm settlement, punching was clearly observed in FE outputs. Stiffness of soil was increased with the application of geocell reinforcement. The curves started to separate when the displacement reached 2mm. In other word, geocell reinforcement needs some displacement to take effect. This effect was already discussed in experimental results. These numerical curve are not smooth like experimental curves.

Bearing capacity of reinforced sand was estimated in different U/B ratio. Maximum bearing capacity was observed in the case of U/B ratio between 0 and 0.5. It was observed that the geocell is not effective after U/B>1.This honeycomb model results

are very close to experimental results. So it can be concluded that honeycomb shape could be modeled using 3D modelling.

It is important to note that when U/B=1.0, the effect of geocell reinforcement becomes negligible. The reinforced soil behaves similar to unreinforced soil. The failure mechanism is also similar to unreinforced case.

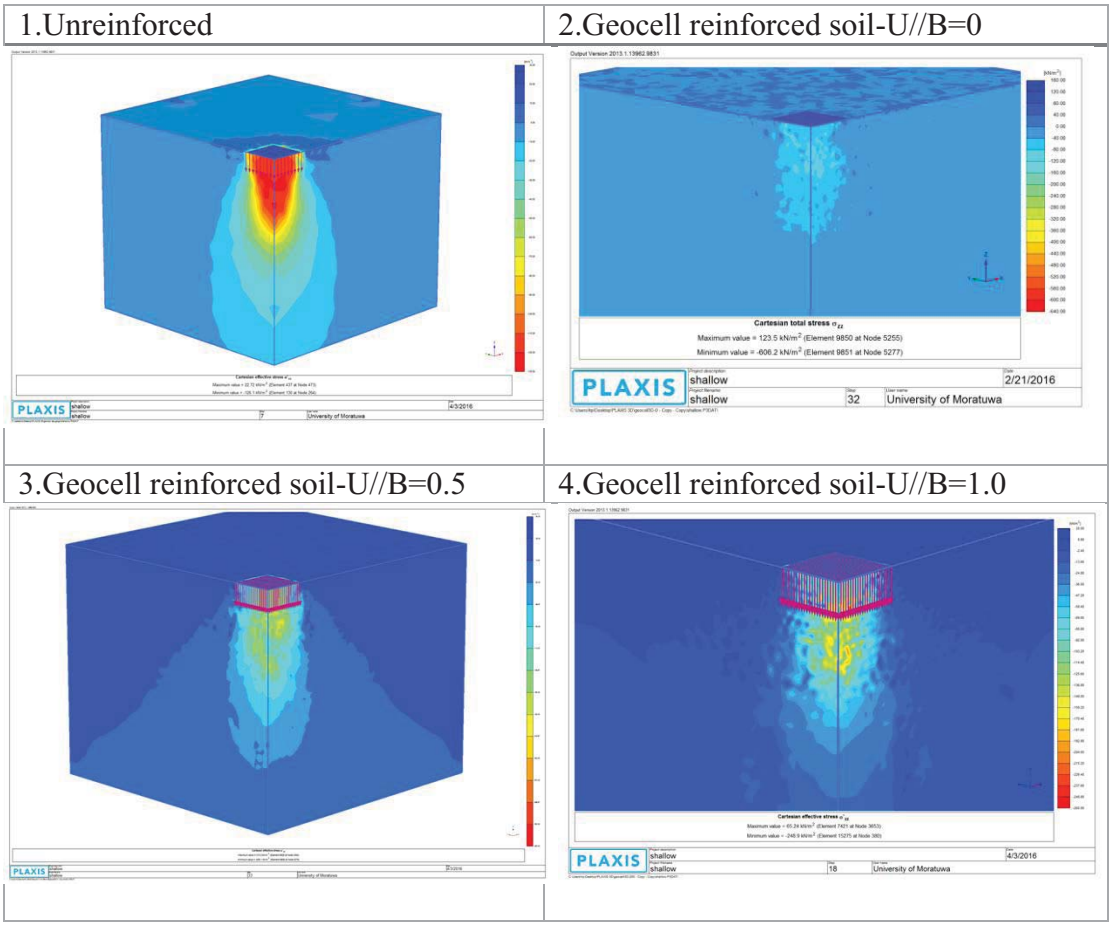

Figure 4.12 Vertical stress distribution of reinforced and unreinforced conditions

The results of the vertical stress distribution for reinforced and unreinforced soil are shown in Figure 4.12. In unreinforced soil, uniform vertical stress distribution up to large depth was observed. In reinforced soil, the stresses are transferred to a shallow depth. But this varies with U/B ratio. In case of U/B=0, the stresses are transferred to a relatively shallow depth as compared to other cases. Same observation was made by Hegde (Hegde and Sitharam, 2015a). These stress contours clearly show that model tank boundaries are quite adequate and satisfied the boundary conditions.

1.Unreinforced	2.Geocell reinforced soil-U//B=0
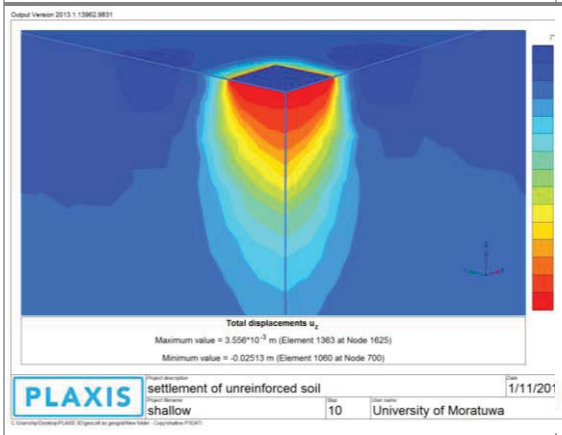	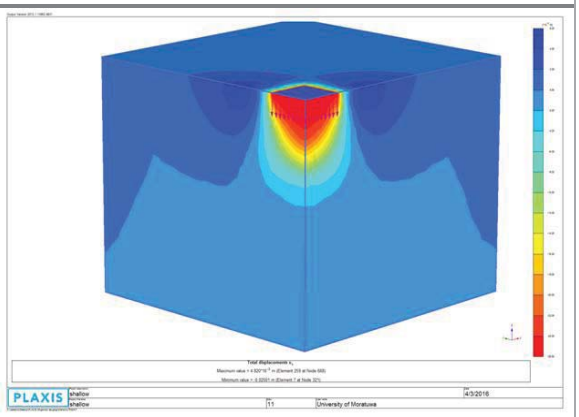
2.Geocell reinforced soil-U//B=0.5	2.Geocell reinforced soil-U//B=1.0
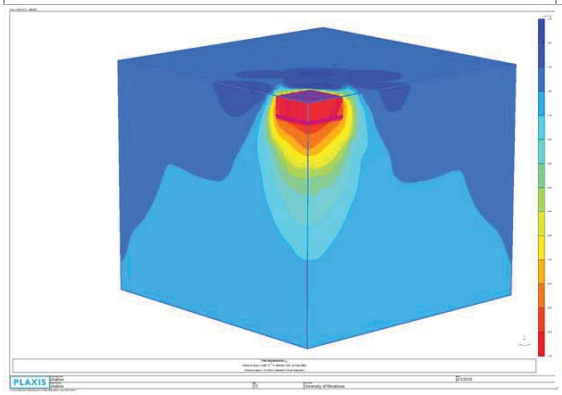	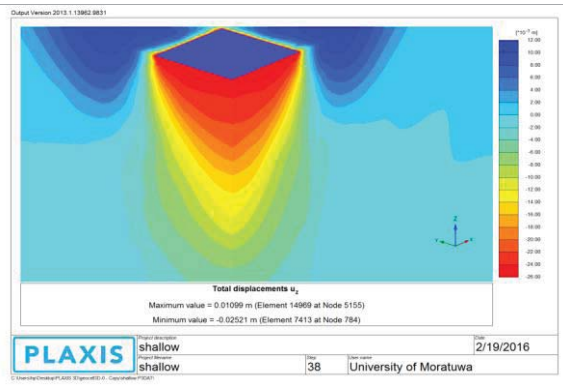

Figure 4.13 Vertical displacement of reinforced and unreinforced conditions

The vertical settlement contours for different cases is shown in Figure 4.13. Distribution of the settlement contours indicates the uniform settlement of reinforced and unreinforced soil. Punching shear failure was observed in high loads. It was validated from experimental observation as well. Latha (Madhavi Latha and Amit Somwanshi, 2009) has also observed similar uniform settlement contours in FLAC 3D modelling of the unreinforced soil. Theoretically, foundations with high rigidity will result in uniform settlements. In numerical approach, uniform settlements could be expected only as long as the foundation material properties are homogeneous and rate of application of footing pressure is constant (Hegde and Sitharam, 2015b). However in experiments, this will not be the case, as it is nearly impossible to ensure such homogeneous soil properties in reality.

4.3.2.2 Effect of cover thickness of the geocell

Mitchell et al. (1979) suggested that an aggregate cover layer would not increase the bearing capacity or the modulus of the soil, but it would provide protection to the geocells. But Thallak et al. (Thallak, Saride and Dash, 2007) tried placing geocell at different depths in his test and it was concluded that the bearing capacity increased sharply when the geocell was placed at shallow depth.

In this studies maximum bearing capacity was observed in the case of U/B ratio between 0 and 0.5.So, further investigation was carried out to estimate the optimum cover thickness using U/B ration between 0 and 0.5. The optimum cover thickness values proposed by other researchers is presented in Table 4.6.

Table 4.6 cover thickness (u) for geocell reinforced soil foundation

Researcher	year	Geocell type	Soil type	Cover
Mandal and Sah	1992	Geogrid	Clay	0.25B
Dash et al	2001	Bounded geogrid	Clay and Sand	0.1B
Sitharam & Sireesh	2005	Geogrid cell	Sand	0.05B
Moghaddas & Dawson	2009	Planar geotextile thermo welded	Sand	0.1B
Hegde & Sitharam	2015	Honeycomb shape	Clay and Sand	N/A

The bearing pressure-settlement curves obtained from numerical studies for different cover thickness are presented in Figure 4.14. From the results, a suitable cover thickness was found at [depth (U)/width (B)] =0.1 for a square pad footing. These curves are not smooth as expected curves.

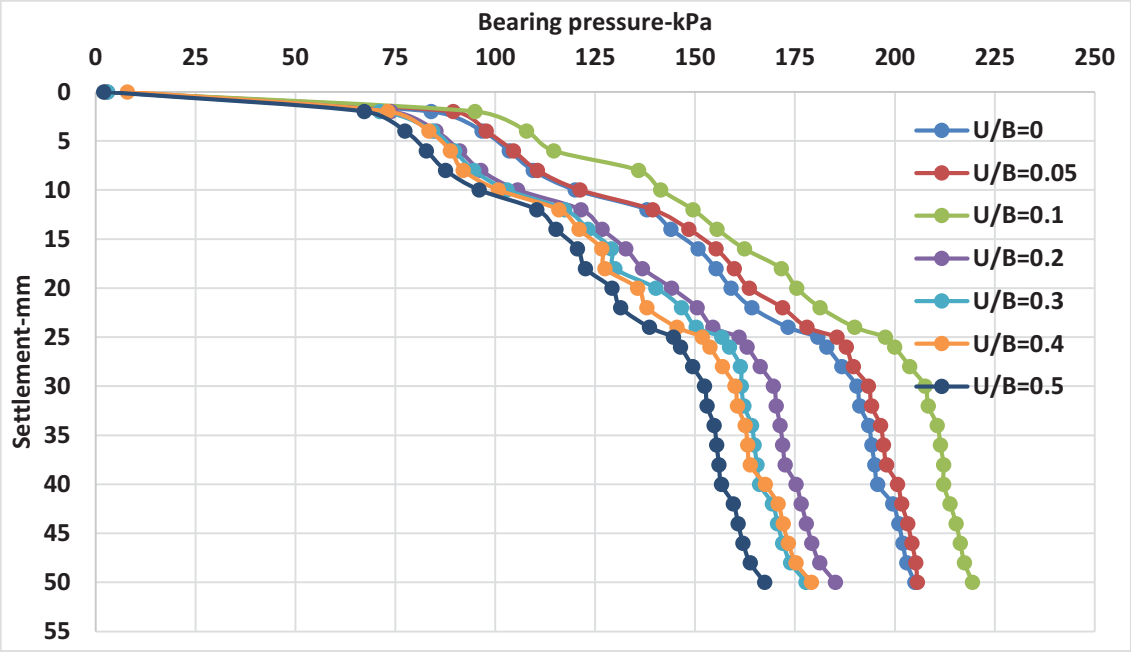

Figure 4.14 Bearing pressure vs settlement of footing under various cover thickness

4.3.2.3 Effect of cell dimension of the geocell

Generally, the bearing capacity increases with the cell height (Dash, 2001) and decreases with the pocket size (Hegde and Sitharam, 2015a). When height of the geocells increase, footing load is distributed over a much area .Due to that, overall load intensity will be reduced and lead to bearing capacity improvement of foundation bed. When geocell pocket size increases, unit volume confinement will be creased, which improve the bearing capacity of foundation bed.

A few researcher considered the aspect ratio (cell height[h]/pocket size[d]) and tried to co relate with the bearing pressure. Rea and Mitchell (1978) found that the optimum cell height to cell width ratio (h/d) was around 2.25, beyond which the improvement was less significant. Mitchell et al. (1979) also confirmed that the optimum cell height to cell width ratio (h/d) was in the order of 2 to 3.

In this study, geocell was used with the aspect ratio (h/d) of 0.5.It was not possible to carry out experimental studies to different aspect ratio of cells due to time and cost. So, numerical study was carried out using geocell with (h/d) ratio of 0.5, 1.0, 1.2, 1.5, 2.0, 2.5, 3 and 4. Optimum cover thickness 0.1B was used in all cases. The bearing pressure-settlement curves obtained from numerical studies for different aspect ratios are presented in Figure 4.15.

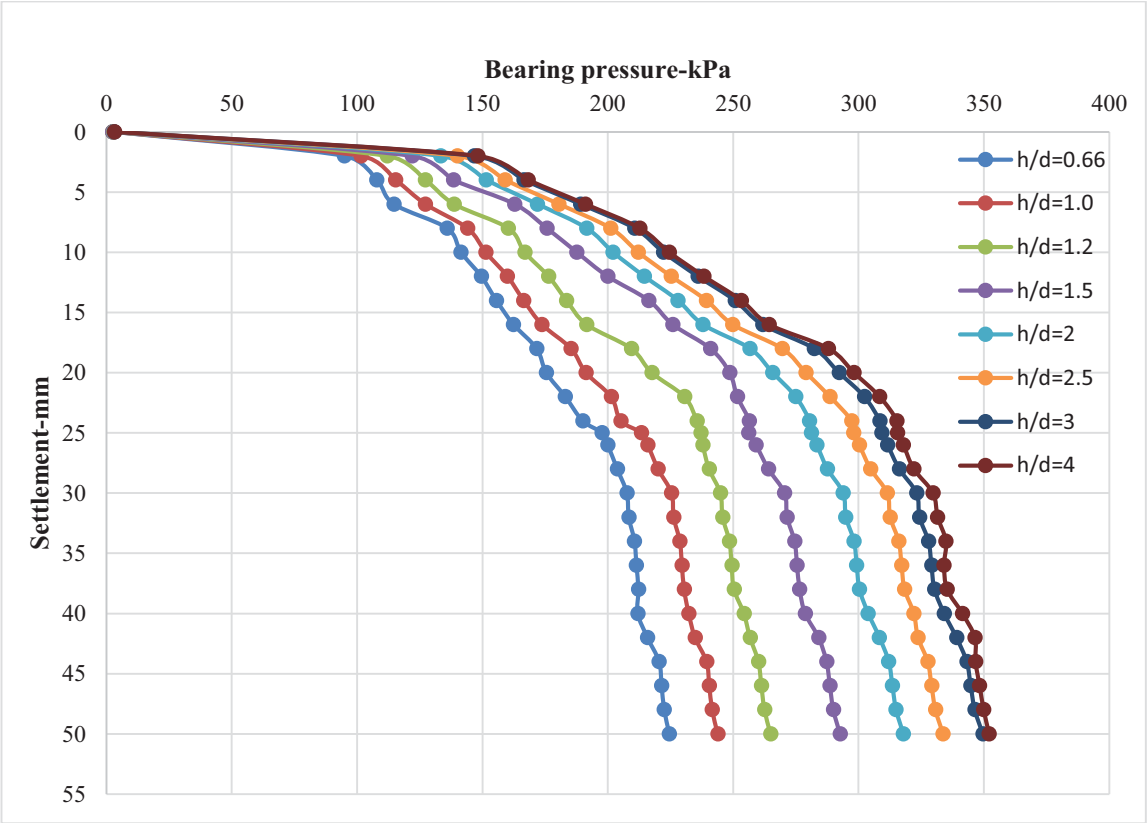

Figure 4.15 Bearing pressure – settlement of footing for different aspect ratios

Numerical results shows that bearing pressure increases with the aspect ratio. Bearing capacity shows a marginal improvement between aspect ratio of 1.5 and 3. Local shear failure and buckling of geocell will occur beyond an aspect ratio of 3.

4.3.2.4 Numerical modelling of Prototype Footing

Prototype model analysis was done using a prototype foundation made up of concrete with young's modulus (E) of 30 GPa and density (γ) of 25kN/m^3. PLAXIS 3D geocell reinforced footing was already validated using experimental. In this study, numerical modelling was used to analyse the prototype footing that was a square footing with thickness=0.5m and width =3.0m**.**

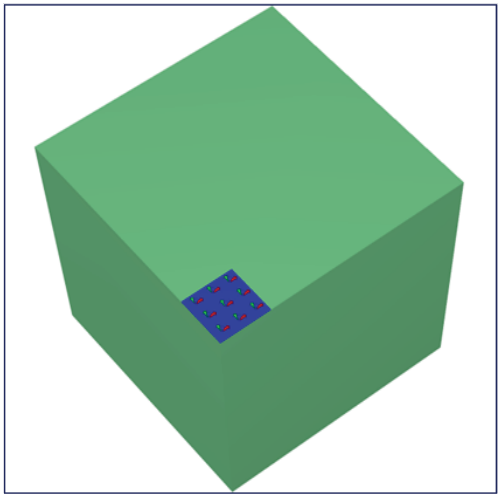

Figure 4.16 3D model of foundation

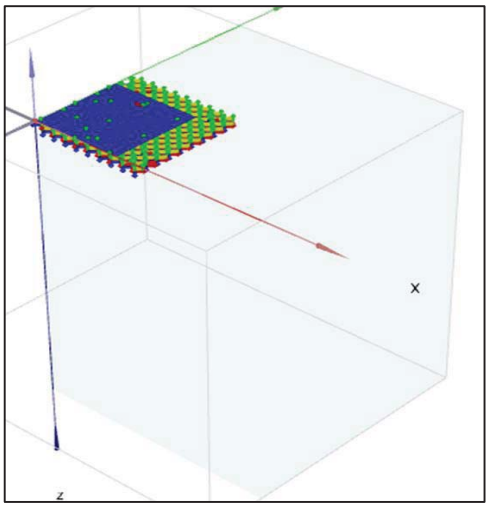

Figure 4.17 placement of geocell

Due to the symmetry of the problem, one quarter of the prototype model was modeled using PLAXIS 3D to simplify the problem. A steadily increasing static displacement was applied within the square area of footing. Geocells are modeled as honeycomb structures. This model considers the curvature to increase the accuracy of the results. (Geocells modelling was already discussed in 4.3.2). Then it was imported to PLAXIS 3D as a solid thin structure. Later, it was defined as geogrid type structures.

The studies were carried out for unreinforced condition, singly reinforced condition and doubly reinforced condition. From previous studies, U/B=0.1 was the optimum (depth/width) ratio for maximum bearing capacity (Hegde and Sitharam, 2015a) (Latha et al., 2009).

Figure 4.18 shows the bearing pressure-settlement curves obtained from numerical studies for different reinforced conditions. Ultimate bearing capacity was estimated in each condition separately. In unreinforced bed case, ultimate bearing capacity was observed in the range of 150kPa. A steep gradual increment curve was observed in the slope of the pressure-settlement. Bearing capacity of singly reinforced sand and doubly reinforced sand were 425kPa and 525kPa respectively. In all analysis, geocell was placed at the depth/width ratio of 0.1 (Latha and Somwanshi, 2009).

Figure 4.19 shows the bearing capacity ratio (BCR) vs. settlement curves for singly and doubly reinforced sand. BCR was 2.75 for singly reinforced and 3.5 for doubly reinforced sand. A similar observation was reported by Henkal (Henkal and Gilbert, 1952).

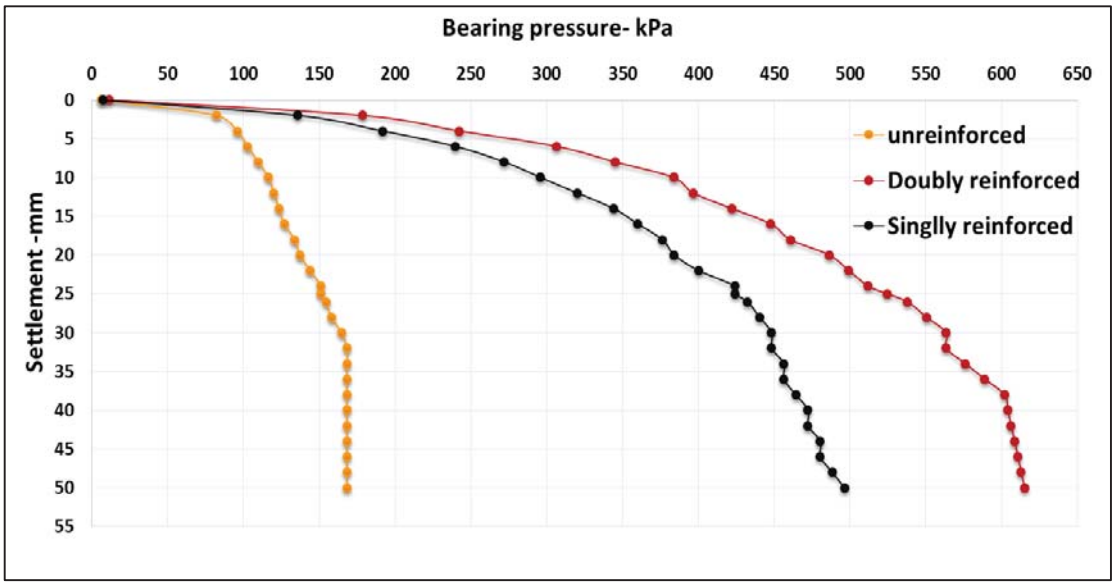

Figure 4.18 Bearing pressure – settlement behaviour of footing under various conditions

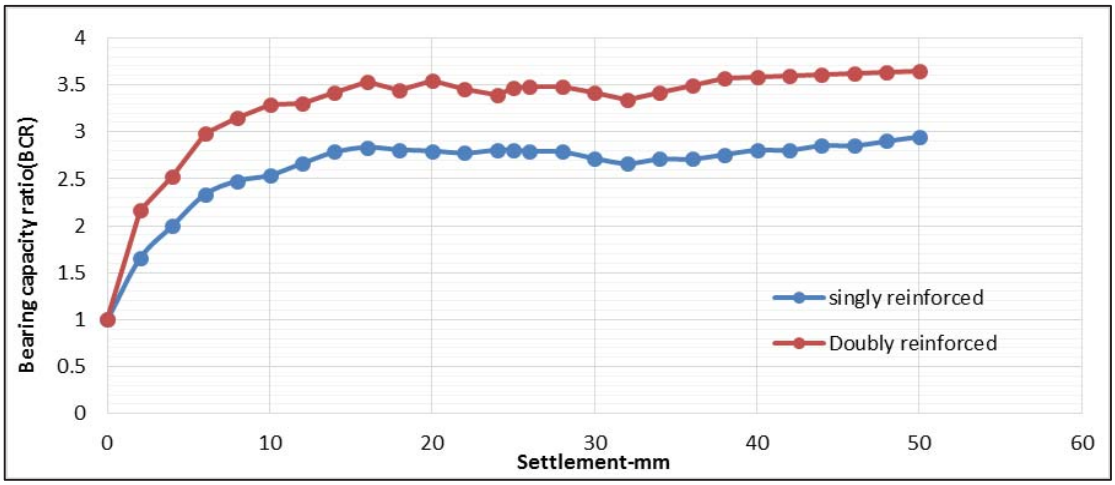

Figure 4.19 Variation of bearing capacity bearing capacity ratio (BCR)

The results of the vertical stress distribution for unreinforced, singly reinforced and doubly reinforced soil are shown in Figure 4.22, 4.24 and 4.26, respectively. In unreinforced soil, uniform vertical stress distribution up to large depth was observed. In reinforced soil, the stresses are transferred to a shallow depth. It shows very shallow depth when doubly reinforced geocell was used. The vertical settlement contours for different cases is shown in Figure 4.21, 4.23 and 4.25. Distribution of the settlement contours indicates the uniform settlement of reinforced and unreinforced soil. Punching shear failure was observed in high loads. Structural performance of geocell is increasing when double layer geocell was used. But it did not much vary with single layer geocell performance.

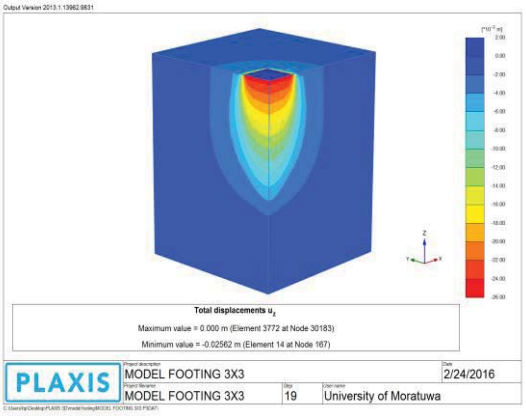

Figure 4.20 Vertical displacement of unreinforced soil

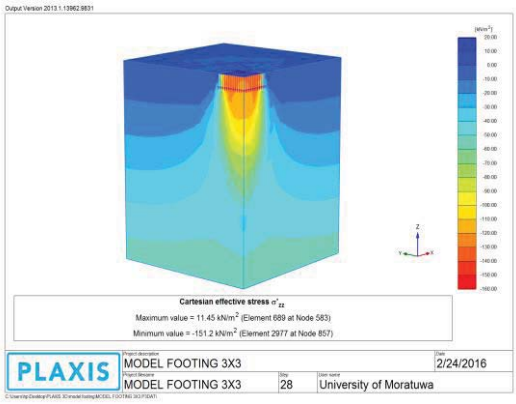

Figure 4.21 Vertical stress of unreinforced soil

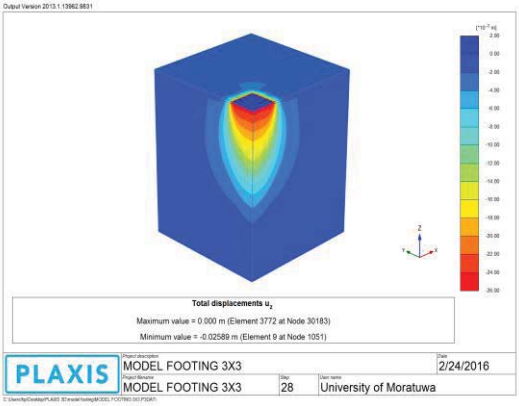

Figure 4.22 Vertical displacement of singly reinforced soil

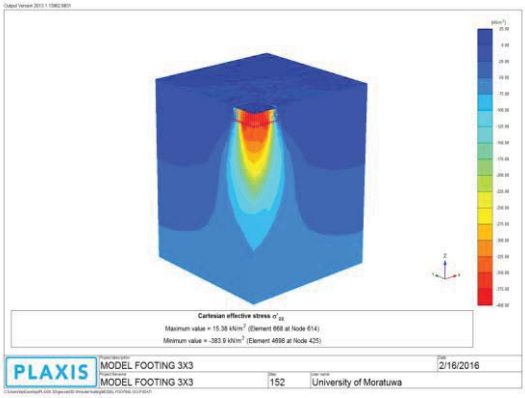

Figure 4.23 Vertical stress of singly reinforced soil

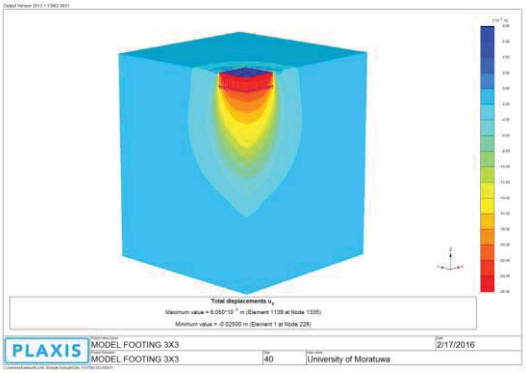

Figure 4.24 Vertical displacement of doubly reinforced soil

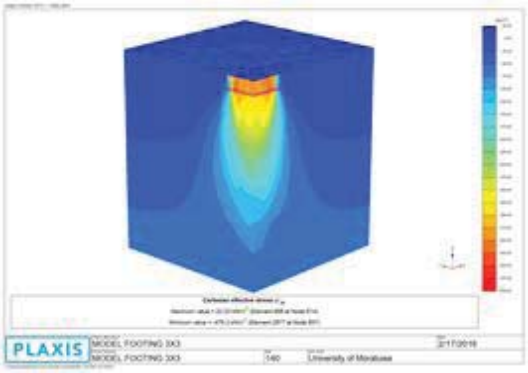

Figure 4.25 Vertical stress of doubly reinforced soil

4.3.3 Numerical analysis of model footing on the Geogrid reinforced soil

Most of the geogrid related geotechnical problems were solved using 2D analyse. Most of the time geogrid was simplified using truss 2D elements. A few researchers analyzed these problems using 3D structural based 3D FEM software like ABAQUS or ANSYS. PLAXIS 3D doesn't have much advanced features like ABAQUS or ANSYS. In this study, it was focused to validate reliability of the existing geogrid element in PLAXIS 3D and analyse the influence of different number of layers of geogrid reinforced soil.

Geogrids are elastic flexible elements with a normal stiffness and no bending stiffness. The PLAXIS 3D program allows for orthotropic and anisotropic material behavior in geogrid elements. Biaxial geogrid was used in this studies with square apertures. Hence, geogrid was modeled as orthotropic material. Table 4.7 shows the properties used in numerical modelling.

Table 4.7 properties of geogrid

Parameters	Name	Geocell	Unit
Material model	model	geogrid	-
Type of material behavior	type	Isotropic Elastic	-
Axial/Normal Stiffness	EA	560	kN/m

Finite element analysis was conducted using same geometry of experimental studies. Foundation modeling is already discussed under 3D modelling of geocell foundation. Figure 4.26 shows the very fine mesh of PLAXIS 3D models used in the analysis. Here, a very fine mesh was used because of the small thickness of geogrid (1.25mm). These FE analysis requires large computer memory and time. In these studies each analysis took 10-20 minutes to mesh and analyze the results.

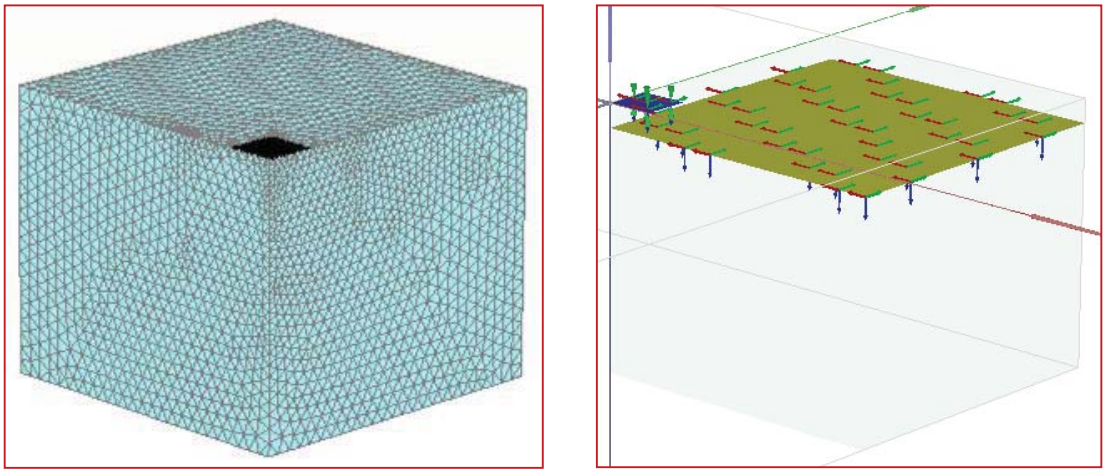

Figure 4.26 mesh of PLAXIS 3D model and 3D view of geogrid reinforced soil footing

Numerical studies were carried out by changing the number of geogrid layers where (N) was changed from 0 to 4. The bearing pressure-settlement curves obtained from numerical and experimental studies for different reinforced conditions presented in Figure 4.27. Ultimate bearing capacity was estimated from using numerical analyze

and compared with experimental studies. In unreinforced bed case, ultimate bearing capacity was observed in the range of 70kPa. A steep gradual increment curve was observed in the slope of the pressure-settlement. After 30mm settlement, punching was clearly observed. The curves started to separate when the displacement reached 2mm.

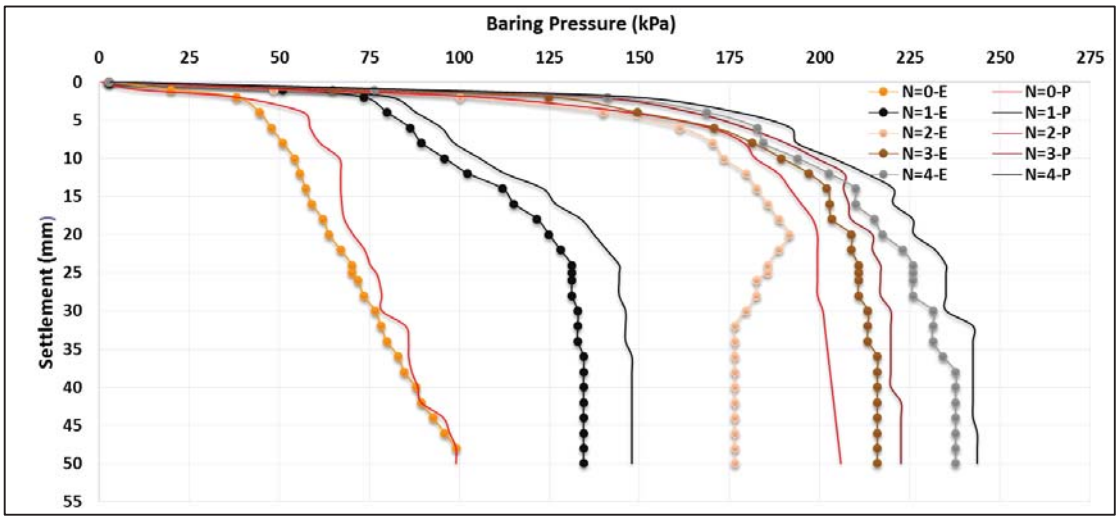

Figure 4.27 Bearing pressure – settlement behaviour of footing under various conditions

Variation between numerical and experimental result is less than 10kPa.This variation might occurred because of geogrid apertures and properties that were directly used from manufacture's specifications and foundation sand properties. Unexpected failure was occurred in experimental studies, two geogrid layers were used. It may be due to improper end fixing of geogrids and density variation of soil. Geogrid was modeled as a geogrid plate element without considering the apertures and the sizes. In PLAXIS 3D, it was a big challenge to model the interlocking effect between soil and geogrid due to very fine meshing. PLAXIS 3D is programmed for large scale analysis. So it is not easy to model actual geogrid with apertures. It is known that soil-geogrid interlocking plays an important role in the load-carrying capacity of foundations over geogrid-reinforced soils (Guido et al., 1986; Liu, 2015; Pinho-Lopes et al., 2015). The interlocking of soil particles through the grid apertures mobilizes the tensile strength in the reinforcing layer and generates an anchoring effect that leads to better geotechnical performance. Modeling such interactions considering the explicit geogrid geometry has been reported by Tran et al. (2014) (Tran, Meguid and Chouinard, 2014) and Hussein et al. (2016) (Hussein and Meguid, 2016) using the finite-discrete element method. Even though with these limitations, the numerical model functions were relatively close to the experimental model.

The results of the vertical stress distribution for reinforced and unreinforced soil are shown in Figure 4.28. In unreinforced soil, uniform vertical stress distribution up to large depth was observed. In reinforced soil, the stresses are transferred to a shallow depth. But this varies with number of geogrids. It shows very shallow depth when N=4. It was observed that bearing capacity increment rate reduces after second layer. The same observation was made by Kolay et al. (2013) and Demir et al. (2013). These stress contours clearly shows that model tank boundaries are quite adequate and satisfied the boundary conditions.

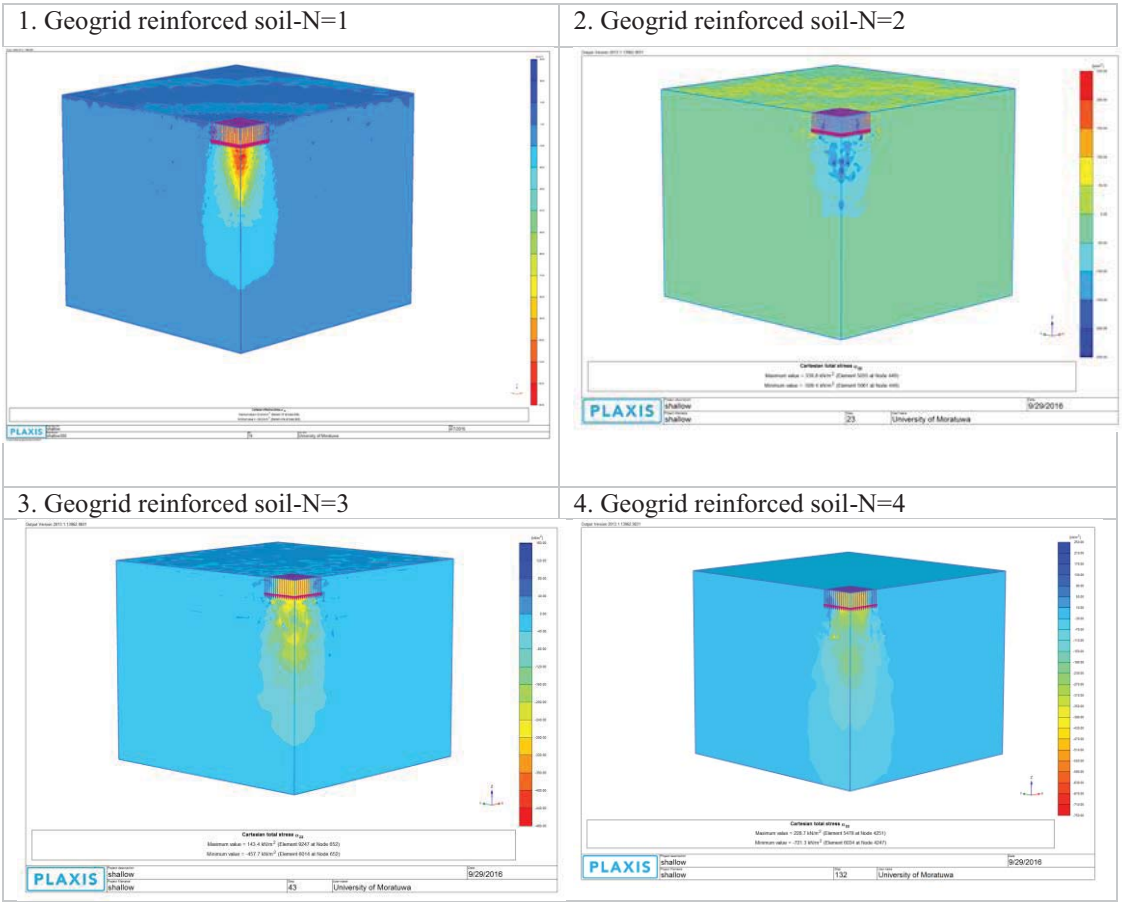

Figure 4.28 Vertical stress distribution of reinforced and unreinforced conditions

The vertical settlement contours for different cases is shown in Figure 4.29. Distribution of the settlement contours indicates the uniform settlement of reinforced and unreinforced soil. When comparing reinforced and unreinforced contours, a clear reduction in the vertical displacements for the reinforced case compared could be seen to the unreinforced case. Punching shear failure was observed in high loads. It was validated from experimental observation as well. Latha (Latha and Amit Somwanshi, 2009) has also observed similar uniform settlement contours in FLAC 3D modelling of the unreinforced soil. Theoretically, foundations with high rigidity will result in uniform settlements. In numerical approach, uniform settlements could be expected only as long as the foundation material properties are homogeneous and the rate of application of footing pressure is constant. However in experiments, this will not be the case, as it is nearly impossible to ensure such homogeneous soil properties in reality.

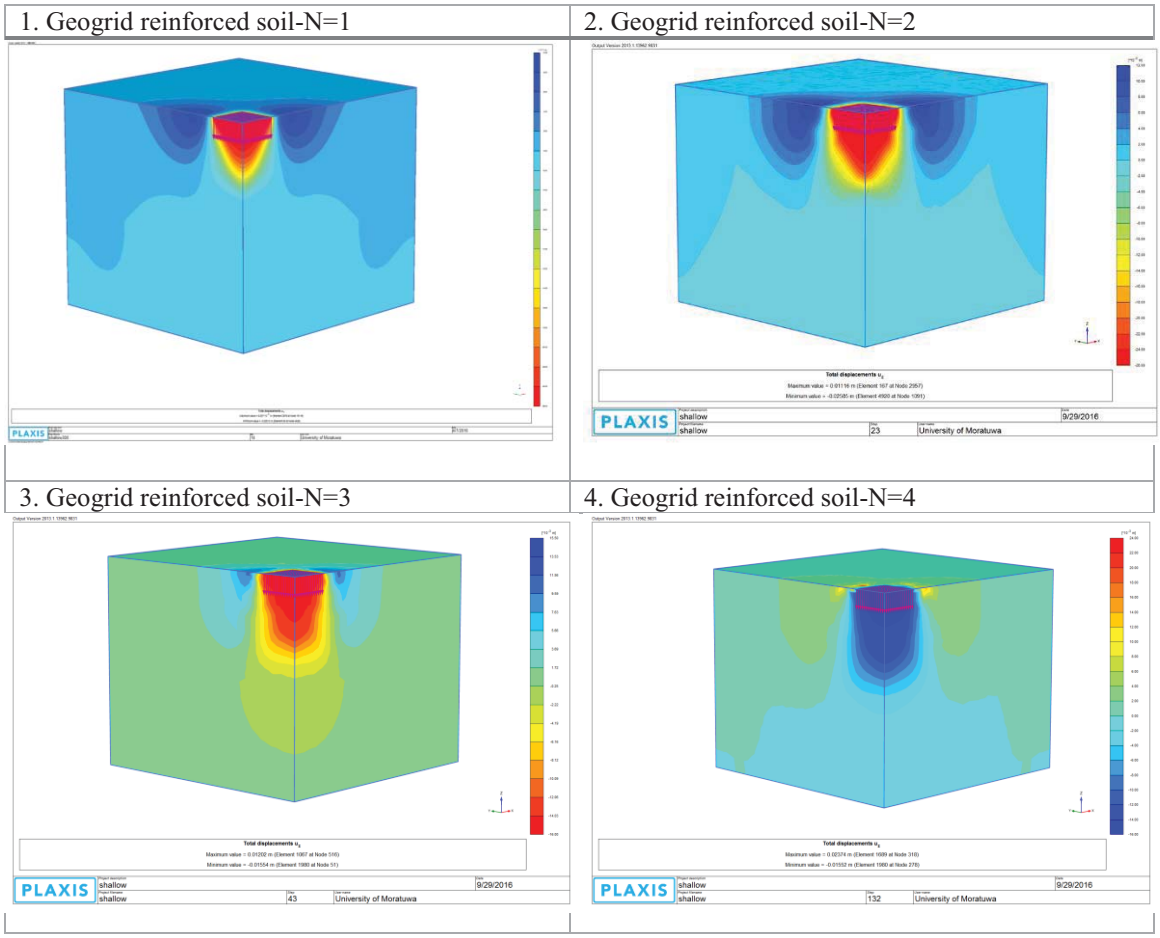

Figure 4.29 Vertical displacement of reinforced and unreinforced conditions

The geogrid reinforced soil behaves as a rigid slab (Ahmet Demir et al., 2014) below the shallow foundation and distributes the load over a large area into the underlying ground. This reduces the pressure distribution and vertical displacements, resulting in uniform settlement. Furthermore, the interlocking between soil and geogrid can reduce the vertical displacement and heaving near the footing. Consequently, potential tensile strain of each geogrid layer is restrained. As a result, bearing capacity of soil is increased and vertical deformation of soil is reduced.

4.3.4 Bearing capacity of shallow foundations on Geogrid –Geocell combinations

Geogrids and geocells are not alternatives to each other in construction applications. The choice of the reinforcement depends on the subgrade modulus as well as the design bearing capacity. Geogrids are cheaper than geocells and easy to lay, but if the required improvement in strength and modulus is very high, multiple layers of geogrids should be placed at regular intervals over considerable depth below the footing, whereas a layer of geocells filled with sand works out to be economical. Geocells are the speedy solution over emergencies, whereas geogrids though simple and easy to install, are not applicable over softer subgrades. Moreover, geocells provide higher lateral confinement and beam effect, thus increasing the bearing capacity of reinforced soil significantly. For many geotechnical problems, savings in time and assured performance of the solution play vital role than economical aspects.

Dash et al. (Sujit Kumar Dash et al., 2001) reported that a layer of planar geogrid placed at the base of the geocell mattress further enhances the performance of the footing in terms of load-carrying capacity and stability against rotation. The beneficial effect of this planar reinforcement layer becomes negligible at large heights of geocell mattress. Further, he mentioned that a layer of planar geogrid placed on top of geocell mattress does not yield much beneficial effect because of low pullout capacity. This technique is cost effective one when compare with double layer geocell.

In some geotechnical problems, it is required to improve the bearing capacity to very high values. In those situations, double layer geocell or multiple layer geogrid could be used. But there may be some construction conflicts. Geocells are the speedy solution over geogrid in most of geotechnical problems. Here combination of geogrid and geocell was analysed using numerical analysis. Two different cases were investigated, namely 'geocell+geogrid' combination and 'geogrid+geocell' combination which are shown in Figure 4.30.

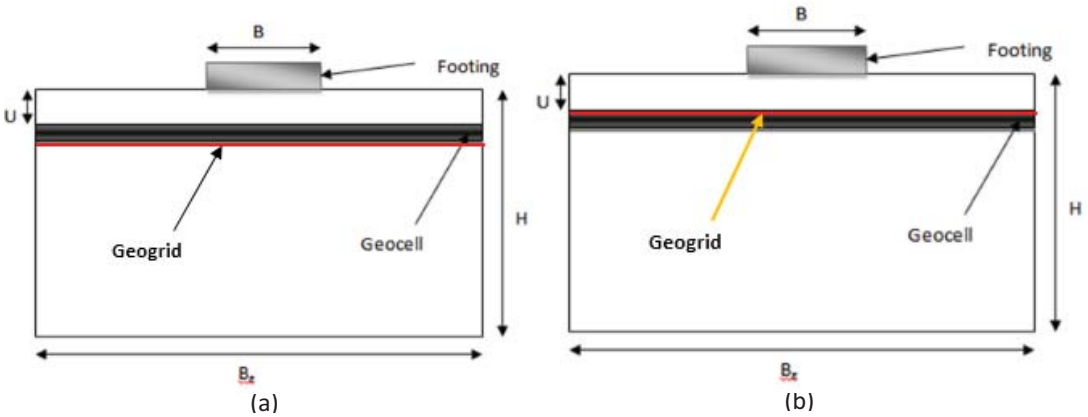

Figure 4.30 Geometry view of (a) Geocell– Geogrid layer reinforced soil (b) Geogrid –Geocell layer reinforced soil

Table 4.8 presents the dimensions of model shallow foundations used in the numerical analysis. The constitutive models and parameters of the sand is summarized in Table 4.1. Balau timber plank was used as rigid square footing with 50mm thickness and

200mm width. Constitutive model properties of timber is shown in Table 4.2. General properties of geocell and constitutive models are presented in Table 4.5. Geogrid was modeled as orthotropic material. Table 4.7 shows the properties of geogrid used in numerical modelling. Figure 4.31 shows the both cases of PLAXIS 3D models used in the analysis.

Table 4.8 Geometry parameter of model foundation

Parameter	Symbol	Unit	Values
Footing width	B	mm	200
Cover thickness (a)	U(a)	mm	20
Cover thickness (b)	U(b)	mm	20
Depth	H	mm	550
Width	Bx	mm	1300

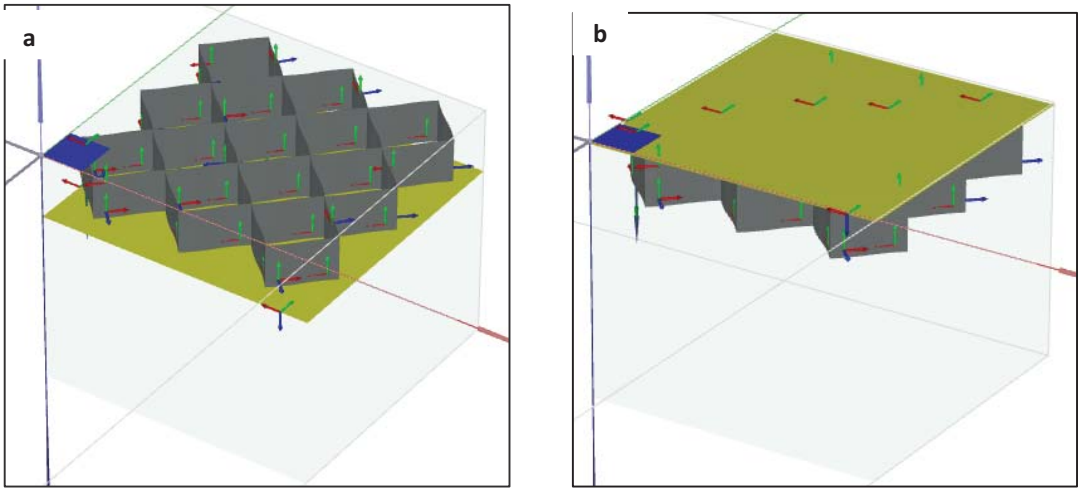

Figure 4.31 (a) Geocell– Geogrid layer reinforced soil (b) Geogrid –Geocell layer reinforced soil

Figure 4.32 shows the vertical stress and vertical distribution of both combinations. Ultimate bearing capacity of 'geocell+geogrid' combination and 'geogrid+geocell' combination are 302kPa and 266kPa, respectively. It can be observed that the provision of a planar geogrid layer at the base or top of the geocell mattress appreciably improves the bearing pressure of the footing as well as the stiffness of the foundation bed. Its rigidity also will increase leading to more uniform settlements at the base of the geocell layer.

A layer of planar geogrid placed at the base of the geocell mattress improve the bearing capacity significantly. For geocell mattress of shallow height (h/d <2), the sand in the cell directly below the footing tends to move downwards due to footing penetration. At higher settlements, this sand overcomes the frictional resistance on geocell wall to push down and move laterally away inducing rotation in the footing (Sujit Kumar Dash et al., 2001). But the presence of a planar geogrid layer at the base of the goecell mattress inhibits the downward as well as the lateral movement of the sand through bearing at the soil to grid interface. Further, the basal geogrid layer by virtue of its flexural

strength improves the overall rigidity of the geocell mattress system leading to more uniform pressure distribution. These two factors might have reduced the footing rotation to a practically negligible value (Dashet al., 2001).

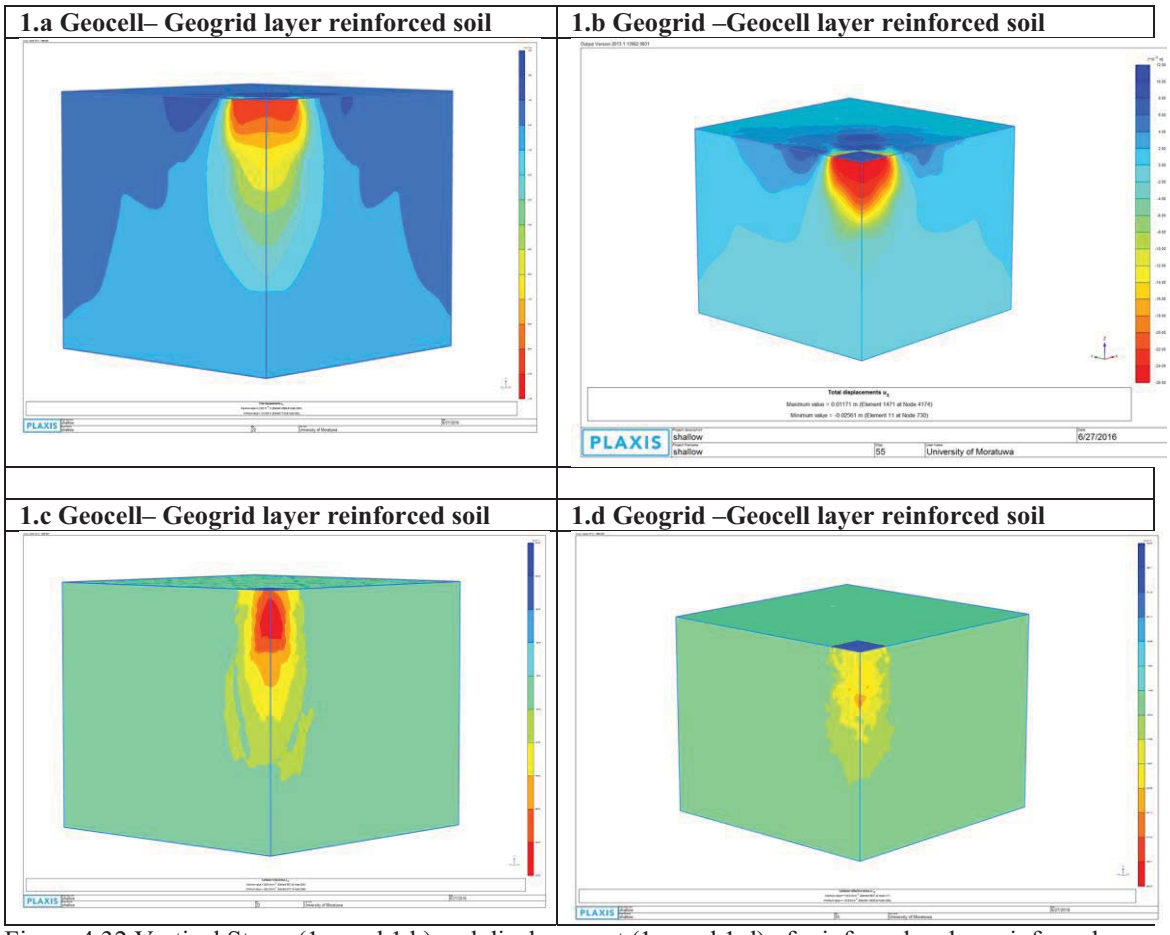

Figure 4.32 Vertical Stress (1.a and 1.b) and displacement (1.c and 1.d) of reinforced and unreinforced conditions

Provision of geogrid above the geocell layer is not much significant for geocell with (h/d) ratio 0.5 (h-geocell height, B-footing width). This is because the overburden pressure on this reinforcement layer was small to generate enough frictional resistance against the tie pullout due to downward penetration of the footing. The improvement is lower than the case with geogrid layer at the base of the geocell mattress. The significant improvement noticed might be due to the contribution of the reinforcement layer by virtue of its stiffness, as a planar reinforcement in sand bed (Sitharam, and Saride, 2006).

4.4 Summary

This chapter describes the development of a numerical model for geocell reinforced soil under a static load and validation of geogrid reinforced soil. These numerical models were validated experimental results. Important conclusions are drawn from this study.

4.4.1 Geocell

This study proposes a relatively accurate method of modeling geocell by using PLAXIS 3D. PLAXIS 3D has not much been used in past to model geocell. There the actual geocell structure was modeled using geogrid elements. In ECA approach, infill soil and geocell were modeled as composite material. That's why failure criteria might differ from actual case (Yang, 2010). But in proposed model, the soil was modeled using the Mohr Coulomb model, and the geocell was modeled using a linear elastic plate model. By considering curvature we contend that the propose model increases the accuracy of the results.

In this direction, this work contributes to the advancement of the knowledge in the numerical simulations of geocells close to reality. From the experimental results, suitable depth was found at depth (U) / width (B) =0.1 for a square pad footing. With experimental results the numerical results also were validated. It was found that the ECA overestimates the bearing capacity of the geocell-reinforced soil beds. Compared to ECA, the PLAXIS-3D modeling is more elegant, representative, and accurate (A. Hegde and T.G. Sitharam, 2015a; 2015b). However, the current 3D modeling approach proposed here is also having a few limitations such as failing to capture the non-homogenous nature of the soil. Further in this analysis the geocells are modeled as geogrid structures, where it is hard to provide all the properties of the geocell. Despite these limitations we hope that the model may function as a relatively close to experimental model. Further, some conclusions can be drawn from this part of study:

- The bearing capacity of the footing was greatly improved with the inclusion of geocell. The stiffness of the soil was also increased, but the benefit started to exhibit after about 2mm displacement was developed on the top surface. This result is consistent with the static load test data obtained from the geocell-reinforced sand.
- These stress contours clearly show that model tank boundaries are quite adequate and satisfied the boundary conditions.
- Suitable cover thickness was found at [depth (U)/width (B)] =0.1 for a square pad footing.
- Numerical results shows that bearing pressure increase with the aspect ratio. Bearing capacity show a marginal improvement after aspect ratio of 3. Local shear failure and Bucking of geocell will occur beyond an aspect ratio of 3.
- Structural performance of geocell is increasing when double layer geocell was used. But it was not much vary with single layer geocell performance.

4.4.2 Geogrid

Geogrid was modeled as a geogrid plate element without considering the apertures and the sizes. In PLAXIS 3D, it is a big challenge to model the interlocking effect between soil and geogrid due to very fine meshing. Even though with these limitations the numerical model functions relatively close to experimental model.

The bearing capacity of reinforced soil increases with increasing number of reinforcement layers. However, the significance of an additional reinforcement layer decreases with the increase in number of layers.

The geogrid reinforced soil behaves as a rigid slab below the shallow foundation and distributes the load over a large area into the underlying ground. This reduces the pressure distribution and vertical displacements, resulting in uniform settlement. Furthermore, the interlocking between soil and geogrid can reduce the vertical displacement and heaving near the footing. Consequently, potential tensile strain of each geogrid layer is restrained. As a result, bearing capacity of soil is increased and vertical deformation of soil is reduced.

4.4.3 Geogrid –Geocell combinations

It shows that a layer of planar geogrid placed at the base of the geocell mattress improve the bearing capacity significantly compare with provision of geogrid above the geocell layer.

5 THEORETICAL ANALYSIS

5.1 Overview

The purpose of this study is to examine the existing analytical solutions and to compare the results with numerical and experimental results. Numerical and experimental are time consuming approaches when compare with theoretical solutions. But accuracy and applicability is the important factor which should be considered in selection of methods. In this study, bearing capacity of geocell and geogrid reinforced soil foundation are separately discussed using appropriate proposed methods.

5.2 Theoretical Analysis-geocell reinforced soil

Neto etc.al (2013) (J. O. Avesani Neto et al, 2013) proposed a bearing capacity calculation method for geocell-reinforced soil by considering confinement effect and stress dispersion effect. The empirical equation is addition of an unreinforced subgrade bearing capacity (p_u) and bearing capacity improved by geocell (I).

$$p_r = p_u + I$$

5.2.1 Unreinforced subgrade bearing capacity (p_u)

In this method, Terzaghi's method which is more accurate method (Bowles, 1996), was used to calculate the subgrade bearing capacity. Terzaghi's equation is shown as equation 5.1.

$$\boldsymbol{p_u = cN_cS_c + \frac{1}{2}\gamma BN_\gamma S_\gamma} \quad \ldots\ldots (5.1)$$

Where:

$\boldsymbol{p_u}$-unreinforced subgrade bearing capacity
$\boldsymbol{c}$ - Subgrade soil cohesion
$\boldsymbol{\gamma}$ -subgrade soil unit weight
$\boldsymbol{B}$ - loading width
$\boldsymbol{N_c}$ & $\boldsymbol{N_\gamma}$ - bearing capacity factors
$\boldsymbol{S_c}$ -loading shape factor related to cohesion (1.0)
$\boldsymbol{S_\gamma}$ -loading shape factor related to the soil unit weight (0.8)

5.2.2 Confinement effect improvement

The confinement effect improvement depends directly on the load magnitude, the fill material, the material itself and the geocell pocket dimensions. Figure 5.1 (Neto et al, 2013) shows the cross sectional view and unitary pocket shear force. Thus, proposed equation for confinement effect improvement (force) is

$$\Delta F_\tau = 4\frac{h}{d}k_0pBL\tan\delta$$

Where:

$\boldsymbol{\Delta F_\tau}$-sum of unitary pocket shear forces under the load

$\frac{h}{d}$ - Geocell aspect ratio

k_0 - Lateral earth pressure coefficient at rest

B&L - loading width

p -load at the top of the geocell mattress

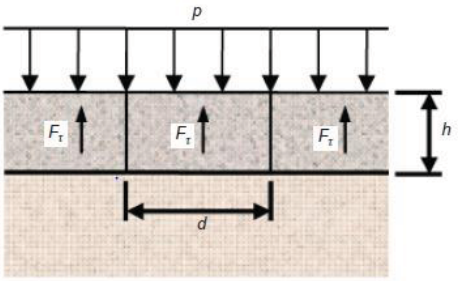

Figure 5.1 cross sectional view and unitary pocket shear force (Neto et al, 2013)

5.2.3 Stress dispersion effect

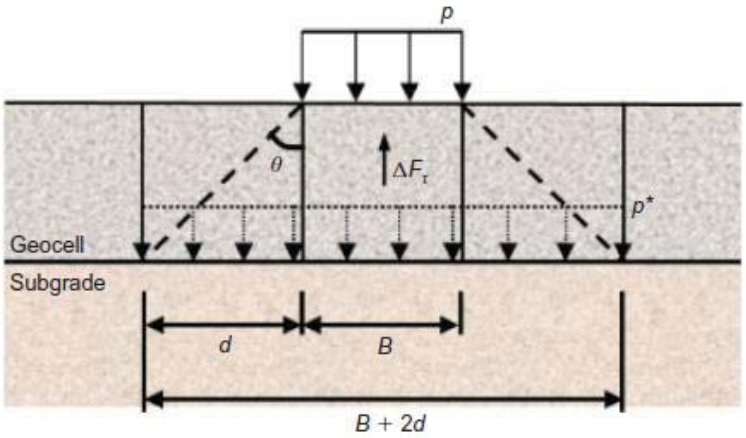

Figure 5.2 illustration of the stress dispersion effect (J. O. Avesani Neto et al, 2013)

The improvement due to this effect is expressed as a function of the load shape and size (boards, footing, tires, etc.), occurring only in finite-sized loads, and the geocell pocket size. In this calculation, a stress spreading a distance equal to one pocket is used which is illustrated in Figure 5.2.

The theoretical dispersion angles calculated by the proposed method were similar to those obtained by Dash et al. (2007) in experiments, mainly for geocell aspect ratio greater than 1. For aspect ratios smaller than 1 and geocell depth of placement greater than 0.25B, the proposed method overestimated values of dispersion angle.

Thus, the stress that effectively acts on the subgrade soil (p^*) can be defined by Equation 5.2.

$$p^* = \left(p - 4\frac{h}{d}k_0 pBL\tan\delta\right)e \quad \text{..... (5.2)}$$

Where: e is a stress redistribution parameter.

$$e = \frac{BL}{(B+2d)(L+2d)} \quad \text{..... (5.3)}$$

5.2.4 Bearing capacity of geocell-reinforced soil (p_τ)

The improvement in the bearing capacity due to geocell reinforcement (I) can be defined as the difference between the stress on the top of the geocell mattress (p) and the stress acting on its bottom (p^*). Thus, the bearing capacity of the geocell-reinforced soil, as shown in Equation 5.4, 5.5, is

$$p_\tau = p_u + (p - p^*) \quad \text{..... (5.4)}$$

$$p_\tau = p_u + 4\frac{h}{d}k_0 p \tan\delta\, e + (1-e)p \quad \text{..... (5.5)}$$

5.2.5 Theoretical bearing capacity calculation

Cross sectional view of the test configuration of geocell reinforcement is shown in Figure 5.3. By changing the cover thickness, experimental studies were carried out. Bearing capacity was calculated using theoretical approach discussed above.

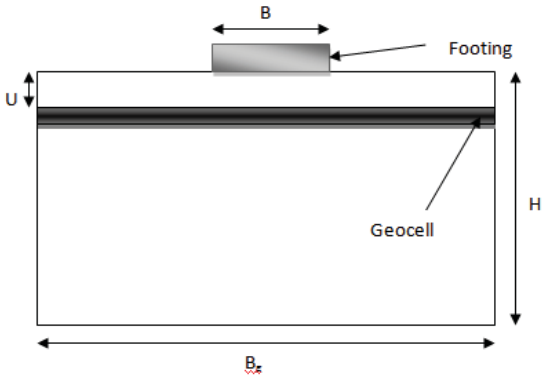

Figure 5.3 Geometry of the geocell reinforced foundation

Figure 5.3 shows the parameters used in the calculation which were used in experimental studies. Geometry parameters of the model footing are shown in Table 5.1.

Table 5.1 Dimensions of geometry

Parameter	Symbol	Unit	Values
Footing			
Footing width	B	mm	200
Depth	H	mm	550
Width	Bx	mm	1300
Embedded depth	D_f	mm	0

The material properties of the soil and other design parameters used in the study are presented in Table 5.2.

Table 5.2 material properties of the soil and other design parameters

Parameters	Symbol	unit	Value
coefficient of active earth pressure	ko	-	0.24
surcharge load	p	kN/m	83.08
interface shear angle	δ	o	15
cohesion of soil	c	kN/m^2	0
bearing capacity factor	Nc	-	61
loading shape factor related to cohesion	Sc	-	1.25
bearing capacity factor	Nq	-	48
loading shape factor related to surcharge load	Sq	-	1.25
subgrade soil unit weight	γ	kN/m^3	16
loading width	B	m	0.2
bearing capacity factor	Nγ	-	64
loading shape factor related to the soil unit weight	Sγ	-	0.6
geocell aspect ratio	h/d	-	0.5
stress redistribution parameter	e	-	0.104

Sample calculation process is shown below when geocell was placed just below the footing:

Step 1: Subgrade bearing capacity

$$(5.1) \quad p_u = cN_cS_c + \frac{1}{2}\gamma BN_\gamma S_\gamma$$

$$= 61.44 \text{ kN/m}^2$$

Step 2: Geocell bearing capacity improvement

$$I = 4\frac{h}{d}k_0 pe \tan\delta + (1-e)$$

$$= 4 \times 0.5 \times 0.4 \times 83.08 \times 0.104 \times 0.268 + (1 - 0.10406) \times 83.08$$

$$= 76.29 kN/m^2$$

Step 3: Bearing capacity of geocell-reinforced soil (p_r)

$$p_r = p_u + I$$

$$p_r = 61.44 kN/m^2 + 76.29 kN/m^2$$

$$p_r = 137.73 kN/m^2$$

Table 5.3 comparison of bearing capacity using different methods

Cases	**Experimental**	**FEM**	**Theoretical**		
			Meyerhof	**Hansen**	**Vesic**
Unreinforced	70.2	76.2	100.3	60.7	73.9
Reinforced			**Koerner**	**Presto**	**Neto**
U/B=0	131	144	156.9	112.3	137.7
U/B=0.5	169.7	182	185.3	132.5	174.2

Estimated results using Neto's method showed a good fit to the results of the experiments and numerical studies. The comparison between the current bearing capacity methods for geocell-reinforced soil (Table 5.3) showed that the Neto's method generally has a better approach than the other methods (Koerner's and Presto's) for sandy foundation soils.

5.3 Theoretical approach of estimating the bearing capacity of geogrid

5.3.1 Analytical solution

The superposition method could be used to calculate the contribution of geogrid reinforcement, and an additional term,Δq_T, is added to include the effect of tensile force T. The ultimate bearing capacity can be given by modifying Meyerhof and Hanna's (1978) solution to incorporate the effect of tensile force T as follows for strip footing on a reinforced soil foundation with horizontal reinforcement:

$$q_{u(R)} = 1.3cN_c + qN_q + 0.4\gamma BN_\gamma + \Delta q_T \quad \text{(5.6)}$$

Where $q_{u(R)}$ is the bearing capacity of unreinforced soil foundation, Δq_T is the increased bearing capacity due to the tensile force of the reinforcement; c is the cohesion of soil; q is the surcharge load; γ is the unit weight of soil; and N_q, N_c, and N_γ are bearing capacity factors, which are dependent on the friction angle of soil φ.

5.3.1.1 Ultimate bearing capacity of the square footing on reinforced sand soil (FHWA/LA.08/424)

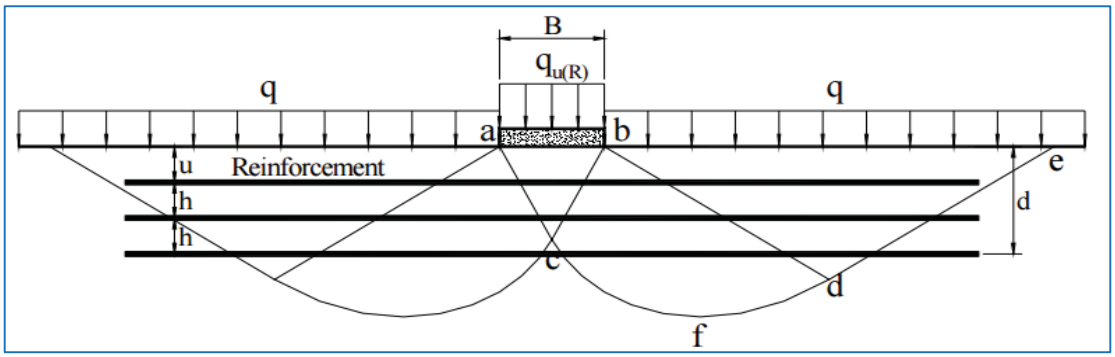

Figure 5.4 failure mode of reinforced soil foundation-failure within reinforced zone (Sharma et.al 2008)

For two or more layers of reinforcement, the increased bearing capacity Δq_T can be given as:

$$\Delta q_T = \sum_{i=1}^{N} \frac{12T_i[u+(i-1)h]r_T}{B^2} \quad \text{(5.7)}$$

Where T_i is the tensile force in the i^{th} reinforcement layer. It should be noted here that all reinforcement layers must be placed above the failure zone, i.e., above the point f in Figure 5.4, to contribute for improving the performance of the soil foundation. The ultimate bearing capacity of the square footing on reinforced soil with horizontal reinforcement can then be given as follows:

$$\boldsymbol{q_{u(R)} = 1.3cN_c + qN_q + 0.4\gamma BN_\gamma + \sum_{i=1}^{N} \frac{12T_i[u+(i-1)h]r_T}{B^2}} \quad \text{(5.8)}$$

$$r_T = \begin{cases} \left[1 - 2\frac{u+(i-1)h}{B}\tan\left[\frac{\pi}{4} - \frac{\varphi}{2}\right]\right] & for\ u + (i-1)h < \frac{B}{2}\tan\left[\frac{\pi}{4} + \frac{\varphi}{2}\right] \\ \frac{1}{2} - \frac{u+(i-1)h}{2H_f} & for\ u + (i-1)h \geq \frac{B}{2}\tan\left[\frac{\pi}{4} + \frac{\varphi}{2}\right] \end{cases} \quad \ldots\ldots\ldots \quad (5.9)$$

Where $\boldsymbol{H_f}$ is the depth of failure surface and can be evaluated as:

$$\boldsymbol{H_f = \frac{B}{2\cos\left[\frac{\pi}{4}+\frac{\varphi}{2}\right]} e^{\left(\frac{\pi}{4}+\frac{\varphi}{2}\right)\tan\varphi}\ \cos\varphi} \ldots\ldots\ldots\ldots\ldots\ldots\ldots\ldots\ldots\ldots\ldots\ldots\ldots\ldots\ldots \quad (5.10)$$

5.3.1.2 Determine the amount of settlement at reinforcement level (Se). Schmertmann et al. (1978)

Tensile force should be estimated to calculate the bearing capacity of geogrid reinforced soil. Sharma et al. (2009) mentioned that strain development along the geogrid is related with footing settlement. For a given footing settlement, the vertical settlement distribution at a certain depth in reinforced soil is assumed to be the same as that in unreinforced soil. At a certain settlement level, the shape of deformed reinforcement should be compatible with the vertical settlement distribution of surrounding foundation soil.

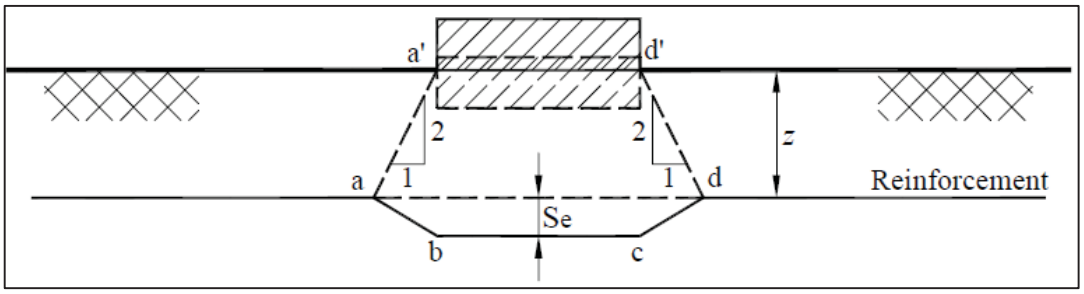

Figure 5.5 Simplified distribution of vertical settlement in sand (Sharma et.al 2008)

Since the distribution of vertical settlement at each reinforcement level is now known, the next step is to determine the amount of settlement at each reinforcement level (Se). Schmertmann et al. (1978) proposed a practical distribution of vertical strain along the depth below the footings in terms of strain influence factor. To calculate the elastic settlement Se at any depth in sand, we can integrate the strain in sand below this depth with respect to depth, and the following formula suggested by Schmertmann et al. (1978) can be applied:

$$\boldsymbol{S_e = C_1 C_2 C_3 (q - \gamma D_f) \sum \frac{I_\varepsilon \Delta z}{E_s}} \quad \ldots\ldots\ldots\ldots\ldots\ldots\ldots\ldots\ldots\ldots\ldots\ldots\ldots\ldots\ldots\ldots \quad (5.11)$$

where C_1 is a correction factor for the depth of embedment; C_2 is a correction factor for secondary creep in sand; C_3 is a correction factor for the footing shape; q is the surcharge load; g is the unit weight of soil; D_f is the embedment depth of the footing; I_ε is the strain influence factor; Δz is the thickness of subdivided soil layer; and E_s is the elastic modulus of sand.

$$C_1 = 1 - 0.5\frac{\gamma D_f}{q-\gamma D_f} \quad \text{(5.12)}$$

$$C_2 = 1 + 0.2\log\left(\frac{t}{0.1}\right) \quad \text{(5.13)}$$

$$C_3 = 1.03 - 0.03L/B \geq 0.73 \quad \text{(5.14)}$$

Schmertmann et al. (1978) suggested a practical distribution of strain influence factor $I_{\varepsilon p}$ along the depth below the footings as shown in Figure 5.5. The peak value of the strain influence factor $I_{\varepsilon p}$ is evaluated by the following equation:

$$I_{\varepsilon p} = 0.5 + 0.1\sqrt{\frac{q-\gamma D_f}{\sigma_{vp}'}} \quad \text{(5.15)}$$

$$\sigma_{vp}' = \gamma(D_f + 0.5B) \quad \text{(5.16)}$$

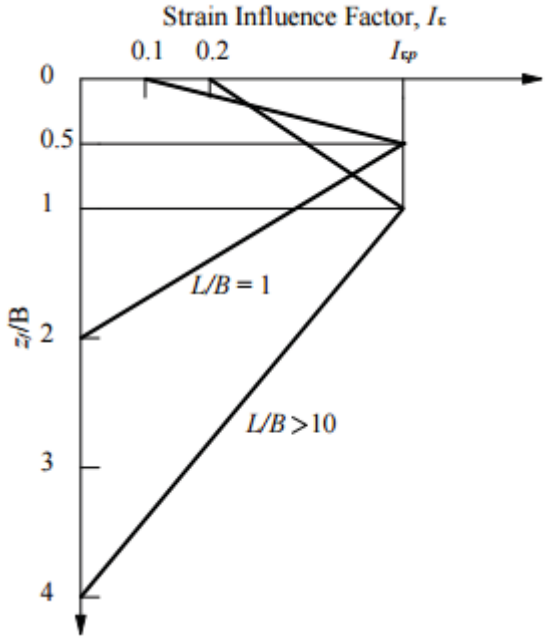

where:
D_f -embedment depth
E_s-Elastic modulus of sand
$I_{\varepsilon p}$-strain influence factor
Q- Bearing pressure of footing
t- Time since application of load

Figure 5.6 Strain influence factor distribution diagrams (Sharma et.al 2008)

The tensile force, T, developed at a certain point in reinforcement can then be evaluated by the following equation:

$$T = J\varepsilon \quad \text{(5.17)}$$

Where T is the tensile force in reinforcement, J is the tensile modulus of reinforcement and ε is strain at a point in geogrid.

5.3.2 Theoretical bearing capacity calculation-geogrid reinforced soil

Cross sectional view of the test configuration of geogrid reinforcement is shown in Figure 5.7. By changing the number of geogrid layers, experimental studies were carried out. Bearing capacity was calculated using theoretical approach discussed above for different number of geogrids.

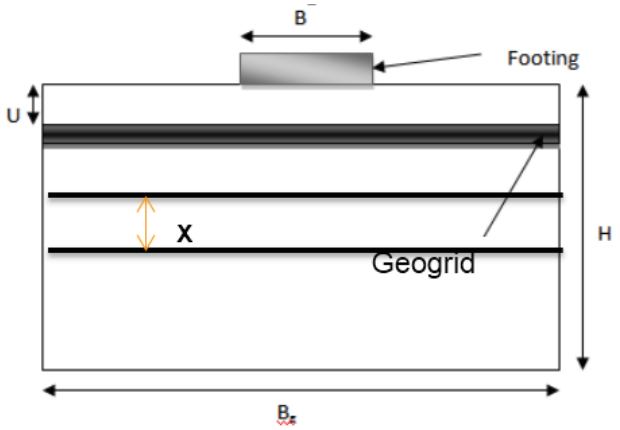

Figure 5.7 Geometry of the geogrid reinforced foundation

Table 5.4 show the parameters used in the calculation which were used in experimental studies.

Table 5.4 Properties of different material used in calculation

Parameter	Symbol	Unit	Values
Footing			
Footing width	B	mm	200
Cover thickness	u	mm	50
Spacing	x	mm	50
Depth	H	mm	550
Width	Bx	mm	1300
Embedded depth	D_f	mm	0
Geogrid			
Thickness	t	mm	1.5
Density	ρ	g/cm^3	1.05
Number of geogrids	N	Nos	0,1,2,3,4
Tensile strength	T	kN	18.2
Tensile modulus	J	kN/m	420
Sand			
Friction angle	φ	^{o}	38
Elastic modulus of sand	Es	kN/m^2	12500

5.3.2.1 Settlement at the first layers of reinforcement: Layer 1

First geogrid layer is at the depth 50mm from the top surface. Here, Z/B=2 is the influence depth. Total influence depth of 400mm was divided into 50 mm layers and further calculations were carried out. Table 5.5 shows the calculation of $\frac{I_\varepsilon \Delta z}{E_s}$ for each 50mm layers.

Table 5.5 Settlement at the first layers of reinforcement

Δz-(mm)	Z-(mm)	z/B	I_ε	$\frac{I_\varepsilon \Delta z}{E_s}$
50	75	0.375	0.925	3.85417E-06
50	125	0.625	1.1	4.58333E-06
50	175	0.875	0.9	3.7500 E-06
50	225	1.125	0.7	2.91667E-06
50	275	1.375	0.5	2.08333E-06
50	325	1.625	0.3	1.2500 E-06
50	375	1.875	0.1	4.16667E-07
			∑	1.88542E-05

Then final settlement was calculated using coefficientsC_1, C_2, C_3 and $\frac{I_\varepsilon \Delta z}{E_s}$.

$(5.12) \longrightarrow C_1 = 1 - 0.5\frac{\gamma D_f}{q - \gamma D_f}$ =1

$(5.13) \longrightarrow C_2 = 1 + 0.2\log\left(\frac{t}{0.1}\right)$ =1

$(5.14) \longrightarrow C_3 = 1.03 - 0.\frac{03L}{B} = 1.01 - 0.03 = 1.00 \geq 0.73$

Total Elastic settlement due to layer 1 geogrid reinforcement.

$(5.11) \longrightarrow S_{e\,1} = C_1 C_2 C_3 (q - \gamma D_f) \sum \frac{I_\varepsilon \Delta z}{E_s}$

= **1.49mm**

Settlement at the different layers of reinforcement is summarized in Table 5.6:

Table 5.6 Settlement at the different layers

N	Se(mm)
1	1.49
2	1.18
3	0.82
4	0.53

5.3.2.2 Tensile forces in the first and second layers of reinforcement: Layer 1

The average strain (ε_{avg}) in reinforcement for a given footing settlement was calculated. Finally, developed tensile force in the reinforcement was estimated.

$$\Delta L = 2\sqrt{{S_e}^2 + (0.5z)^2} - z$$

$$\varepsilon_{avg} = \frac{\Delta L}{L_{ad}} = 0.035376$$

$$T = J\varepsilon$$

= 14.85778kN/m

Developed tensile force in the each reinforcement layers is presented in Table 5.7**.**

Table 5.7 Settlement at the different layers

N	T(kN/m)
1	14.86
2	9.41
3	4.54
4	1.86

5.3.2.3 Increased bearing capacity ΔqT

The increased bearing capacity $\Delta \boldsymbol{q_T}$ was calculated using following equation:

(5.8), (5.9) & (5.10)−→

$$\Delta \boldsymbol{q_T} = \sum_{\boldsymbol{i=1}}^{\boldsymbol{N}} \frac{\mathbf{12}\boldsymbol{T_i}[\mathbf{u} + (\boldsymbol{i}-\mathbf{1})\boldsymbol{h}]\left[\mathbf{1} - \mathbf{2}\frac{\boldsymbol{u}+(\boldsymbol{i}-\mathbf{1})\boldsymbol{h}}{\boldsymbol{B}}\boldsymbol{tan}\left[\frac{\boldsymbol{\pi}}{\mathbf{4}} - \frac{\boldsymbol{\varphi}}{\mathbf{2}}\right]\right]}{\boldsymbol{B^2}}$$

Table 5.8 bearing capacity improvement at the different layers

N	T(kN/m)	Δq_T(kPa)
1	14.86	60.84
2	9.41	38.52
3	4.54	18.58
4	1.86	7.61

5.3.2.4 Ultimate bearing capacity of reinforced sand

The total bearing capacity of geogrid reinforced sand was calculated using following relationship.

$$q_{u(R)} = q_u + \Delta q_T$$

Table 5.9 shows the bearing capacity of reinforced soil for different number of geogrid layers.

Table 5.9 bearing capacity of reinforced soil for different N

N	T(kN/m)	Δq_T(kPa)	$q_{u(R)}$(kPa)
1	14.86	60.84	140.84
2	9.41	38.52	179.37
3	4.54	18.58	197.95
4	1.86	7.61	205.56

5.3.3 Comparison of Ultimate Bearing Capacity

Table 5.10 Summary of bearing capacity for different approaches

Number of Geogrid layer-N	Ultimate Bearing Capacity-kPa		
	Experimental	Numerical	Theoretical
1	131.2	144.3	140.84
2	185.6	199.3	179.37
3	210.7	216.8	197.95
4	225.9	235.1	205.56

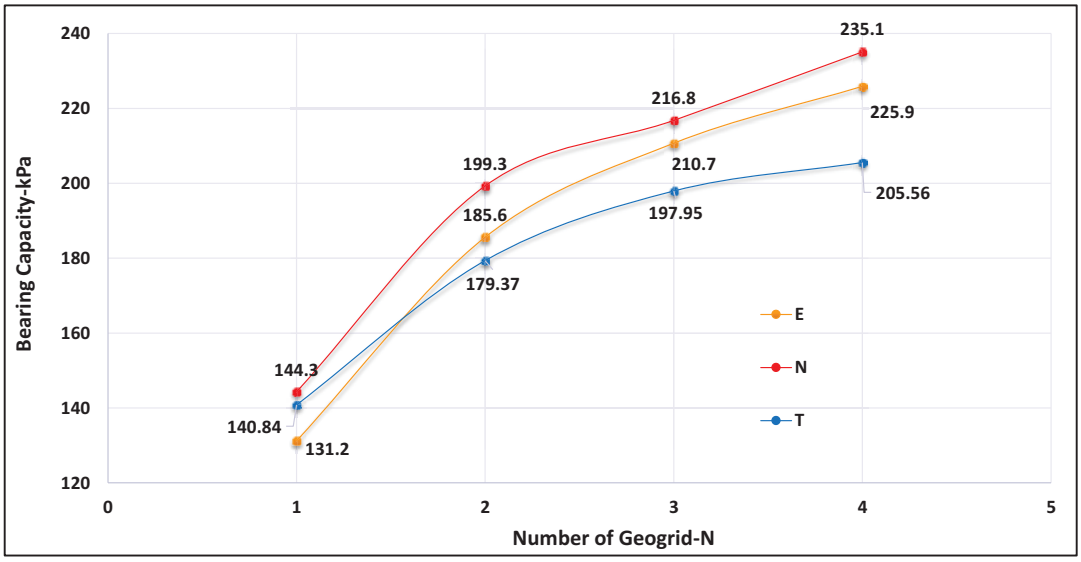

Figure 5.8 Comparison of Ultimate Bearing Capacity

Table 5.10 presents the comparison between the experimental, numerical and theoretical bearing capacities of geogrid reinforced soil. The values predicted by using the analytical solution (Radhey Sharma et al., 2008) are in good agreement with the

experimental and numerical results. All results are presented in graphical view in Figure 5.8. All approaches show the same trend in improvement of bearing capacity. Theoretical results show a realistic solution .Same observation was recorded by Sharma etc.al (Radhey Sharma et al., 2008).

5.4 Summary

Bearing capacity of geocell and geogrid reinforced soil are calculated using theoretical solutions proposed by researchers. Based on the results of the study, the following conclusions can be drawn:

5.4.1 Geocell

In this study, approach proposed by Neto et al (J. O. Avesani Neto et al., 2013) was used to estimate the bearing capacity of geocell reinforced soil. This solution was based on geocell reinforcement mechanisms (confinement effect and stress dispersion effect) and verified through comparison with laboratory experimental results from several authors.

Estimated results using Neto's method showed a good fit to the results of the experiments and numerical studies. The comparison between the current bearing capacity methods for geocell-reinforced soil (Table 5.3) showed that the Neto's method generally has a better approach than the other methods (Koerner's and Presto's) for sandy foundation soils.

5.4.2 Geogrid

The theoretical solutions proposed by R. Sharma etc.al (Radhey Sharma et al., 2008) was used in this study to rationally evaluate the ultimate bearing capacity of geogrid reinforced soil foundations for sand.

The values predicted by using the analytical solution (Chen, 2007) are in good agreement with the experimental and numerical results. Figure 5.9 shows comparison among experimental, numerical and theoretical results for different number of geogrid. However, several simplifying assumptions were made by authors (Radhey Sharma et al., 2008; Chen, 2007) in the derivation of tensile force in geogrid.

The bearing capacity of reinforced soil increases with increasing number of reinforcement layers. However, the significance of an additional reinforcement layer decreases with the increase in number of layers. The reinforcing effect becomes negligible below the influence depth (Chen, 2007; Gu, 2011).

6 COST FEASIBILITY STUDY OF GEOCELL REINFORCED SHALLOW FOUNDATION

6.1 Cost feasibility study for geocell reinforcement

Cost analyse is important for any type of products. Whenever, implementation of new technique should be financially feasible.

Here, initially 3mx3m footing was used to cost calculation. It was assumed that transferred axial column load to footing was 1200kN. Hence, required bearing capacity was calculated based on this axial load. Then, cost was calculated for unreinforced, singly reinforced and doubly reinforced cases separately

Table 6.1 summary of cost calculation

Features	Unreinforced	Single reinforced	Single reinforced	Doubly reinforced	Doubly reinforced
Foundation size-m^2	3.0x3.0	3.0x3.0	2.0x2.0	3.0x3.0	1.6x1.6
Foundation depth-m	0.5	0.5	0.4m	0.5m	0.3m
Geocell area-m^2	-	64	36	64	16
Geocell depth-m	-	0.1	0.1	0.2	0.2
Bearing Capacity-kN/m^2	151.2	425.2	320.4	525.5	470.5
Concrete Volume-m^3	4.5	4.5	1.6	4.5	0.3
Reinforced steel volume- kg	273.6	273.6	97.28	273.6	18.24
Expected cost-Lkr	124596	162996	65901	200396	41351
Bearing Capacity with respect to the expected cost	**1.21**	**2.61**	**4.86**	**2.65**	**11.38**

Then bearing Capacity with respect to the expected cost ratio was estimated for each cases using 3.0m x 3.0m footing. Finally, the optimum footing size was obtained by trial and error method using different size of footing. Table 6.1 shows the summary of calculation.

Initially, footing size was kept as constant (3mx3m) and cost analyse was carried out. Doubly reinforced geocell sand shows high feasible ratio among all cases. At the same time, singly reinforced sand also shows high ratio as doubly reinforced. Then optimum size of footing was estimated for singly and doubly reinforced cases. Singly reinforced footing could be designed as 2.0mx2.0m (optimum size) and doubly reinforced footing was as 1.6mx1.6m. Finally, the optimum bearing pressure/cost ratios were compared among themself. Doubly reinforced footing showed high feasible ratio and 65% cost reduction. So, it could be recommended to use doubly reinforced geocell for financially feasible footing design. On the other hand there could be some construction issue when doubly reinforced is used.

6.2 Summary

When doubly reinforced geocell was used, footing size was reduced by 40% and cost was reduced by 65%. This will lead for cost effective foundation design.

7 CONCLUSIONS AND RECOMMENDATIONS

As discussed the benefits of using geosynthetics to reinforce soils have been widely recognized. Past research works available in the literature demonstrated that the use of reinforcements could significantly increase the bearing capacity of the soil foundation and reduce the settlement of the footing. The objective of this study is to investigate the effect of geosynthetic type, spacing and cover thickness/placing depth on the bearing capacity of shallow foundation using experimental and numerical studies.

This research was undertaken to investigate the potential benefits of using reinforcement to improve the bearing capacity and reduce the settlement of shallow foundations on soils. Experimental studies were done using geocell, geogrid and combination of both geocell and geogrid cases. Then, appropriate numerical models were developed using PLAXIS 3D and validated using experimental studies. Finally, a theoretical approach was used to validate the final results of each case. Following sections discuss the drawn conclusions based on the results of the present study.

7.1 Conclusions from experimental studies

In this study, a series of laboratory static-load tests were performed using HDPE geocells and biaxial geogrids to validate and calibrate the numerical models. Following conclusions can be drawn from the test results:

7.1.1 Geocell

- From the results, suitable cover thickness was found at [depth (U)/width (B)] ratio between 0 and 0.5 for a square pad footing.
- The static load test showed that with the provision of HDPE geocells, bearing capacity of soil can be improved by a factor up to 2.5 times of unreinforced soil.
- Estimated modulus of subgrade reaction (Ks)(1.25mm) for different cases in sand beds showed that improvement of Ks value is not significant in sand beds even with the addition of geocell reinforcement. Therefore, soil reinforcements show marginal improvement in stiffness of composite mass. However, bearing pressure has suddenly increased, when the load was applied gradually on bed. This shows that composite mass will have higher stiffness than soil from beginning and resist the loading.
- Geocell reinforcement needs some displacement to take be effective. The reason for this phenomenon may be the hoop stress from the geocell is proportional to the tensile stress of geocell. Therefore, the geocell provides more and more confining stress to sand as the tensile stress (or strain) in the geocell increases which was validated by estimating the K_{25}(subgrade reaction for 25mm settlement)

7.1.2 Geogrid

- The inclusion of reinforcement resulted in increasing the ultimate bearing capacity of soils and reducing the footing settlement.

- The bearing capacity of reinforced soil increases with increasing number of reinforcement layers (at same vertical spacing). However, the significance of an additional reinforcement layer decreases with the increase in number of layers.
- Maximum bearing capacity improvement was observed when four layer of geogrids (N=4) was used as reinforcement which was 2.86 times of unreinforced bearing capacity.

7.2 Conclusions from numerical studies

This section describes the significant conclusions from the process of development of the numerical model for geocell reinforced soil under a static load and validation of geogrid reinforced soil.

7.2.1 Geocell

In geocell reinforced soil model, the soil was modeled using the Mohr Coulomb model, and the geocell was modeled using a linear elastic plate model. Following conclusions can be drawn from this part of study:

- The bearing capacity of the footing was greatly improved by about 250% with the inclusion of geocell. The stiffness of the soil also increased, but the benefit started to exhibit after about 2mm displacement was developed on the top surface. This result is consistent with the static load test data obtained from the geocell-reinforced sand.
- Vertical stress and displacement contours clearly show that model tank boundaries are quite adequate and satisfied the boundary conditions.
- Suitable cover thickness can be found at [depth (U)/width (B)] =0.1 for a square pad footing.
- Numerical results shows that bearing pressure increase with the aspect ratio. Bearing capacity show a marginal improvement after aspect ratio of 3.0. Local shear failure and Buckling of geocell will occur beyond an aspect ratio of 3.0.
- Structural performance of geocell is increasing when double layer geocell was used. But it does not much vary with single layer geocell performance.

7.2.2 Geogrid

Geogrid was modeled as a geogrid plate element without considering the apertures and the sizes. In PLAXIS 3D, it is a big challenge to model the interlocking effect between soil and geogrid due to very fine meshing. Even though with these limitations the numerical model functions relatively close to experimental model.

The bearing capacity of reinforced soil increases with increasing number of reinforcement layers. However, the significance of an additional reinforcement layer decreases with the increase in number of layers.

The geogrid reinforced soil behaves as a rigid slab below the shallow foundation and distributes the load over a large area into the underlying ground. This reduces the pressure distribution and vertical displacements, resulting in uniform settlement. Furthermore, the interlocking between soil and geogrid can reduce the vertical displacement and heaving near the footing. Consequently, potential tensile strain of each geogrid layer is restrained. As a result, bearing capacity of soil is increased and vertical deformation of soil is reduced.

7.2.3 Geocell-Geogrid combination

It shows that a layer of planar geogrid placed at the base of the geocell mattress improve the bearing capacity significantly compared with provision of geogrid above the geocell layer.

7.3 Conclusions from theoretical studies

Bearing capacity of geocell and geogrid reinforced soil are calculated using theoretical solutions proposed by researchers (Chen, 2007) (Neto, J.O.A., Bueno, B.S. and Futai, M.M., 2013). Based on the results of the study, the following conclusions can be drawn:

7.3.1 Geocell

In this study, approach proposed by Neto et al (Neto, J.O.A., Bueno, B.S. and Futai, M.M., 2013) was used to estimate the bearing capacity of geocell reinforced soil. This solution was based on geocell reinforcement mechanisms (confinement effect and stress dispersion effect) and verified through comparison with laboratory experimental results from several authors.

Estimated results using Neto's method showed a good fit to the results of the experiments and numerical studies. The comparison between the current bearing capacity methods for geocell-reinforced soil showed that the Neto's method generally has a better approach than the other methods (Koerner's and Presto's) for sandy foundation soils.

7.3.2 Geogrid

The values predicted by using the analytical solution (Chen, 2007) are in good agreement with the experimental and numerical results. However, several simplifying assumptions were made by Sharma and Chen (Chen, 2007) (Sharma, R. , Chen, Q , Abu-Farsakh,M. and Yoon, S., 2008) in the derivation of tensile force in geogrid.

The bearing capacity of reinforced soil increases with increasing number of reinforcement layers. However, the significance of an additional reinforcement layer decreases with the increase in number of layers. The reinforcing effect becomes negligible below the influence depth of 1.25B (Chen, 2007) (Gu, 2011) .

7.4 Recommendations for reinforced soil foundation design

Based on the overall study following are the key recommendations that can be made for the improvements of reinforced soil foundation design.

- Based on the experimental and numerical test results of this study and literature survey, typical design parameters for reinforcement layout are recommended in Table 7.1 and Table 7.2.

Table 7.1 Recommended design parameters for geocell reinforcement layout

Parameters	Symbol	Typical value	Recommended
Cover thickness	U/B	0.0-0.5	0.1
Length of geogrid	Bx/B	4-6	5
Aspect ratio	h/d	2-3	3
Bearing capacity ratio	BCR	2-3.5	3

Table 7.2 Recommended design parameters for geogrid reinforcement layout

Parameters	**Symbol**	**Typical value**	**Recommended**
Cover thickness	U/B	0.2-0.5	0.2
Vertical spacing	x/B	0.2-0.5	0.25
Influence depth	d/B	1.3-1.7	1.25
Length of geogrid	Bx/B	4-6	5
Number of geogrids	N	3-4	4
Bearing capacity ratio	BCR	2-3	3

- In this study it showed that doubly geocell reinforced footing shows high BCR compare with singly reinforced foundation. When doubly reinforced geocell was used, footing size was reduced by 40% and cost was reduced by 65%. Therefor it's apparent that using double reinforced geocell will lead to cost effective foundation designs.
- A layer of planar geogrid placed at the base of the geocell mattress improve the bearing capacity significantly. Therefore this practice is recommended for better performance of geocell.
- Looking at the high agreement of numerical model and experimental results, PLAXIS 3D recommended to be used to model the geocell and geogrid reinforced soil foundations.
- Based on the sustainability study, it is found that geocell could be used as reinforced soil with higher structural and financial performance along significant positive environmental impact.

7.5 Recommendations for Future Research

This work presents a detailed study toward understanding the behavior of geosynthetic reinforced soil foundations. However, the performance of reinforced soil foundation is influenced by numerous factors. Due to limited time and resources, this study cannot address all these factors. The future research is recommended to address the following:

- Given that the work carried out in the thesis was based on finite element analysis and small scale experimental studies of reinforced soil foundation, there is a need to verify the findings of this study using full-scale reinforced soils, such as static loading of reinforced shallow foundation.
- Most previous experimental studies were focused on short-term behavior of reinforced soil foundations. The future work is recommended to investigate the long-term performance of reinforced soil foundation.
- The future work is recommended to investigate the performance of reinforced soil with the variation of soil's moisture content and unloading cases.
- Most of bearing pressure –settlement curves of geocell reinforced soil were not smooth as experimental curves. The future work is recommended to investigate the problem and suggest the solution to overcome this problem.
- The numerical models developed in this study can well simulate the behavior of the geocell-reinforced soil under static loads. However, it takes significant time to run the model. To better implement the geocell technology, a future study is needed to develop a simplified numerical model considering membrane effect.

8 REFERENCES

Adams, M. T., and Collin, J. G., 1997. Large model spread footing load tests on geosynthetic reinforced soil foundations. Journal of Geotechnical and Geoenvironmental Engineering, 123(1), pp. 66-72.

Ahmed, A, E-Tohami, A. M. K. and Marei, N. A,, 2008. Two-Dimensional Finite Element Analysis of Laboratory Embankment Model. s.l., s.n.

Alamshahi, S. and Hataf, N., 2009. Bearing capacity of strip footings on sand slopes reinforced with geogrid. Geotextiles and Geomembranes, 27(3), p. 217–226.

Alawaji, H., 2001. Settlement and bearing capacity of geogrid-reinforced sand over collapsible soil. Geotextiles and Geomembranes, 19(2), pp. 75-88.

Basudhar, P. K., Dixit, P. M., Gharpure, A and Deb, K, 2008. Finite element analysis of geotextile-reinforced sand-bed subjected to strip loading. Geotextiles and Geomembranes, Volume 26, p. 91–99.

Bathrust, R.J. and Karpurapu, R, 1993. Large scale triaxial compression testing of geocell reinforced granular soils. Geotech. Tes, 16(3), pp. 296-303.

Bathurst, R. J., and Knight, M. A., 1998). Analysis of Geocell Reinforced-Soil Covers over Large Span Conduits. Computers and Geotechnics, 22(3), pp. 205-219..

Belal, A., Nagy,N., and Elshesheny, A., 2015. Numerical Evaluation of Bearing Capacity of Square Footing. Ottawa, Ontario, Canada, s.n.

Biabani, M. Mahdi., Indraratna, B.and Ngo, N., 2016. Modelling of geocell-reinforced subballast subjected to cyclic loading. Geotextiles and Geomembranes, 44 (4), pp. 489-503..

Biswas, A., 2013. Influence of subgrade strength on the performance of geocell-reinforced foundation systems. Geosynthetics International, 20(6), pp. 376-388.

Chen, Q., 2007. AN EXPERIMENTAL STUDY ON CHARACTERISTICS AND BEHAVIOR OF REINFORCED SOIL FOUNDATION, Louisiana , USA: Louisiana State University.

Chesworth, W., 2007. Encyclopedia of Soil Science. Netherland: Springer Science & Business Media.

Das, B. M., 2015. Principles of Foundation Engineering. Boston, USA: Cengage Learning.

Dash, S.K, Rajagopal, K and Krishnaswamy, N.R, 2001. Strip footing on geocell reinforced sand beds with additional planar reinforcement. Geotextiles and Geomembranes, Volume 19, pp. 529-538.

Dash,S.K., Rajagopal,K. and Krishnaswamy, N.R., 2007. Behaviour of geocell-reinforced sand beds under strip loading. Canadian Geotechnical, Volume 44, pp. 905-915.

Demir, A., Yildiz, A., Laman, M. and Ornek, M., 2014. Experimental and numerical analyses of circular footing on geogrid-reinforced granular fill underlain by soft clay. Acta Geotechnica, 9(4), p. 711–723.

Evan, M. D., 1994. Geocell Mattress effects on the Embankment Settlements. In: Vertical and horizontal deformations of foundations and embankments:Settlement '94. s.l.:s.n., pp. 584-597.

Ghareh, S., 2015. Numerical Modeling of the Effect of Geocell Elements' Dimensions on Behavior of Circular Footings. Journal of Structural Engineering and Geotechnics, 5(3), pp. 9-14.

Ghazavi, M. and Lavasan,A.A., 2008. Interferenceeffect of shallow foundations constructed on sand reinforced with geosynthetics. Geotextiles and Geomembranes , 26(5), pp. 404-415.

Guido, V.A., Biesiadecki, G.L., and Sullivan, M.J., 1985. Bearing capacity of a geotextile reinforced foundation. San Francisco, s.n.

Gu, J., 2011. COMPUTATIONAL MODELING OF GEOGRID REINFORCED SOIL FOUNDATION AND GEOGRID REINFORCED BASE IN FLEXIBLE PAVEMENT, USA: Louisiana State University.

Han, J., Yang, X.M., Leshchinsky, D. and Parsons, R.L, 2008. Behavior of geocellreinforced sand under a vertical load. Journal of Transportation Research Board, Volume 2045, pp. 95-101.

Hegde, A. and Sitharam, T.G. , 2015a. 3-Dimensional numerical modelling of geocell reinforced sand beds. Geotextiles and Geomembranes, Volume 43, pp. 171-181.

Hegde, A., Sitharam, T.G., 2013. Experimental and numerical studies on footings supported on geocell reinforced sand and clay bed. International Journal of Geotechnical Engineering, 7(4), pp. 347-354.

Hegde, A.M. and Sitharam, T.G. , 2015b. Three-dimensional numerical analysis of geocell-reinforced soft clay beds by considering the actual geometry of geocell pockets. Canadian Geotechnical, 14 February , Volume 52, pp. 1-12.

Hejazia,S.M. , Sheikhzadeha,M., Abtahib, S.M. and Zadhoush, A., 2012. A simple review of soil reinforcement by using natural and synthetic fibers. Construction and Building Materials, Volume 30, pp. 100-116.

Henkal,D.J and Gilbert,G.D, 1952. the effect of rubber membrane on the measured triaxial compression strength of clay samples. Geotechnique, 3(1), pp. 20-29.

Hussein, M.G. and Meguid, M.A., 2016. A three-dimensional finite element apporach for modeling biaxial geogrid with application to geogrid-reinforced soils. Geotextiles and Geomenbranes, Volume 44, pp. 295-307.

Janbu.N, 1963. soil compressibility as determined by odometer and triaxial tests. Wiesbaden,Germany, s.n.

Koerner, R., 1997. Design with Geosynthetics. New Jersy.: 4th edition, Prentice Hall,Upper Saddle River.

Kolay, P.K., Kumar, S. and Tiwari, D., 2013. Improvement of Bearing Capacity of Shallow foundation on Geogrid Reinforced Silt Clay and Sand. Journal of Construction Engineering.

Latha, G.M. and Somwanshi, A., 2009. Effect of reinforcement form on the bearing capacity of square footings on sand. Geotextiles and Geomembranes, Volume 27, pp. 409-422.

Latha,G.M, 2000. Investigation on the bahaviour og geocell supported embankments, Madras,India: s.n.

Latha, G.M. and Somwanshi, S.A., 2009. Bearing capacity of square footings on geosynthetic reinforced sand. Geotextiles and Geomembranes, 27(4), pp. 281-294..

Latha, G.M., Dash, S.K. and Rajagopal.K., 2009. Numerical Simulation of the Behavior of Geocell Reinforced Sand in Foundations. INTERNATIONAL JOURNAL OF GEOMECHANICS, Issue August, pp. 143-152.

Maharaj, D. K., 2003. Nonlinear finite element analysis of strip footing on reinforced clay. The Electronic Journal of Geotechnical Engineering, 8(Bundle C).

Mandal, J. N., and Gupta, P., 1994. Stability of geocell-reinforced soil. Construction and building materials, 8(1), pp. 55-62.

McGown, A., Andrawes, K. Z. and Al-Hasani, M.M, 1978. Effect of inlusion properties on the behavior of sand. Geotechnique, 28(3), pp. 327-346.

Moghaddas Tafreshi, S.N. and Dawson, A.R., 2010. Comparison of bearing capacity of a strip footing on sand with geocell and with planar forms of geotextile reinforcement. Geotextiles and Geomembranes, Volume 28, pp. 72-84.

Mosallanezhad, M. , Taghavi, S.H.S., Hataf, N. and Alfaro, M.C. , 2016. Experimental and numerical studies of the performance of the new reinforcement system under pull-out conditions. Geotextiles and Geomembranes, 44(1), pp. 70-80.

Mosallanezhad,M., Taghavi,S.H.S., Hataf,N. and Alfaro,M., 2016. Experimental and numerical studies of the performance of the new reinforcement system under pull-out conditions. Geotextiles and Geomembranes, 44(1), pp. 70-80.

Murad Y. Abu-Farsakh,and Qiming Chen, 2008. Use of Reinforced Soil Foundation (RSF) to Support Shallow Foundation, Louisiana ,USA: Louisiana Transportation Research Center -FHWA.

Neto, J.O.A., Bueno, B.S. and Futai, M.M., 2013. A bearing capacity calculation method for soil reinforced with a geocell. Geosynthetics International, 20(3), pp. 129-141.

Patra, C.R., Das, B.M., and Atalar, C, 2005. Bearing capacity of embedded strip foundation on geogrid-reinforced sand. Geotextiles and Geomembranes, Volume 23, pp. 454-462.

Pinho-Lopes, M., Paula, A.M. and Lopes, M.L, 2015. Pull-out response of geogrids after installation. Geosynthetics International, 22(5), pp. 339-354.

Pokharel, S. ,Han, J. , Leshchinsky, D. and Parsons, R., 2010. "Investigation of factors influencing behavior of single geocell-reinforced bases under static loading. Geotextiles and Geomembranes journal, 28(6), pp. 570-578.

Rajagopal, K., Krishnaswamy, N. R., and Latha, G. M, 1999. Behaviour of Sand Confined with Single and Multiple Geocells. Geotextiles and Geomembranes,, Volume 17, pp. 171-184.

Raji, M., 2013. Endochronic Constitutive Model for Sand and its Applications to Geotechnical problems, Bangalore,India: s.n.

Ramaswamy, S. D. and Puroshothama, 1992. Model footings of geogrid reinforced clay. India, s.n.

Rea, C., and Mitchell, J. K, 1978. Sand reinforcement using paper grid cells. Pittsburgh, s.n.

Saride, S., Gowrisetti, S., Sitharam, T.G. and Puppala, A.J., 2009. Numerical simulations of sand and clay. Ground improvement, 162(14), pp. 185-198.

Sawwaf, M. A. E., 2007. Behavior of strip footing on geogrid-reinforced sand over a soft clay slope. Geotextiles and Geomembranes, 25(1), pp. 50-60.

Sharma, R. , Chen, Q , Abu-Farsakh,M. and Yoon, S., 2008. Analytical modeling of geogrid reinforced soil foundation. Geotextiles and Geomembranes, Volume 27, p. 63–72.

Sitharam .T .G., and Saride, S., 2006. Effects of base geogrid on geocell-reinforced foundation beds. Geomechanics and Geoengineering, 1(3), pp. 207-216.

Sitharam, G.Thallak, Saride, S. and Dash, S.K., 2007. Performance of surface footing on geocell-reinforced soft clay beds. Geotechnical and Geological Engineering, Volume 25, pp. 509-524.

Sitharam,T.G., Sireesh,S. and Dash, S.K., 2005. Model studies of a circular footing supported on geocell-reinforced clay. Canadian Geotechnical, Volume 42, pp. 693-703.

Sitharam.G and Sireesh.S, 2005. Behaviour of embedded footings supported on geogrid cell reinforced foundations beds. Geitechnical Testing Journal, 25(5), pp. 452-463.

Sladen, J. A. and & Handford G., 1987. A potential systematic error in laboratory testing of very loose sands. Canadian Geotechnical Journal, Volume 24, pp. 462-466.

Sugimoto, M. and Alagiyawanna, A. M. N., 2003. Pullout behavior of geogrid by test and numerical analysis. Journal of Geotechnical and Geoenvironmental Engineering, 129(4), pp. 361-371.

Swaraj, C. and Shakti, S., 2015. A Review of Studies on Geocell-reinforced Foundations. Research Journal of Recent Sciences, Volume 4, pp. 24-30.

Tran,V. D. H., Meguid, M. A. and Chouinard, L. E. , 2014. Three-Dimensional Analysis of Geogrid-Reinforced Soil. International Journal of Geomechanics, 15(4), p. 04014066.

Towhata, I., 2008. Geotechnical Earthquake Engineering. 1 ed. s.l.:Springer Science & Business Media.

Vidal, H., 1978. The Development and Future of Reinforced Earth. Pittsburgh, PA, s.n.

Webster, S. L., and Watkins, J. E., 1977. Investigation of Construction Techniques for Tactical Bridge Approach Roads Across Soft Ground, Vicksburg, MS: Technical Report S-77-1, U.S. Army Engineer Waterways Experiment.

Webster, S. L., 1977a. Investigation of Beach Sand Trafficability Enhancement Using Sand-Grid Confinement and Membrane Reinforcement Concepts;Report 1, Sand Test Sections 1 and 2, Vicksburg, MS: Technical Report GL-79-20,Geotechnical Laboratory, US Army Corps of Engineers Waterways Experimentation Station.

Webster, S. L., 1977b. Investigation of Beach Sand Trafficability Enhancement Using Sand-Grid Confinement and Membrane Reinforcement Concepts; Report 2, Sand Test Sections 3 and 4, Vicksburg, MS: Technical Report GL-79-20,Geotechnical Laboratory, US Army Corps of Engineers Waterways Experimentation Station.

Wesseloo, J., 2004. The Strength and Stiffness of Geocell Support Packs, Pretoria, South Africa: Ph.D.Dissertation, University of Pretoria.

Yang, X., 2010. Numerical Analyses of Geocell-Reinforced Granular Soils under Static and Repeated Loads, New Jersey: University of Kansas.

Yarbasi, N., Kalkan, E. and Akbulut, S., 2007. Modification of freezing–thawing properties of granular soils with waste additives. Col Reg Sci Technol, Volume 48, pp. 44-54.

Yetimoglu, T., Wu, J. T. H. and Saglamer, A., 1994. Bearing capacity of rectangular footings on geogrid-reinforced sand.. Journal of Geotechnical Engineering, ASCE, 120(12), pp. 2083-2099..

Yogaarajah, I., and Yeo, K.C, 1994. Finite element modeling of pull-out tests with load and strain measurements. Geotextiles and Geomembranes, Volume 13, pp. 43-54.

Zhou, B., Maosen,J.X., Zhao and Zeng,Q., 2012. Stability study on naturally filling body in gob-side entry retaining. International Journal of Mining Science and Technology, Volume 22, pp. 423-427.

Zidan, A. F., 2012. Numerical Study of Behavior of Circular Footing on Geogrid-Reinforced Sand Under Static and Dynamic Loading. Geotechnical and Geological Engineering, 30(2), p. 499–510.